

<https://www.mdc-berlin.de/de/veroeffentlichungstypen/clinical-journal-club>

## The weekly Clinical Journal Club by Dr. Friedrich C. Luft

Usually every Wednesday 17:00 - 18:00



### Klinische Forschung

Experimental and Clinical Research Center (ECRC) von MDC und Charité

Als gemeinsame Einrichtung von MDC und Charité fördert das Experimental and Clinical Research Center die Zusammenarbeit zwischen Grundlagenwissenschaftlern und klinischen Forschern. Hier werden neue Ansätze für Diagnose, Prävention und Therapie von Herz-Kreislauf- und Stoffwechselerkrankungen, Krebs sowie neurologischen Erkrankungen entwickelt und zeitnah am Patienten eingesetzt. Sie sind eingeladen, uns beizutreten. [Bewerben Sie sich!](#)



Acute generalized exanthematous pustulosis

Generalized pustular psoriasis

IgA Pemphigus

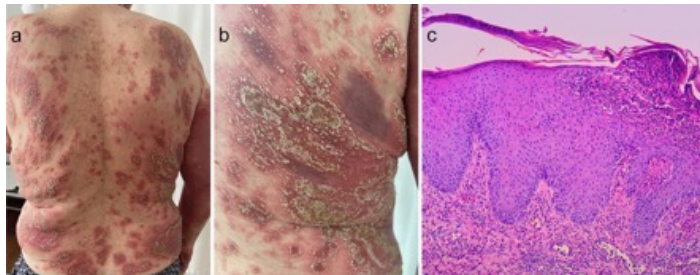
Staphylococcal scalded skin syndrome

Subcorneal pustular dermatosis

A 54-year-old woman with invasive ductal carcinoma of the breast and well-controlled chronic plaque psoriasis presented to the emergency department with a 2-day history of painful rash and fever. Five days before the onset of the rash, the patient had completed a **2-week course of systemic glucocorticoids to treat side effects of chemotherapy**. The body temperature was 38.2°C, and heart rate 137 beats per minute. On physical examination, widespread erythematous patches with overlying, coalescing pustules were seen on the torso, arms, legs, face, and scalp, with sparing of mucosal surfaces. Laboratory testing was notable for neutrophilic leukocytosis and an elevated C-reactive protein level. **Biopsy of the rash in the periumbilical region revealed neutrophil-rich pustules in the epidermis on histopathological testing. What is the most likely diagnosis?**

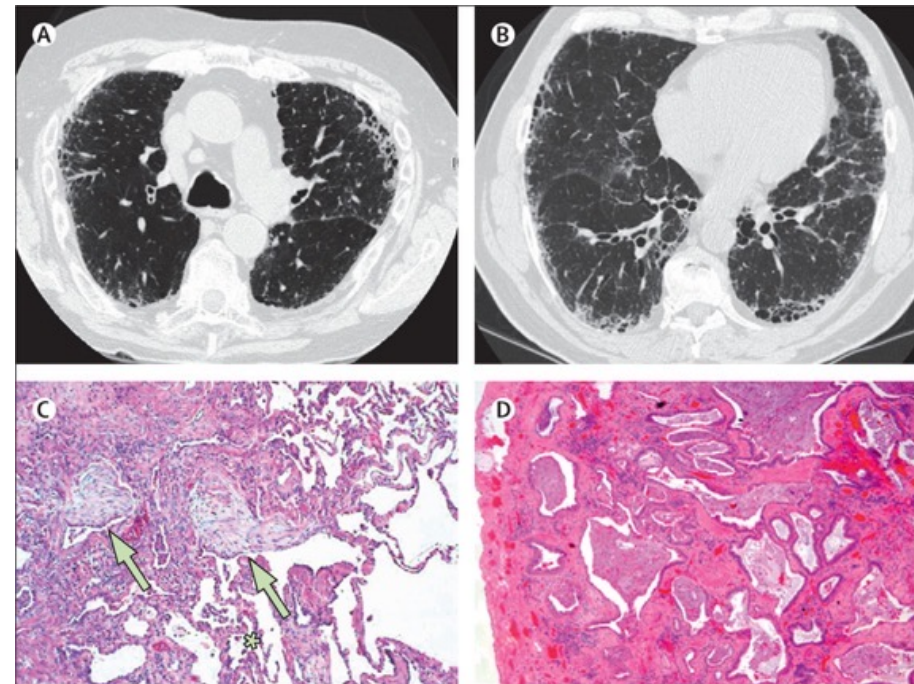
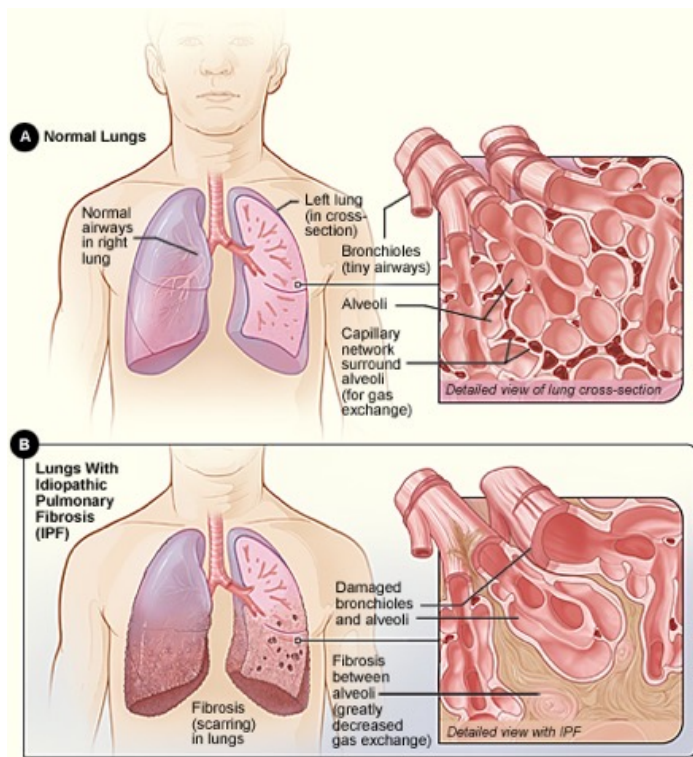
A diagnosis of generalized pustular psoriasis — a rare, autoinflammatory skin disease that manifests as widespread sterile pustules and systemic symptoms — was made. Generalized pustular psoriasis often occurs in patients with plaque psoriasis. It may be spontaneous or triggered by physiological stressors, such as medication withdrawal.

Generalized pustular psoriasis (GPP), also known as von Zumbusch psoriasis, is a rare, severe form of psoriasis characterized by sudden outbreaks of widespread, sterile pustules on the skin, often accompanied by systemic inflammation like fever and fatigue. It can be life-threatening if untreated and may require hospitalization.





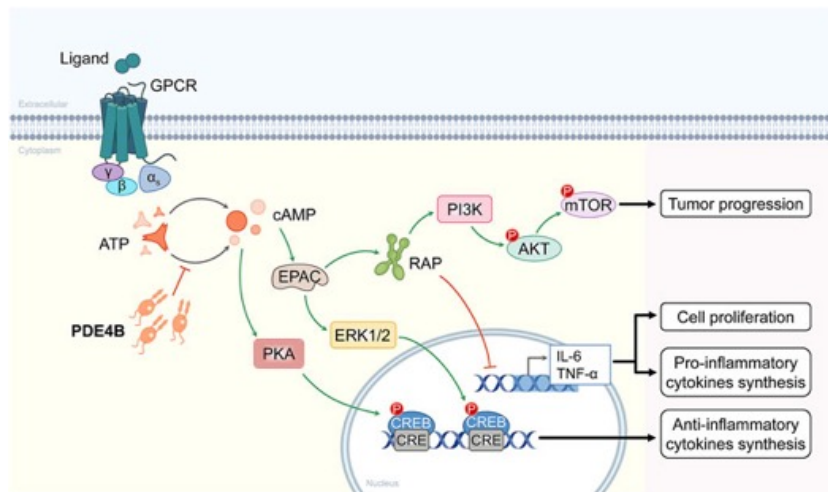
Idiopathic pulmonary fibrosis (IPF) is a progressive lung disease where the lungs become scarred, making it increasingly difficult to breathe. The cause of this scarring is unknown, hence the term "idiopathic". It is a chronic, long-term condition, and there is currently no cure, though treatments can help slow its progression.





**Phosphodiesterase-4-Hemmer** (auch **Phosphodiesterase-IV-Hemmer**, PDE-4-Hemmer) sind Hemmstoffe, die das Enzym Phosphodiesterase IV hemmen. Die Phosphodiesterase IV baut den second Messenger cAMP ab. PDE-4-Hemmer **erhöhen daher die Konzentration von cAMP im Zytosol**. Das Enzym kommt unter anderem in der Lunge und im Gehirn vor.

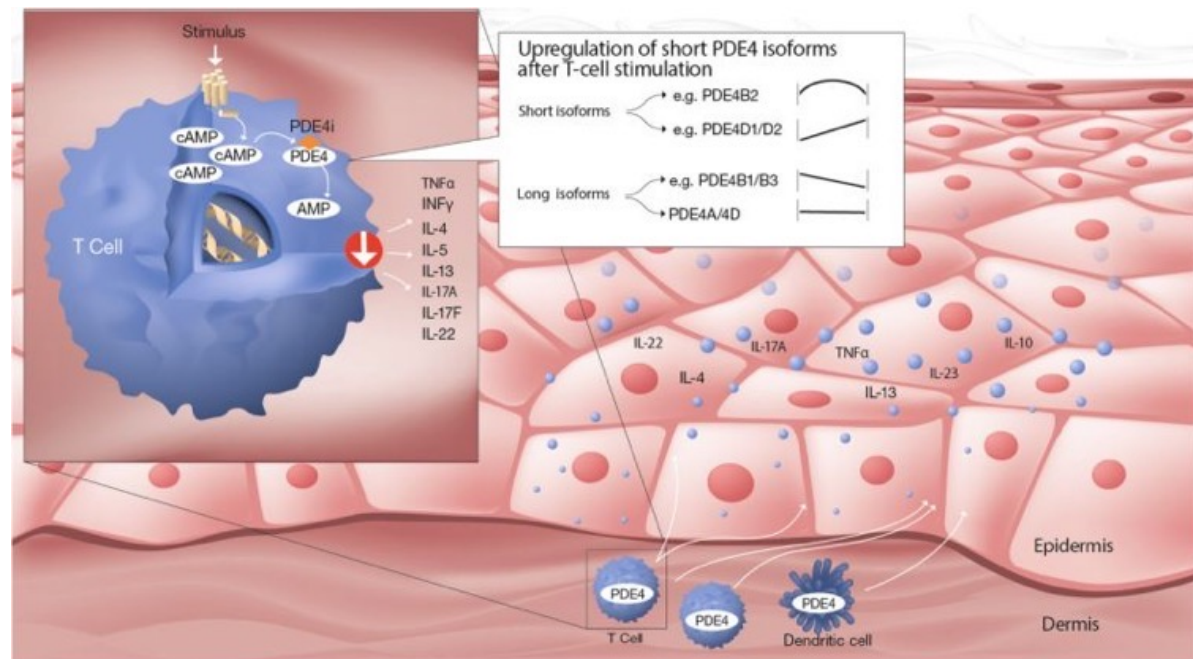
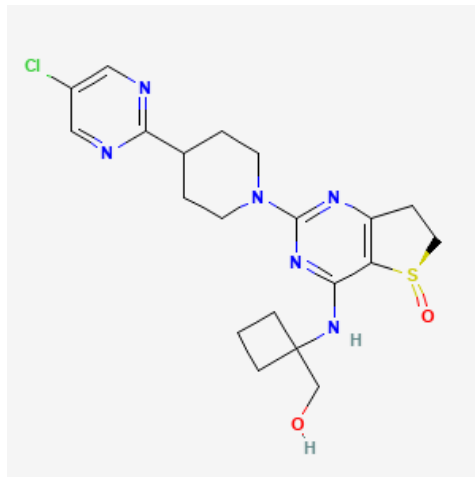
PDE-4-Hemmer wirken entzündungshemmend und wurden unter anderem in den Anwendungsgebieten **Chronisch obstruktive Lungenerkrankung (COPD), Asthma bronchiale, Depression und Multiple Sklerose untersucht**. Der Prototyp der Phosphodiesterase-4-Hemmer ist Rolipram. Rolipram bindet eine Aminosäure-Sequenz im katalytischen Zentrum der carboxyterminalen Proteindomäne der PDE-4 und wirkt dadurch kompetitiv hemmend. In Zellen des Zentralnervensystems liegt die PDE-4 in einer Proteinfaltungsform mit hoher Bindungsaffinität für Rolipram vor, während die PDE in verschiedenen Immunzellen eine niedrigere Bindungsaffinität zu Rolipram aufweist.



**Phosphodiesterase 4b (PDE4B) does not catabolize cGMP.** PDE4B is a phosphodiesterase that has high specificity for hydrolyzing cyclic adenosine monophosphate (cAMP).

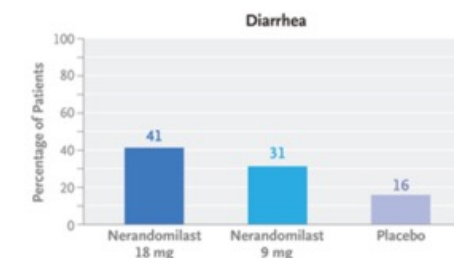
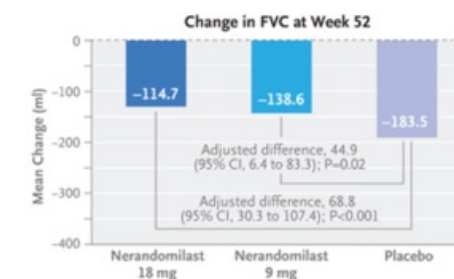
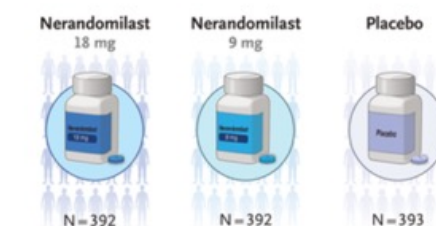
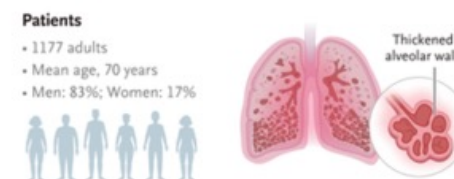
Exchange protein activated by cAMP (Epac) as a guanine nucleotide exchange factor for Rap GTPases has shed light on protein kinase A (PKA)-independent functions of cAMP signaling in neural tissues.

**Nerandomilast** ist ein experimenteller Arzneistoff, der als potenzieller Wirkstoff zur Behandlung von Lungenfibrose untersucht wird. Es ist ein oraler, **selektiver Inhibitor der Phosphodiesterase 4B (PDE4B)**, der antifibrotische und immunmodulierende Eigenschaften besitzt. Nerandomilast hat sich in Studien gezeigt, dass er das Fortschreiten der idiopathischen Lungenfibrose (IPF) verlangsamt.



## Nerandomilast in Patients with Idiopathic Pulmonary Fibrosis

Nerandomilast (BI 1015550) is an orally administered preferential inhibitor of phosphodiesterase 4B with antifibrotic and immunomodulatory effects. In a phase 2 trial involving patients with idiopathic pulmonary fibrosis, treatment with nerandomilast stabilized lung function over a period of 12 weeks. In this phase 3, double-blind trial, we randomly assigned patients with idiopathic pulmonary fibrosis in a 1:1:1 ratio to receive nerandomilast at a dose of 18 mg twice daily, nerandomilast at a dose of 9 mg twice daily, or placebo, with stratification according to background antifibrotic therapy (nintedanib or pirfenidone vs. none). The primary end point was the absolute change from baseline in forced vital capacity (FVC), measured in milliliters, at week 52.





Idiopathic pulmonary fibrosis (IPF) is a fibrosing interstitial lung disease characterized by progressive decline in lung function. The pathogenesis of IPF is thought to involve aberrant wound repair in response to alveolar injury, leading to a self-sustaining fibrotic process. Two antifibrotic drugs, nintedanib and pirfenidone, slow decline in lung function in patients with IPF and have become the standard of care. However, these drugs do not halt progression, and their gastrointestinal side effects often prevent treatment initiation or result in discontinuation. There remains a need for effective, well-tolerated drugs for IPF that can be used as monotherapy or in combination with other therapies to preserve lung function.

Nerandomilast (BI 1015550) is an orally administered preferential inhibitor of phosphodiesterase 4B. In preclinical models of lung fibrosis, nerandomilast showed antifibrotic and immunomodulatory effects. In a phase 2 trial involving 147 patients with IPF, nerandomilast at a dose of 18 mg twice daily stabilized lung function over a period of 12 weeks, with acceptable safety. We conducted the phase 3 FIBRONEER-IPF trial to investigate the efficacy and safety of nerandomilast at a dose of 9 mg twice daily or 18 mg twice daily, as monotherapy or with background antifibrotic therapy, in patients with IPF.

## **Patients**

The first patient was screened on October 6, 2022, and the last patient completed the week 52 visit on August 16, 2024. Eligible patients were 40 years of age or older and had IPF, a forced vital capacity (FVC) of at least 45% of the predicted value, and a diffusing capacity of the lungs for carbon monoxide (DLCO) of at least 25% of the predicted value. IPF was diagnosed by the investigator according to guidelines, on the basis of a high-resolution computed tomographic (CT) scan obtained no more than 12 months before screening.

## **Randomization and Follow-up**

Patients were randomly assigned in a 1:1:1 ratio to receive nerandomilast at a dose of 18 mg twice daily, nerandomilast at a dose of 9 mg twice daily, or placebo twice daily with the use of interactive response technology. Randomization was stratified according to use of background antifibrotic therapy (nintedanib or pirfenidone vs. none). Visits occurred at baseline; weeks 2, 6, 12, 18, 26, 36, 44, and 52; and every 12 weeks thereafter.

## **End Points**

The primary end point was the absolute change from baseline in FVC at week 52. Spirometry was performed with SpiroSphere (Clario) spirometers in accordance with the recommendations of the American Thoracic Society and European Respiratory Society. The key secondary end point was a first acute exacerbation, hospitalization for a respiratory cause, or death, assessed in a time-to-event analysis over the duration of the trial.

### Characteristics of the Patients at Baseline.

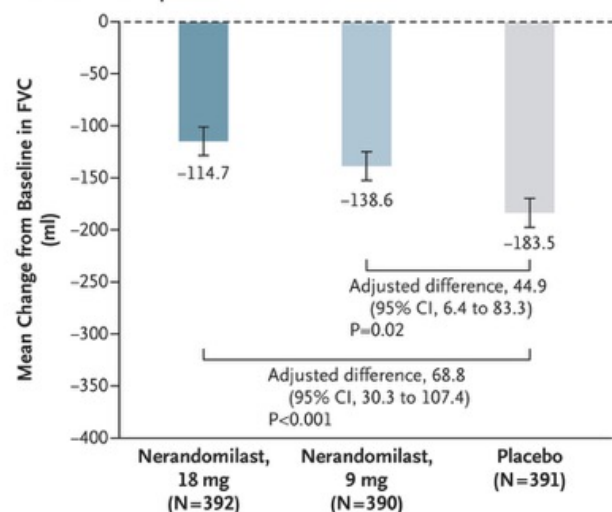
Characteristic	Nerandomilast, 18 mg (N = 392)	Nerandomilast, 9 mg (N = 392)	Placebo (N = 393)
Male sex — no. (%)	323 (82.4)	317 (80.9)	337 (85.8)
Age — yr	70.3±7.8	70.5±7.8	69.9±7.5
Weight — kg	76.3±14.0	76.1±15.8	77.5±14.5
Smoking status — no. (%)			
Never smoked	109 (27.8)	119 (30.4)	113 (28.8)
Former smoker	272 (69.4)	263 (67.1)	275 (70.0)
Current smoker	11 (2.8)	10 (2.6)	5 (1.3)
Time since diagnosis of IPF — yr	3.6±2.8	3.5±2.6	3.5±2.7
FVC			
Mean value — ml	2827±758	2837±781	2864±805
Percentage of predicted value	78.4±16.8	79.0±16.7	77.3±18.3
DLco — percentage of predicted value†	51.5±17.5	51.7±15.5	49.4±15.8
Background antifibrotic treatment — no. (%)			
Nintedanib	178 (45.4)	184 (46.9)	173 (44.0)
Pirfenidone	127 (32.4)	120 (30.6)	133 (33.8)
None	87 (22.2)	88 (22.4)	87 (22.1)
Supplemental oxygen therapy — no. (%)	90 (23.0)	68 (17.3)	90 (22.9)



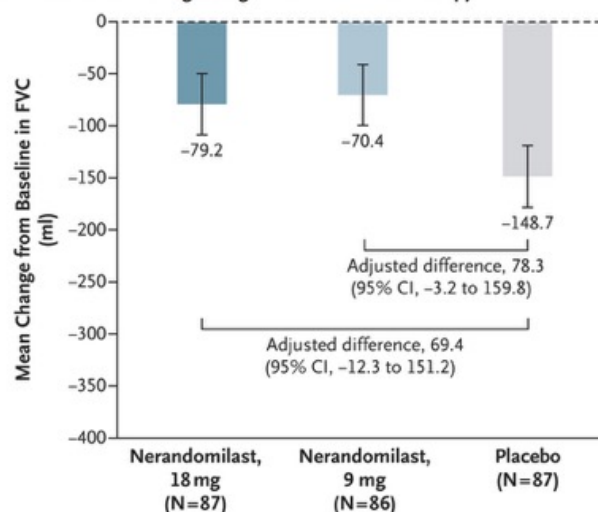
## Time-to-Event End Points up to First Database Lock.

End Point	Nerandomilast, 18 mg (N=392)	Nerandomilast, 9 mg (N=392)	Placebo (N=393)	Hazard Ratio (95% CI)	
	<i>number with event (percent)</i>			Nerandomilast, 18 mg, vs. Placebo	Nerandomilast, 9 mg, vs. Placebo
Key secondary end point					
First acute exacerbation, hospitalization for a respiratory cause, or death	85 (21.7)	79 (20.2)	80 (20.4)	1.17 (0.86–1.59)†	1.03 (0.75–1.41)‡
Other secondary end points					
Acute exacerbation or death	50 (12.8)	51 (13.0)	49 (12.5)	1.11 (0.75–1.65)	1.12 (0.76–1.67)
Hospitalization for a respiratory cause or death	75 (19.1)	68 (17.3)	73 (18.6)	1.13 (0.82–1.56)	0.98 (0.70–1.36)
Death	21 (5.4)	26 (6.6)	28 (7.1)	0.81 (0.46–1.43)	1.03 (0.60–1.76)
Absolute decline in percentage of predicted value of FVC of >10 percentage points from baseline or death	94 (24.0)	107 (27.3)	111 (28.2)	0.84 (0.64–1.10)	0.96 (0.74–1.25)
Absolute decline in percentage of predicted value of DLco of >15 percentage points from baseline or death	59 (15.1)	59 (15.1)	66 (16.8)	0.88 (0.62–1.26)	0.98 (0.69–1.41)

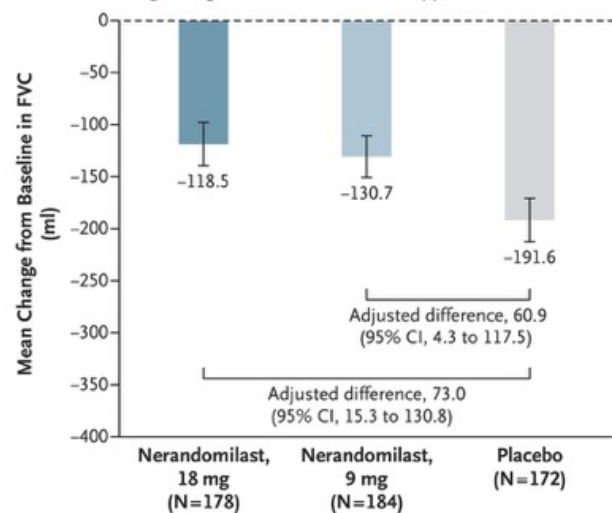
**A Overall Trial Population**



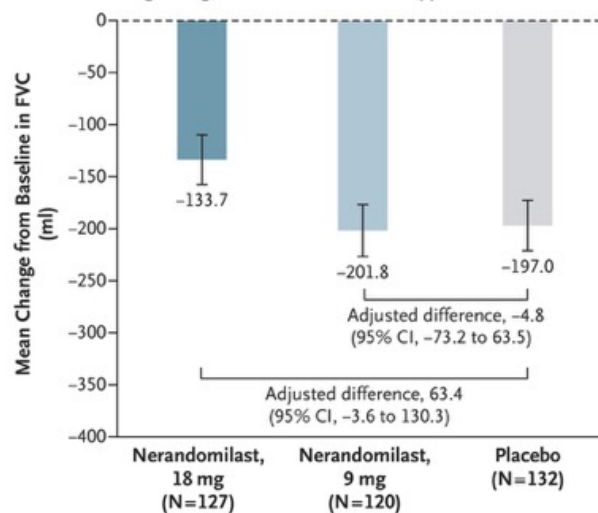
**B Patients Not Taking Background Antifibrotic Therapy**



**C Patients Taking Background Nintedanib Therapy**



**D Patients Taking Background Pirfenidone Therapy**



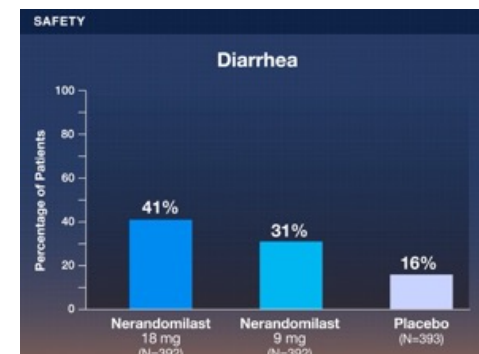
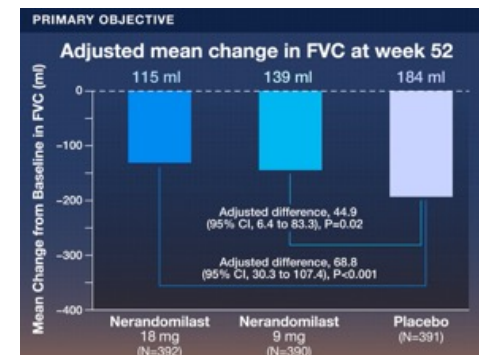
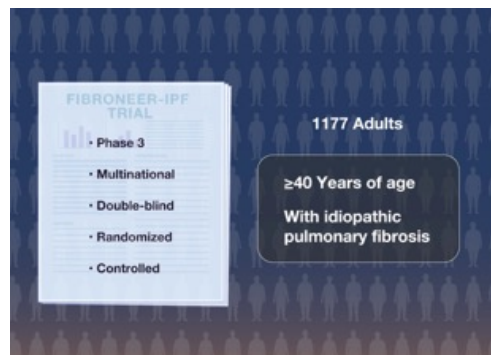
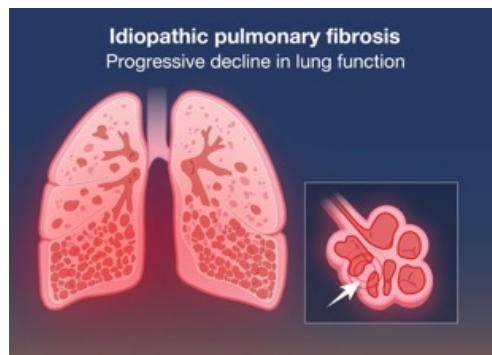
## Change from Baseline in Forced Vital Capacity at Week 52.

Patients were randomly assigned in a 1:1:1 ratio to receive nerandomilast at a dose of 18 mg twice daily, nerandomilast at a dose of 9 mg twice daily, or placebo twice daily. I bars indicate standard errors.

## Adverse Events over a Period of 52 Weeks.

Event Category	All Patients		No Background Antifibrotic Therapy				Background Nintedanib Therapy			Background Pirfenidone Therapy		
			Placebo (N=393)			Placebo (N=87)			Placebo (N=173)			Placebo (N=133)
	Nerandomilast			Nerandomilast			Nerandomilast			Nerandomilast		
	18 mg (N=392)	9 mg (N=392)		18 mg (N=87)	9 mg (N=88)		18 mg (N=178)	9 mg (N=184)		18 mg (N=127)	9 mg (N=120)	
number of patients (percent)												
Any event	372 (95)	364 (93)	371 (94)	79 (91)	77 (88)	83 (95)	174 (98)	175 (95)	163 (94)	119 (94)	112 (93)	125 (94)
Most frequent events†												
Diarrhea	162 (41)	122 (31)	63 (16)	23 (26)	15 (17)	7 (8)	110 (62)	91 (49)	46 (27)	29 (23)	16 (13)	10 (8)
Cough	55 (14)	65 (17)	65 (17)	9 (10)	12 (14)	4 (5)	21 (12)	28 (15)	31 (18)	25 (20)	25 (21)	30 (23)
Covid-19	51 (13)	59 (15)	45 (11)	14 (16)	8 (9)	5 (6)	17 (10)	30 (16)	21 (12)	20 (16)	21 (18)	19 (14)
URT infection	49 (12)	39 (10)	40 (10)	13 (15)	10 (11)	8 (9)	24 (13)	17 (9)	14 (8)	12 (9)	12 (10)	18 (14)
Dyspnea	35 (9)	39 (10)	50 (13)	6 (7)	2 (2)	12 (14)	14 (8)	21 (11)	23 (13)	15 (12)	16 (13)	15 (11)
Nasopharyngitis	35 (9)	40 (10)	44 (11)	8 (9)	9 (10)	12 (14)	17 (10)	19 (10)	19 (11)	10 (8)	12 (10)	13 (10)
Condition aggravated	38 (10)	32 (8)	40 (10)	7 (8)	3 (3)	10 (11)	18 (10)	16 (9)	17 (10)	13 (10)	13 (11)	13 (10)
Weight decreased	40 (10)	35 (9)	30 (8)	6 (7)	1 (1)	5 (6)	28 (16)	24 (13)	19 (11)	6 (5)	10 (8)	6 (5)
Events leading to discontinuation of trial regimen												
Any	55 (14)	46 (12)	42 (11)	6 (7)	7 (8)	7 (8)	38 (21)	31 (17)	22 (13)	11 (9)	8 (7)	13 (10)
Diarrhea	24 (6)	7 (2)	2 (1)	1 (1)	0	0	23 (13)	4 (2)	2 (1)	0	3 (2)	0
Event leading to interruption of trial regimen	76 (19)	72 (18)	56 (14)	11 (13)	12 (14)	13 (15)	48 (27)	45 (24)	21 (12)	17 (13)	15 (12)	22 (17)
Serious events‡												
Any	117 (30)	121 (31)	131 (33)	20 (23)	22 (25)	28 (32)	56 (31)	62 (34)	50 (29)	41 (32)	37 (31)	53 (40)
Fatal event	6 (2)	16 (4)	18 (5)	0	3 (3)	7 (8)	4 (2)	9 (5)	5 (3)	2 (2)	4 (3)	6 (5)

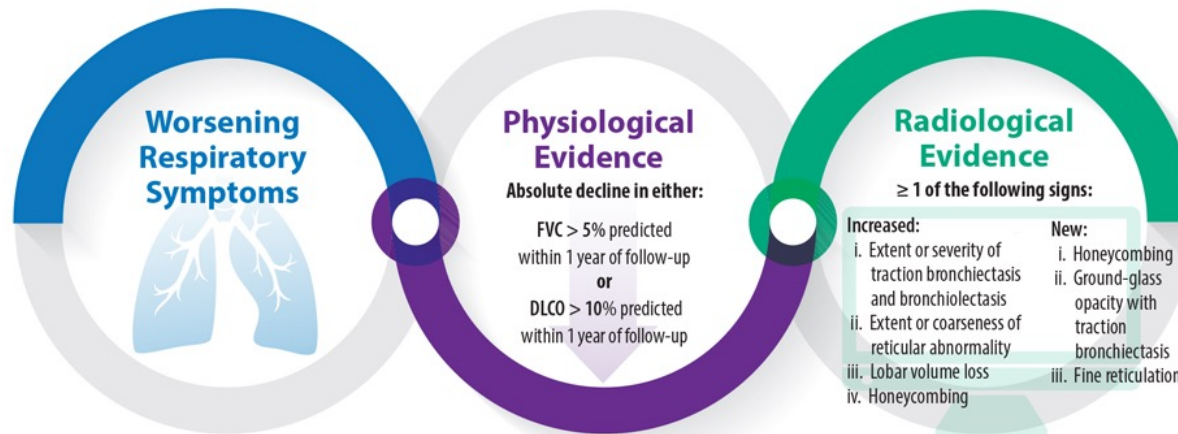




Progressive pulmonary fibrosis (PF) is a condition where lung scarring (fibrosis) worsens over time, leading to difficulty breathing and other complications. It can be a life-threatening disease with a high mortality rate and low quality of life, particularly in advanced stages. Idiopathic Pulmonary Fibrosis (IPF) is a specific type of progressive fibrosing interstitial lung disease (ILD) where the cause is unknown. Progressive Pulmonary Fibrosis (PPF) is a broader term referring to progressive ILD with fibrosis, but not specifically IPF. Essentially, PPF can include IPF, but also other forms of ILD that exhibit progressive fibrosis.

#### New Definition for PPF<sup>1</sup>

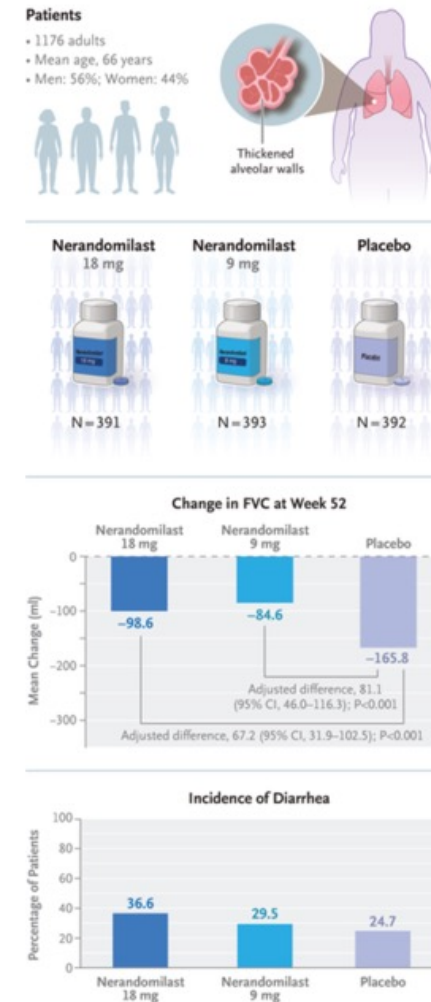
In 2022, the American Thoracic Society established a new definition for PPF, formerly referred to as progressive fibrosing interstitial lung disease.<sup>1,4</sup> Patients with ILD with radiological evidence of pulmonary fibrosis meet the criteria for PPF if they have at least 2 of the following findings with no alternative known cause:



# Nerandomilast in Patients with Progressive Pulmonary Fibrosis

Nerandomilast (BI 1015550) is an orally administered preferential inhibitor of phosphodiesterase 4B with antifibrotic and immunomodulatory properties.

Nerandomilast has been shown to slow the progression of idiopathic pulmonary fibrosis, but an assessment of its effects in other types of progressive pulmonary fibrosis is needed. In a phase 3, double-blind trial, we randomly assigned patients with progressive pulmonary fibrosis in a 1:1:1 ratio to receive nerandomilast at a dose of 18 mg twice daily, nerandomilast at a dose of 9 mg twice daily, or placebo, with stratification according to background therapy (nintedanib vs. none) and fibrotic pattern on high-resolution computed tomography (usual interstitial pneumonia-like pattern vs. other patterns). The primary end point was the absolute change from baseline in the forced vital capacity (FVC), measured in milliliters, at week 52.





Interstitial lung diseases (ILDs) are disorders characterized by inflammation, fibrosis, or both of the alveolar interstitium. The term progressive pulmonary fibrosis is used to describe a progressive disease course in persons with a fibrosing ILD other than idiopathic pulmonary fibrosis (IPF). The only approved therapy for progressive pulmonary fibrosis is nintedanib, which slows the decline in the forced vital capacity (FVC) but is associated with a gastrointestinal side-effect profile that often leads to treatment discontinuation or deters treatment initiation. Many patients with progressive pulmonary fibrosis are not receiving a therapy that has proven efficacy in slowing disease progression.

Nerandomilast (BI 1015550) is an orally administered preferential inhibitor of phosphodiesterase 4B (PDE4B). In preclinical models of lung fibrosis, nerandomilast showed antifibrotic and immunomodulatory effects. After a phase 2 trial of nerandomilast, the phase 3 FIBRONEER-IPF trial showed that treatment with nerandomilast at a dose of 18 mg twice daily or 9 mg twice daily resulted in a smaller decline in the FVC than placebo over a period of 52 weeks in patients with IPF, with acceptable adverse-event and safety profiles. We conducted the phase 3 FIBRONEER-ILD trial to investigate the efficacy and safety of nerandomilast at a dose of 18 mg twice daily or 9 mg twice daily in patients with progressive pulmonary fibrosis.

## **Patients**

The first patient was screened on November 16, 2022, and the last patient completed the week 52 visit on December 18, 2024. Eligible patients were 18 years or older with a diagnosis of ILD other than IPF and a fibrotic lung disease extent of more than 10% on the basis of a high-resolution computed tomographic (CT) scan obtained no more than 12 months before screening and confirmed by central review. Patients had an FVC of least 45% of the predicted value and a diffusion capacity of the lungs for carbon monoxide (DLCO) of at least 25% of the predicted value.

## **Randomization and Follow-up**

Patients were randomly assigned in a 1:1:1 ratio to receive nerandomilast at a dose of 18 mg twice daily, nerandomilast at a dose of 9 mg twice daily, or placebo twice daily with the use of interactive response technology.

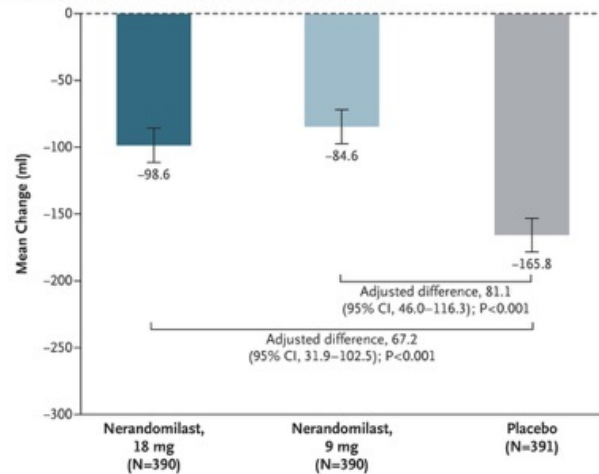
## **End Points**

The primary end point was the absolute change from baseline in the FVC at week 52. Spirometry was conducted with the use of SpiroSphere (Clario) spirometers in accordance with recommendations of the American Thoracic Society and European Respiratory Society. The key secondary end point was a first acute exacerbation of ILD, hospitalization for a respiratory cause, or death as assessed in a time-to-event analysis over the duration of the trial. An acute exacerbation of ILD was defined in accordance with published criteria for an acute exacerbation of IPF.

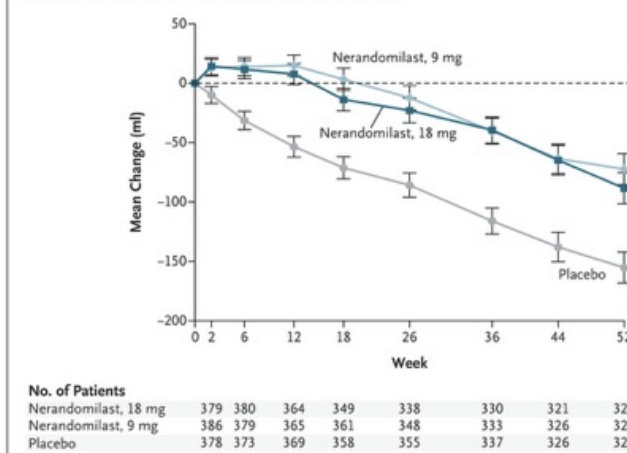
## Characteristics of the Patients at Baseline.

Characteristic	Nerandomilast, 18 mg (N = 391)	Nerandomilast, 9 mg (N = 393)	Placebo (N = 392)
Male sex — no. (%)	220 (56.3)	203 (51.7)	231 (58.9)
Age — yr	66.0±9.8	66.5±9.8	66.6±10.3
Weight — kg	73.2±17.1	72.1±17.5	73.4±17.9
Smoking status — no. (%)			
Never smoked	191 (48.8)	200 (50.9)	186 (47.4)
Former smoker	189 (48.3)	186 (47.3)	200 (51.0)
Current smoker	11 (2.8)	7 (1.8)	6 (1.5)
Time since diagnosis of ILD — yr	4.6±4.8	4.1±4.3	3.9±3.6
FVC			
Mean value — ml	2381±723	2326±768	2354±766
Percentage of predicted value	70.4±15.5	70.3±15.7	69.7±16.2
Percentage of predicted DLco†	49.4±17.5	48.7±16.8	49.7±16.5
Background nintedanib therapy — no. (%)‡	171 (43.7)	173 (44.0)	170 (43.4)
UIP or UIP-like fibrotic pattern on high-resolution CT — no. (%)	275 (70.3)	290 (73.8)	275 (70.2)
ILD diagnosis			
Autoimmune ILD	113 (28.9)	112 (28.5)	100 (25.5)
Hypersensitivity pneumonitis	73 (18.7)	83 (21.1)	77 (19.6)
Unclassifiable idiopathic interstitial pneumonia	73 (18.7)	76 (19.3)	82 (20.9)
Idiopathic nonspecific interstitial pneumonia	82 (21.0)	73 (18.6)	73 (18.6)
Other ILD	50 (12.8)	49 (12.5)	60 (15.3)
Supplemental oxygen therapy — no. (%)§	117 (29.9)	97 (24.7)	110 (28.1)

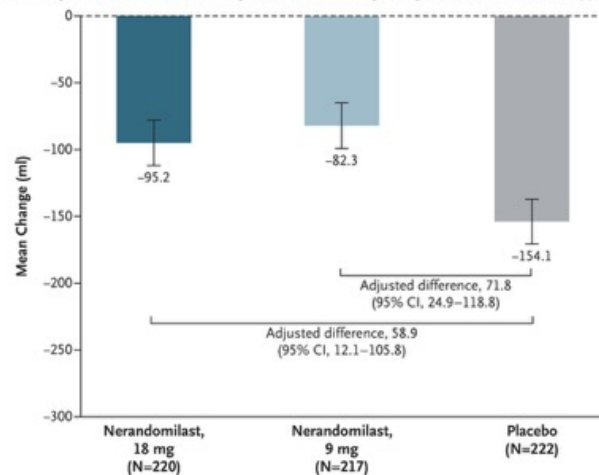
**A** Change in FVC at Week 52 in the Overall Trial Population



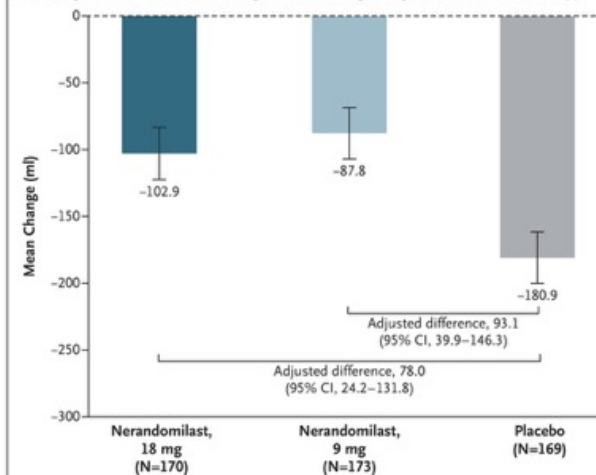
**B** Change in FVC over Time in the Overall Trial Population



**C** Change in FVC at Week 52 among Patients Not Taking Background Nintedanib Therapy



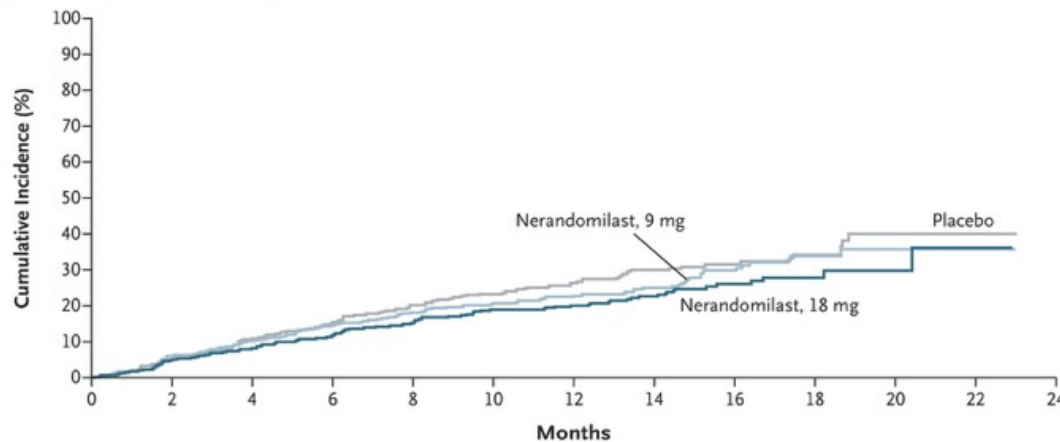
**D** Change in FVC at Week 52 among Patients Taking Background Nintedanib Therapy



**Changes from Baseline to Week 52 in the Forced Vital Capacity (FVC).**

Patients were randomly assigned in a 1:1:1 ratio to receive nerandomilast at a dose of 18 mg twice daily, nerandomilast at a dose of 9 mg twice daily, or placebo twice daily. Two patients included in the group taking background nintedanib therapy received pirfenidone rather than nintedanib and were classified as having protocol deviations. I bars indicate standard errors.

**A Time to a First Key Secondary End-Point Event up to First Database Lock**



**B Analyses of Key Secondary End Point and Related Secondary End Points up to First Database Lock**

End Point	Nerandomilast no. with event/no. of patients	Placebo no. with event/no. of patients	Hazard Ratio (95% CI)	P Value
<b>Key secondary end point</b>				
Nerandomilast, 18 mg	95/391	122/392	0.77 (0.59–1.01)	0.06
Nerandomilast, 9 mg	110/393	122/392	0.88 (0.68–1.14)	0.34
<b>Acute exacerbation of ILD or death</b>				
Nerandomilast, 18 mg	48/391	83/392	0.59 (0.41–0.84)	
Nerandomilast, 9 mg	65/393	83/392	0.78 (0.56–1.08)	
<b>Hospitalization for respiratory cause or death</b>				
Nerandomilast, 18 mg	84/391	110/392	0.75 (0.56–1.00)	
Nerandomilast, 9 mg	97/393	110/392	0.83 (0.63–1.10)	
<b>Death</b>				
Nerandomilast, 18 mg	24/391	50/392	0.48 (0.30–0.79)	
Nerandomilast, 9 mg	33/393	50/392	0.60 (0.38–0.95)	

Key Secondary End Point and Related Secondary End Points.


The key secondary end point was a first acute exacerbation of ILD, hospitalization for a respiratory cause, or death as assessed in a time-to-event analysis over the duration of the trial. Nerandomilast was administered at a dose of 18 mg twice daily or 9 mg twice daily. The first database lock took place after the last patient had completed the week 52 visit.



## Adverse Events over a Period of 52 Weeks.

Event Category	All Patients			No Background Nintedanib Therapy			Background Nintedanib Therapy†		
	Nerandomilast		Placebo	Nerandomilast		Placebo	Nerandomilast		Placebo
	18 mg (N=391)	9 mg (N=393)	(N=392)	18 mg (N=220)	9 mg (N=220)	(N=222)	18 mg (N=171)	9 mg (N=173)	(N=170)
	<i>number of patients (percent)</i>								
Any event	362 (92.6)	362 (92.1)	360 (91.8)	202 (91.8)	200 (90.9)	202 (91.0)	160 (93.6)	162 (93.6)	158 (92.9)
Most frequent events‡									
Diarrhea	143 (36.6)	116 (29.5)	97 (24.7)	59 (26.8)	33 (15.0)	35 (15.8)	84 (49.1)	83 (48.0)	62 (36.5)
Cough	58 (14.8)	49 (12.5)	55 (14.0)	35 (15.9)	24 (10.9)	31 (14.0)	23 (13.5)	25 (14.5)	24 (14.1)
URT infection	46 (11.8)	39 (9.9)	60 (15.3)	31 (14.1)	26 (11.8)	44 (19.8)	15 (8.8)	13 (7.5)	16 (9.4)
Covid-19	42 (10.7)	41 (10.4)	58 (14.8)	26 (11.8)	20 (9.1)	27 (12.2)	16 (9.4)	21 (12.1)	31 (18.2)
Condition aggravated	28 (7.2)	46 (11.7)	57 (14.5)	12 (5.5)	24 (10.9)	34 (15.3)	16 (9.4)	22 (12.7)	23 (13.5)
Depression	40 (10.2)	38 (9.7)	44 (11.2)	23 (10.5)	21 (9.5)	24 (10.8)	17 (9.9)	17 (9.8)	20 (11.8)
Nasopharyngitis	34 (8.7)	45 (11.5)	39 (9.9)	16 (7.3)	21 (9.5)	18 (8.1)	18 (10.5)	24 (13.9)	21 (12.4)
Anxiety	37 (9.5)	40 (10.2)	37 (9.4)	22 (10.0)	20 (9.1)	20 (9.0)	15 (8.8)	20 (11.6)	17 (10.0)
Nausea	40 (10.2)	30 (7.6)	26 (6.6)	13 (5.9)	9 (4.1)	8 (3.6)	27 (15.8)	21 (12.1)	18 (10.6)
Weight decreased	42 (10.7)	27 (6.9)	23 (5.9)	23 (10.5)	11 (5.0)	9 (4.1)	19 (11.1)	16 (9.2)	14 (8.2)
Event leading to discontinua- tion of trial regimen									
Any	39 (10.0)	32 (8.1)	40 (10.2)	19 (8.6)	16 (7.3)	23 (10.4)	20 (11.7)	16 (9.2)	17 (10.0)
Diarrhea	10 (2.6)	5 (1.3)	2 (0.5)	3 (1.4)	0	0	7 (4.1)	5 (2.9)	2 (1.2)
Event leading to interruption of trial regimen	69 (17.6)	68 (17.3)	59 (15.1)	28 (12.7)	31 (14.1)	30 (13.5)	41 (24.0)	37 (21.4)	29 (17.1)
Serious events§									
Any	130 (33.2)	125 (31.8)	138 (35.2)	65 (29.5)	68 (30.9)	82 (36.9)	65 (38.0)	57 (32.9)	56 (32.9)
Fatal event	8 (2.0)	14 (3.6)	20 (5.1)	5 (2.3)	10 (4.5)	11 (5.0)	3 (1.8)	4 (2.3)	9 (5.3)

### Progressive Pulmonary Fibrosis

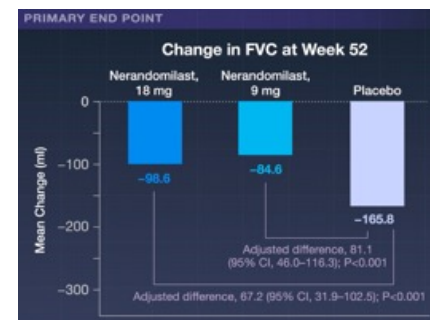


- Slows progression
- Often discontinued because of gastrointestinal events

### FIBRONEER-ILD Trial

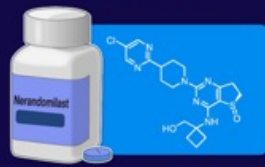
- Phase 3
- Double-blind
- Randomized
- Placebo-controlled

1176 patients with progressive pulmonary fibrosis






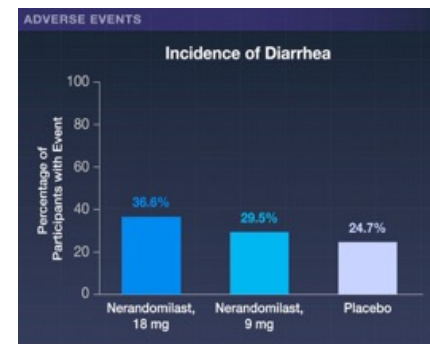
### Progressive Pulmonary Fibrosis

#### Nerandomilast



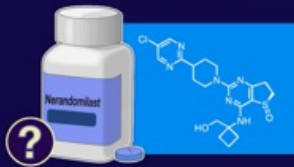
- Effective for idiopathic pulmonary fibrosis

Nerandomilast 18 mg Twice daily	Nerandomilast 9 mg Twice daily	Placebo Twice daily
		
N=391	N=393	N=392






### Progressive Pulmonary Fibrosis

#### Nerandomilast




- Effective for idiopathic pulmonary fibrosis
- Data lacking for progressive pulmonary fibrosis

Nerandomilast 18 mg Twice daily	Nerandomilast 9 mg Twice daily	Placebo Twice daily
		
Approximately 44% received background nintedanib		
N=391	N=393	N=392

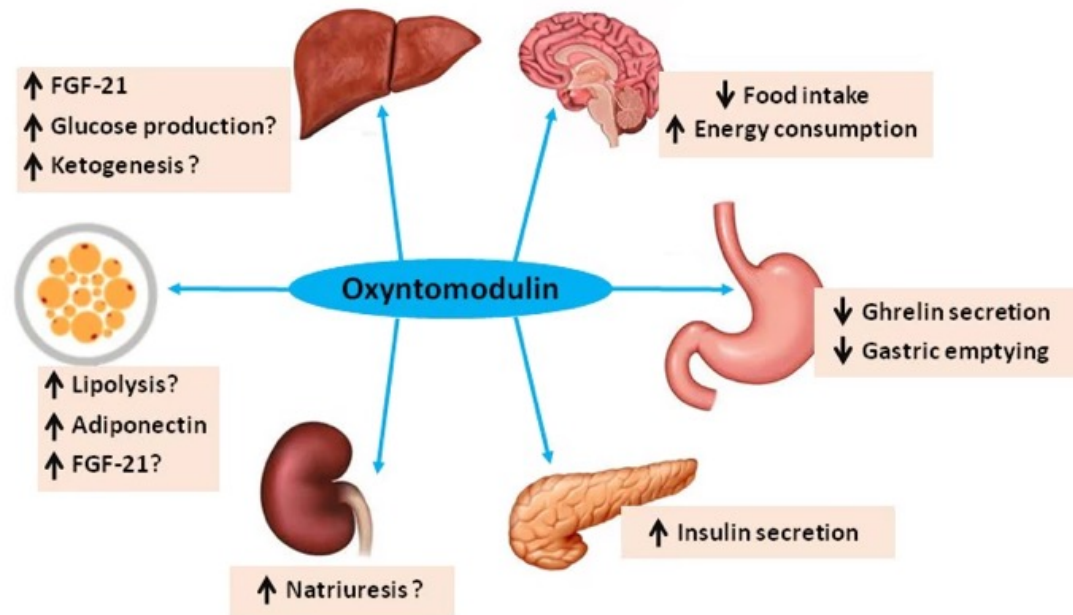
### Progressive Pulmonary Fibrosis

#### Nerandomilast 9 mg or 18 mg twice daily




✓ Reduced the decline in FVC over 52 weeks

Oxyntomodulin, kurz OXM, ist ein Peptidhormon, das eine wichtige, aber noch nicht völlig verstandene Rolle bei der Regulation des Hunger- und Sättigungsgefühls des Menschen spielt. Es wird im Ileum und im Colon von enteroendokrinen L-Zellen gebildet. Oxyntomodulin ist ein Polypeptid aus 37 Aminosäuren. Es bindet an den GLP-1- und Glukagonrezeptoren und unterdrückt Hungergefühle. Wird es vor den Mahlzeiten injiziert, führt es zu einem Gewichtsverlust.




Mazdutid ist ein dualer Agonist, der sowohl am GLP-1-Rezeptor als auch am Glucagon-Rezeptor wirkt. Er wird von Eli Lilly entwickelt und ist ein Analogon des Oxyntomodulins (OXM). Mazdutid ist derzeit in mehreren Phase-III-Studien im Bereich der Behandlung von Übergewicht und Diabetes Typ 2 im Fokus.



**Mazdutide vs  
Tirzepatide for  
Weight Loss:**

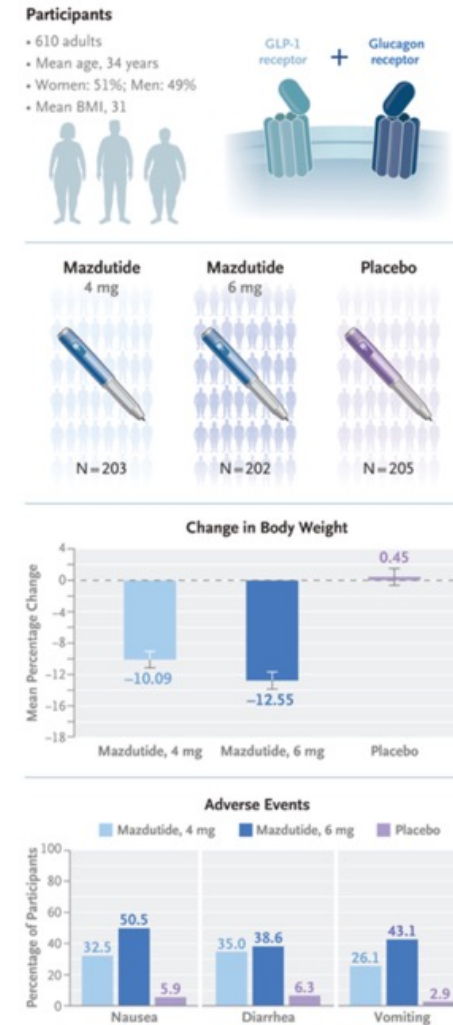
Which One Works Better

[www.ivdrips.com](http://www.ivdrips.com)



# Once-Weekly Mazdutide in Chinese Adults with Obesity or Overweight

Evidence suggests that incretin-based dual agonist pharmacotherapy is helpful in persons with obesity. Mazdutide, a glucagon-like peptide-1 and glucagon receptor dual agonist, may have efficacy in persons with overweight or obesity. In a phase 3, double-blind, placebo-controlled trial in China, we randomly assigned, in a 1:1:1 ratio, adults 18 to 75 years of age who had a body-mass index (BMI; the weight in kilograms divided by the square of the height in meters) of at least 28 or had a BMI of 24 to less than 28 plus at least one weight-related coexisting condition to receive 4 mg of mazdutide, 6 mg of mazdutide, or placebo for 48 weeks. The two primary end points were the percentage change in body weight from baseline and a weight reduction of at least 5% at week 32, as assessed in a treatment-policy estimand analysis (which assessed effects regardless of early discontinuation of mazdutide or placebo and the initiation of new antiobesity therapies).





Obesity is a growing worldwide pandemic. According to Chinese criteria, approximately half the population in China lives with overweight (defined as a body-mass index [BMI; the weight in kilograms divided by the square of the height in meters] of 24 to <28) or obesity (BMI,  $\geq 28$ ). Obesity and overweight are well-recognized risk factors for a wide range of diseases, among which metabolic dysfunction–associated fatty liver disease (MAFLD), dyslipidemia, hypertension, and prediabetes have been most common in China.

Mazdutide (also known as IBI362 or LY3305677), a synthetic peptide analogue of mammalian oxyntomodulin, is a once-weekly GLP-1 and glucagon receptor dual agonist being developed for the treatment of obesity and type 2 diabetes. In phase 2 trials, mazdutide treatment in doses of up to 6 mg led to a marked reduction in body weight in Chinese adults with obesity or overweight and to both effective glycemic control and weight reduction in Chinese patients with type 2 diabetes.

### **Participants**

Adult participants 18 to 75 years of age who had obesity or had overweight accompanied by at least one weight-related coexisting condition (prediabetes, hypertension, dyslipidemia, MAFLD, weight-bearing joint pain, obesity-related dyspnea, or obstructive sleep apnea syndrome) were eligible.

### **End Points and Assessments**

The two primary end points were the percentage change in body weight from baseline to week 32 and a weight reduction of at least 5% by week 32.

## Demographic and Clinical Characteristics of the Participants

Characteristic	Mazdutide, 4 mg (N = 203)	Mazdutide, 6 mg (N = 202)	Placebo (N = 205)	Overall (N = 610)
Age — yr	34.8±7.9	33.2±8.2	34.5±7.9	34.2±8.0
Male sex — no. (%)	101 (49.8)	99 (49.0)	99 (48.3)	299 (49.0)
Body weight — kg	87.9±14.8	87.2±14.1	86.5±13.0	87.2±13.9
Waist circumference — cm	101.7±10.0	101.7±10.1	101.1±9.4	101.5±9.8
Body-mass index	31.0±3.5	31.3±3.8	31.1±3.3	31.1±3.5
Body-mass index category at screening — no. (%)				
<28	31 (15.3)	34 (16.8)	38 (18.5)	103 (16.9)
≥28	172 (84.7)	168 (83.2)	167 (81.5)	507 (83.1)
Systolic blood pressure — mm Hg	122.0±11.4	122.2±12.0	122.8±12.1	122.3±11.8
Diastolic blood pressure — mm Hg	82.5±8.0	81.8±7.7	82.5±7.9	82.3±7.9
Triglycerides — mmol/liter	1.9±1.0	2.1±1.3	2.0±1.2	2.0±1.2
Total cholesterol — mmol/liter	4.7±0.8	4.8±0.9	4.9±0.9	4.8±0.9
LDL cholesterol — mmol/liter	3.2±0.7	3.2±0.7	3.2±0.7	3.2±0.7
Serum uric acid — μmol/liter	366.0±86.7	377.5±90.5	362.5±91.5	368.6±89.7
Alanine aminotransferase — U/liter	36.5±27.6	36.3±24.1	33.6±24.0	35.5±25.3

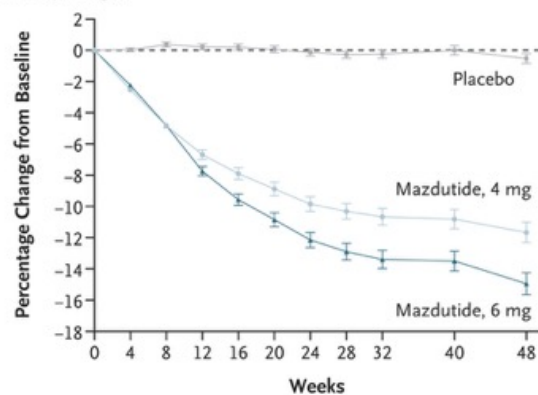
## Primary and Key Secondary End Points (Treatment-Policy Estimand Analysis).

Variable	Mazdutide, 4 mg (N=203)	Mazdutide, 6 mg (N=202)	Placebo (N=205)
No. of participants with body-weight and waist-circumference measures			
At wk 32	200	187	196
At wk 48	190	184	196
<b>Primary end points</b>			
Percentage change in body weight from baseline to wk 32 (95% CI)	-10.09 (-11.15 to -9.04)	-12.55 (-13.64 to -11.45)	0.45 (-0.61 to 1.52)
Difference vs. placebo (95% CI) — percentage points	-10.54 (-11.83 to -9.26)†	-13.00 (-14.31 to -11.70)†	—
Weight reduction of ≥5% at wk 32 (95% CI) — %‡	73.9 (67.8 to 79.9)	82.0 (76.7 to 87.4)	10.5 (6.2 to 14.7)
Relative rate vs. placebo (95% CI)	7.1 (4.6 to 11.0)†	7.9 (5.1 to 12.2)†	—
<b>Key secondary end points</b>			
Percentage change in body weight from baseline to wk 48 (95% CI) — %	-11.00 (-12.27 to -9.73)	-14.01 (-15.36 to -12.66)	0.30 (-0.98 to 1.58)
Difference vs. placebo (95% CI) — percentage points	-11.30 (-12.84 to -9.76)†	-14.31 (-15.88 to -12.74)†	—
Weight reduction of ≥10% at wk 32 (95% CI) — %	49.0 (42.1 to 55.9)	61.6 (54.8 to 68.5)	0.6 (-0.5 to 1.8)
Relative rate vs. placebo (95% CI)	81.7 (19.3 to 346.1)†	101.7 (24.1 to 429.2)†	—
Weight reduction of ≥15% at wk 32 (95% CI) — %‡	27.2 (21.0 to 33.3)	43.6 (36.6 to 50.6)	0.0 (0.0 to 1.8)
Relative rate vs. placebo (95% CI)	113.1 (88.7 to 144.1)†	178.5 (145.8 to 218.6)†	—
Weight reduction of ≥5% at wk 48 (95% CI) — %‡	71.6 (65.3 to 77.9)	81.6 (75.9 to 87.2)	10.8 (6.5 to 15.2)
Relative rate vs. placebo (95% CI)	6.7 (4.4 to 10.1)†	7.6 (5.1 to 11.3)†	—
Weight reduction of ≥10% at wk 48 (95% CI) — %‡	53.5 (46.6 to 60.4)	66.7 (60.0 to 73.4)	2.6 (0.4 to 4.8)
Relative rate vs. placebo (95% CI)	21.1 (7.6 to 58.2)†	26.1 (9.4 to 72.0)†	—
Weight reduction of ≥15% at wk 48 (95% CI) — %‡	35.7 (29.1 to 42.4)	49.5 (42.4 to 56.6)	2.0 (0.1 to 3.9)
Relative rate vs. placebo (95% CI)	18.5 (5.6 to 61.8)†	25.3 (7.6 to 84.0)†	—
Change in waist circumference from baseline to wk 32 (95% CI) — cm	-7.86 (-8.69 to -7.03)	-9.27 (-10.12 to -8.42)	-0.99 (-1.82 to -0.16)
Difference vs. placebo (95% CI)	-6.87 (-7.88 to -5.86)†	-8.28 (-9.30 to -7.25)†	—
Change in waist circumference from baseline to wk 48 (95% CI) — cm	-9.12 (-10.11 to -8.12)	-10.72 (-11.76 to -9.68)	-1.41 (-2.41 to -0.42)
Difference vs. placebo (95% CI)	-7.70 (-8.91 to -6.50)†	-9.31 (-10.54 to -8.08)†	—

**Key Secondary End Points in the Pooled Mazdutide Group, as Compared with Placebo (Treatment-Policy Estimand Analysis).**

Variable	Mazdutide, Pooled (N=405)	Placebo (N=205)	Difference
No. of participants with data at wk 48	374	196	—
Change from baseline to wk 48 (95% CI)			
Systolic blood pressure — mm Hg	−8.56 (−9.90 to −7.23)	−2.13 (−3.78 to −0.48)	−6.44 (−8.22 to −4.65)†
Triglycerides — mmol/liter	−0.65 (−0.77 to −0.54)	−0.16 (−0.28 to −0.03)	−0.50 (−0.64 to −0.36)†
Total cholesterol — mmol/liter	−0.28 (−0.38 to −0.18)	0.15 (0.04 to 0.27)	−0.43 (−0.56 to −0.31)†
LDL cholesterol — mmol/liter	−0.20 (−0.28 to −0.12)	0.10 (0.02 to 0.19)	−0.31 (−0.41 to −0.20)†
Serum uric acid — μmol/liter	−36.70 (−46.01 to −27.39)	7.91 (−2.76 to 18.58)	−44.61 (−56.56 to −32.65)†
Alanine aminotransferase — U/liter	−13.92 (−16.45 to −11.39)	−4.44 (−7.43 to −1.44)	−9.48 (−12.75 to −6.21)†

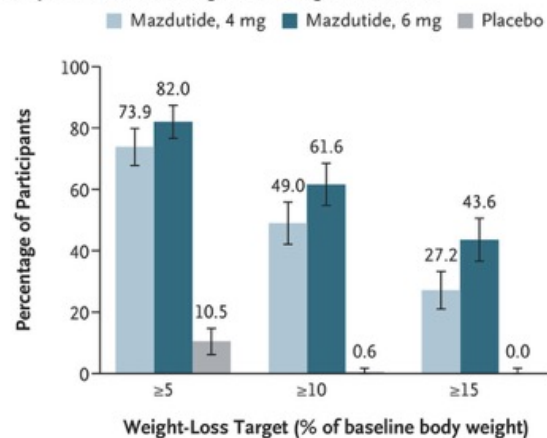
**A Change in Body Weight**



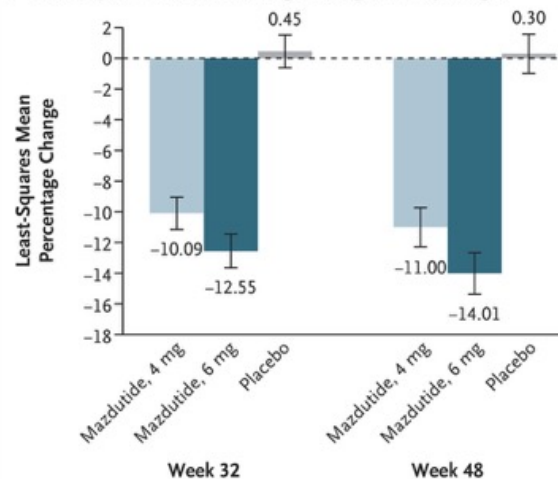
**No. of Participants**

Mazdutide, 4 mg	203	197	200	196	193	192	192	193	200	182	190
Mazdutide, 6 mg	202	190	193	186	186	184	186	185	187	179	184
Placebo	205	199	202	199	197	198	197	196	196	191	196

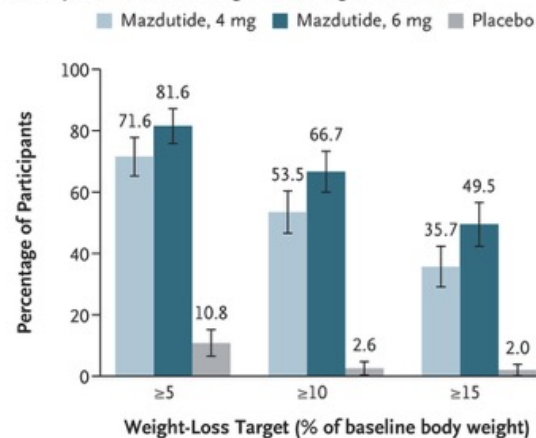
**C Participants Who Met Weight-Loss Target at Week 32**



**B Least-Squares Mean Percentage Change in Body Weight**



**D Participants Who Met Weight-Loss Target at Week 48**



### Effect of Mazdutide on Body Weight (Treatment-Policy Estimand Analysis).

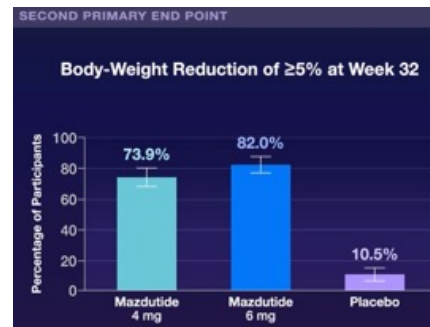
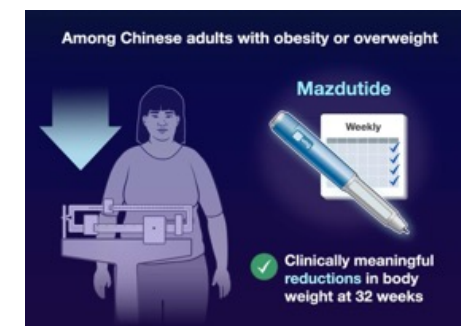
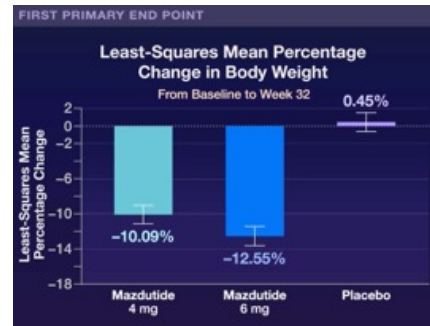
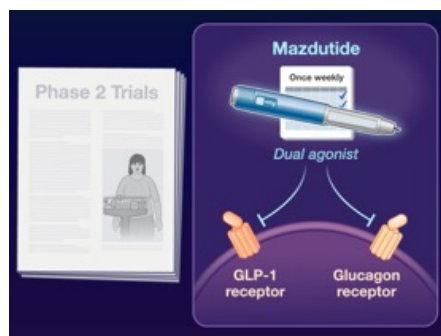
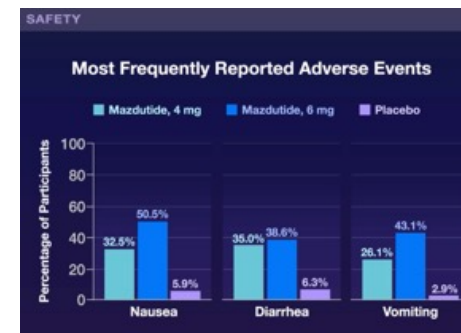
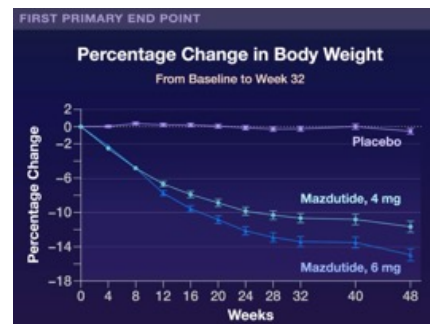
Panel A shows the mean percentage change in body weight over time; I bars indicate the standard error. The numbers of participants with body-weight measurements at various time points are shown. Panel B shows the least-squares mean percentage change in body weight from baseline to week 32 (first primary outcome) and week 48 according to an analysis of covariance. The percentage of participants who had weight reduction of at least 5% at week 32 was the second primary outcome.

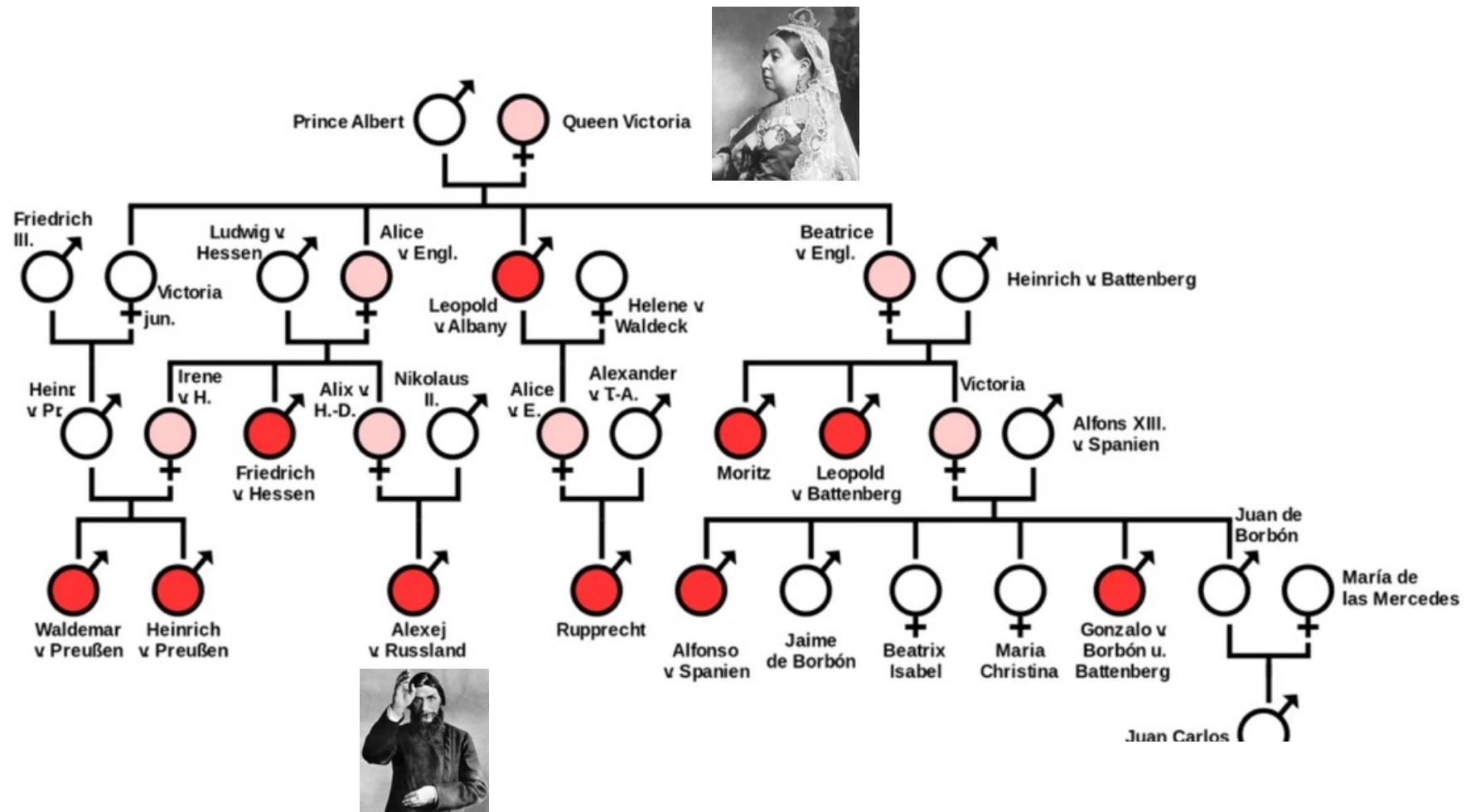
Panel C shows the percentages of participants who met specified weight-loss targets at week 32, and Panel D at week 48. The treatment-policy estimand was used to assess effects regardless of early discontinuation of mazdutide or placebo and the initiation of new antiobesity therapies. Percentages were calculated with the use of Rubin's rules by combining the percentages of participants who met the target in imputed data sets, from a logistic-regression model. In Panels B, C, and D, I bars indicate 95% confidence intervals.



## Adverse Events (Safety Population).

Event	Mazdutide, 4 mg (N = 203)	Mazdutide, 6 mg (N = 202)	Placebo (N = 205)
	<i>number (percent)</i>		
Any adverse event	195 (96.1)	196 (97.0)	183 (89.3)
Serious adverse event	12 (5.9)	8 (4.0)	13 (6.3)
Death	0	0	0
Adverse event leading to discontinuation of mazdutide or placebo	3 (1.5)	1 (0.5)	2 (1.0)
Adverse events occurring in ≥10% of participants in any group†			
Nausea	66 (32.5)	102 (50.5)	12 (5.9)
Diarrhea	71 (35.0)	78 (38.6)	13 (6.3)
Vomiting	53 (26.1)	87 (43.1)	6 (2.9)
Decreased appetite	70 (34.5)	58 (28.7)	10 (4.9)
Covid-19	39 (19.2)	50 (24.8)	40 (19.5)
Upper respiratory tract infection	42 (20.7)	45 (22.3)	41 (20.0)
Urinary tract infection	24 (11.8)	25 (12.4)	22 (10.7)
Hyperuricemia	20 (9.9)	22 (10.9)	42 (20.5)
Abdominal distention	13 (6.4)	28 (13.9)	4 (2.0)
Suspected Covid-19	21 (10.3)	14 (6.9)	27 (13.2)
Other adverse events of clinical interest			
Injection-site reaction‡	14 (6.9)	17 (8.4)	3 (1.5)
Allergic reaction§	6 (3.0)	9 (4.5)	3 (1.5)
Sinus tachycardia	4 (2.0)	9 (4.5)	6 (2.9)
Hypoglycemia	5 (2.5)	5 (2.5)	1 (0.5)
Acute cholecystitis	1 (0.5)	0	0
Cholecystitis	1 (0.5)	0	1 (0.5)
Cholelithiasis	2 (1.0)	3 (1.5)	0
Obstructive pancreatitis	1 (0.5)	0	0





# Sustained Clinical Benefit of AAV Gene Therapy in Severe Hemophilia B

## Background

Adeno-associated virus (AAV)–mediated gene therapy has emerged as a promising treatment for hemophilia B. **Data on safety and durability from 13 years of follow-up in a cohort of patients who had been successfully treated with scAAV2/8-LP1-hFIXco gene therapy are now available.**

## Methods

Ten men with severe hemophilia B received a single intravenous infusion of the scAAV2/8-LP1-hFIXco vector in one of three dose groups (low-dose:  $2 \times 10^{11}$  vector genomes [vg] per kilogram of body weight [in two participants]; intermediate-dose:  $6 \times 10^{11}$  vg per kilogram [in two]; or high-dose:  $2 \times 10^{12}$  vg per kilogram [in six]). Efficacy outcomes included factor IX activity, the annualized bleeding rate, and factor IX concentrate use. Safety assessments included clinical events, liver function, and imaging.

## Conclusions

**A single administration of scAAV2/8-LP1-hFIXco gene therapy resulted in durable factor IX expression, sustained clinical benefit, and no late-onset safety concerns over a period of 13 years.** These data support the long-term efficacy and safety of AAV gene therapy for severe hemophilia B. (Funded by the U.K. Medical Research Council and others.

In 2014, we reported successful gene therapy in patients with severe hemophilia B who had received a single intravenous infusion of a self-complementary, serotype 8 pseudotyped adeno-associated virus (AAV) vector encoding a codon-optimized factor IX transgene (scAAV2/8-LP1-hFIXco). We found that glucocorticoids effectively suppressed immune responses against AAV-transduced hepatocytes, preserving levels of transgenic factor IX. Subsequent studies by other investigators, including those using the Padua gain-of-function factor IX variant, validated these findings, which paved the way for the conditional marketing authorization of the gene therapies etranacogene dezaparvovec (Hemgenix) and fidanacogene elaparvovec (Beqvez) in adults with severe hemophilia. These market-approved therapies result in higher factor IX activity levels than a vector with the wild-type factor IX variant but in similar levels of factor IX protein.

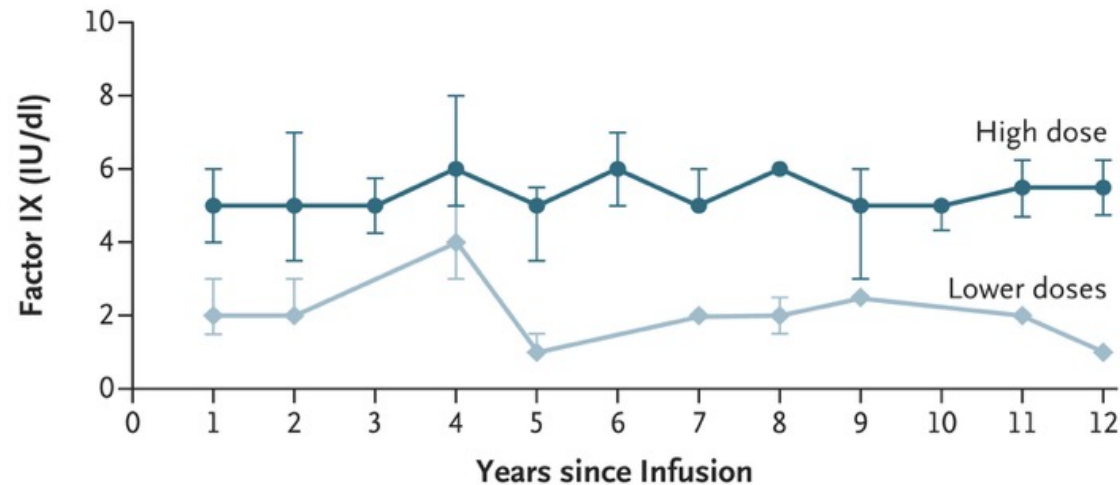
Here, we present safety and efficacy data from 10 men with severe hemophilia B treated with a single bolus infusion of scAAV2/8-LP1-hFIXco who were followed for a median of 13 years. We investigated the long-term safety and durability of transgene expression to assess whether it provided sustained protection from spontaneous bleeding.



## Characteristics of the Participants at Screening and after Gene Transfer, According to Dose Group and Participant Number.

Characteristic	Low Dose		Intermediate Dose			High Dose				
	P1	P2	P3	P4	P5	P6	P7	P8	P9	P10
<b>At baseline</b>										
Age (yr)	31	64	43	29	32	27	22	38	44	33
Factor IX mutation	31280G→A E387K	2-bp del, frameshift	30097G→T W215C	31290G→A A309T	20518C→T R180W	–52 del C	3-bp del, frameshift	1277C→T T426I	698C→A A233D	385G→T G129X
Cross-reacting material status†	Pos	Neg	Pos	Pos	Pos	Neg	Neg	Pos	Pos	Neg
Factor IX prophylaxis	2×/wk	2×/wk	2×/wk	1×/wk	2×/wk	3×/wk	1×/wk	On demand	On demand	On demand
No. of target joints	4	10	6	3	10	2	2	4	5	3
<b>Infection markers</b>										
Hepatitis B surface antigen	Neg	Neg	Neg	Neg	Neg	Neg	Neg	Neg	Neg	Neg
Hepatitis B surface antibody	Pos	Pos	Pos	Pos	Pos	Pos	Neg	Pos	Pos	Pos
HIV antibody	Neg	Neg	Neg	Neg	Neg	Neg	Neg	Neg	Neg	Neg
Hepatitis C antibody	Neg	Pos	Pos	Neg	Pos	Neg	Pos	Pos	Pos	Pos
Hepatitis C RNA	Neg	Neg	Neg	Neg	Neg	Neg	Neg	Neg	Neg	Neg
Anti-AAV8 IgG antibody (relative units)	1	12	37	1	5	8	1	6	6	5
<b>After gene transfer</b>										
Steady-state factor IX activity (IU/dl)‡	1.9±0.7	1.5±0.7	2.7±1.3	1.9±0.8	3.0±1.4	5.8±2.0	4.9±0.7	7.0±1.0	5.5±1.3	2.7±1.9
<b>Elevated ALT level</b>										
Between 1 wk and 12 wk after infusion	No	No	No	No	Yes, at wk 8	Yes, at wk 9	Yes, at wk 7	No	No	Yes, at wk 9
Between 13 wk and 11 yr after infusion	No	No	No	No	No	No	No	No	No	No
Factor IX inhibitor	Neg	Neg	Neg	Neg	Neg	Neg	Neg	Neg	Neg	Neg
Follow-up (yr)	13.8	13.4	13.2	13.2	13.0	12.9	11.8	11.6	11.3	11.1
<b>Annual use of factor IX con- centrate§</b>										
Before gene transfer (IU/kg)	3608	4284	2486	1515	2678	2509	5719	3130	1367	1714
After gene transfer (IU/kg)	798	3559	2723	17	1863	35	497	237	45	106
<b>Annual bleeding rate¶</b>										
Before gene transfer (no.)	3	13	12	12	15	3	22	20	36	29
Mean no. after gene transfer	1.9	4.6	1.9	0.7	5.5	0.3	2.3	0.9	1.1	0.2

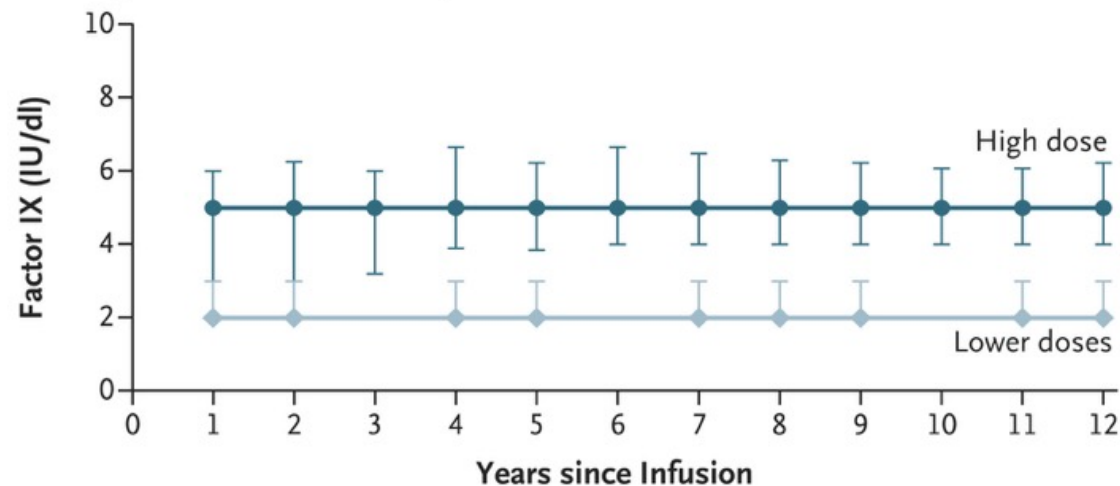
### A Annualized Factor IX Activity



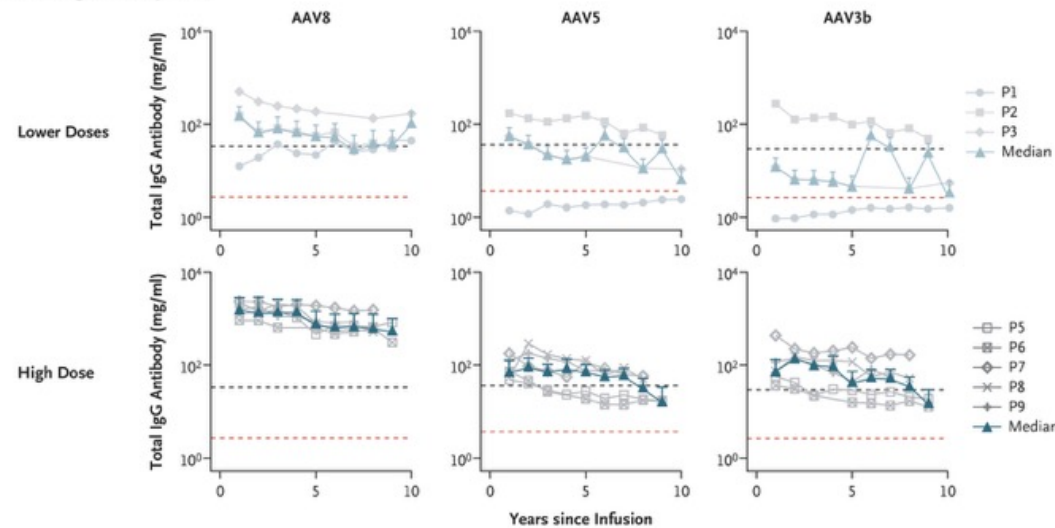
### Factor IX Activity Levels after Administration of scAAV2/8-LP1-hFIXco, with Factor IX Levels Uninfluenced by Prophylaxis Use or Treatment with Factor IX Concentrate.

The annualized and steady-state factor IX activity was determined at the indicated time points with the use of a one-stage clotting assay after the administration of the high dose of scAAV2/8-LP1-hFIXco ( $2 \times 10^{12}$  vector genomes [vg] per kilogram of body weight [in six participants]) as compared with activity seen in participants who received the low or intermediate dose ( $2 \times 10^{11}$  vg per kilogram or  $6 \times 10^{11}$  vg per kilogram [in four participants combined]). The annualized factor IX activity (Panel A) was determined for each group with the use of the median factor IX activity obtained during the indicated year; I bars indicate the interquartile range. Steady-state factor IX activity (Panel B) was the median of all accumulated factor IX activity levels from 5 months after the receipt of gene therapy up to the indicated time point for each group; I bars indicate the interquartile range. Only factor IX levels measured at least 10 days after factor IX use were included.

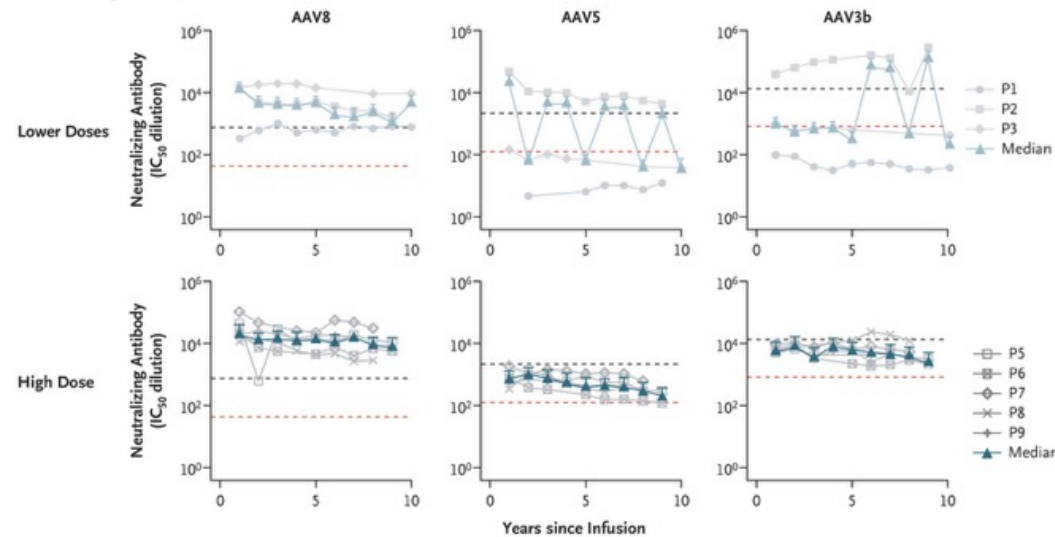
### B Steady-State Factor IX Activity



### A Total IgG Antibody Levels



### B Neutralizing Antibody Levels



### Longitudinal Analysis of Anti-AAV Capsid Antibody Level after Administration of scAAV2/8-LP1-hFIXco.

Total IgG antibody levels as assessed by enzyme-linked immunosorbent assay (Panel A) or neutralizing antibody levels as assessed by transduction inhibition assay (Panel B) against the adeno-associated viruses (AAVs) AAV8, AAV5 and AAV3b in serum samples obtained over time after gene transfer in individual participants who had been treated at the low- and intermediate-dose levels (combined) or the high dose. Shown are antibody levels over time in the individual participants (according to participant number) as well as the overall median values and interquartile ranges (I bars) for the dose level. Data for Participants 4 and 10 were excluded owing to a paucity of sequential samples resulting from nonadherence with study visits. For reference, the dashed black line indicates the maximum, and the dotted red line the median, AAV antibody levels observed in 38 samples obtained from persons who were presumed to have been infected with wild-type AAV.  $IC_{50}$  denotes the 50% inhibitory concentration.

## **Discussion**

This 13-year longitudinal study provided long-term observation data in 10 participants with severe hemophilia B who were successfully treated with AAV gene therapy. Beyond transient elevations in liver aminotransferase levels, no long-term or new AAV-related adverse events were observed. Factor IX expression remained stable, with 7 participants not receiving factor IX prophylaxis. Clinically, AAV gene transfer resulted in reductions by a factor of more than 9 times in the annualized bleeding rate and factor IX concentrate use, which considerably alleviated the disease burden. These findings support the long-term safety and efficacy of AAV gene therapy for hemophilia B, thus offering this group of patients a promising and durable treatment option with recently licensed gene-therapy products.

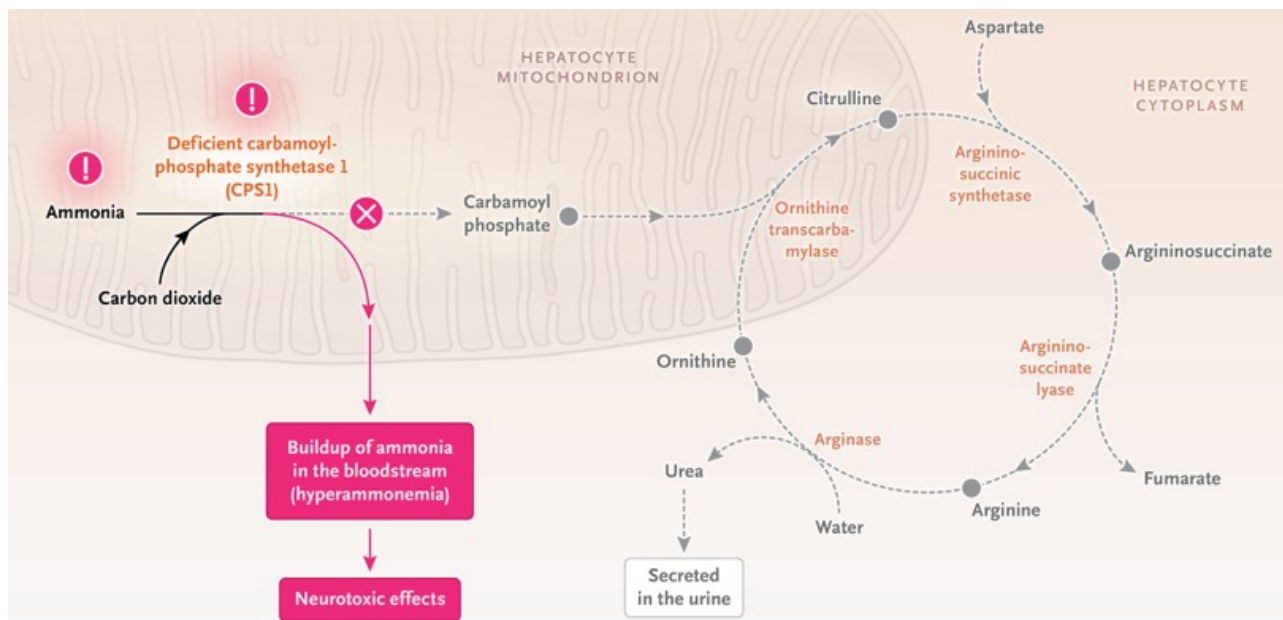
Neoplastic lesions developed in two participants. These lesions were reported as serious adverse events possibly related to AAV, in accordance with the protocol. However, subsequent molecular investigations and expert multidisciplinary review suggested that these events were likely to be unrelated to AAV gene therapy, attributing them instead to age-related or environmental risk factors prevalent in the general population, as previously described.

In this study, 13 years of longitudinal follow-up among men with severe hemophilia B confirmed the long-term safety of AAV gene therapy and durability of factor IX expression, which were accompanied by lasting improvement in hemostasis and a reduction in the use of factor IX prophylaxis.

# Personalized Gene Editing to Treat an Inborn Error of Metabolism

## What Is CPS1?

**Carbamoyl-phosphate synthetase-1 (CPS1)** is a mitochondrial enzyme that catalyzes the first and rate-limiting step of the urea cycle: the conversion of ammonia and bicarbonate to carbamoyl phosphate. This is a crucial detoxification step that occurs primarily in hepatocytes. Without functional CPS1, ammonia accumulates rapidly in the bloodstream and causes hyperammonemia, which is toxic to the brain and can lead to coma or death if untreated.

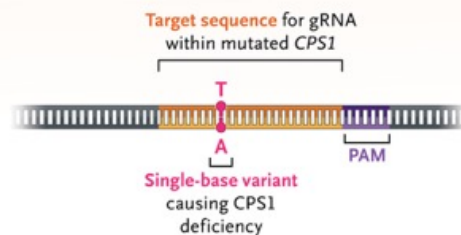


Deficiency of carbamoyl-phosphate synthetase 1 (CPS1) is a recessive urea-cycle disorder caused by damaging or null variants in the gene *CPS1*. The CPS1 enzyme catalyzes the first step in the urea cycle, which takes place in the hepatocyte (Panel A). This step involves the combination of ammonia and carbon dioxide to produce carbamoyl phosphate, thus converting a neurotoxin (ammonia) into a substrate of the urea cycle (carbamoyl phosphate). The product of this cycle, urea, is excreted from the body in the urine. In the absence of adequate levels of CPS1, ammonia levels increase.

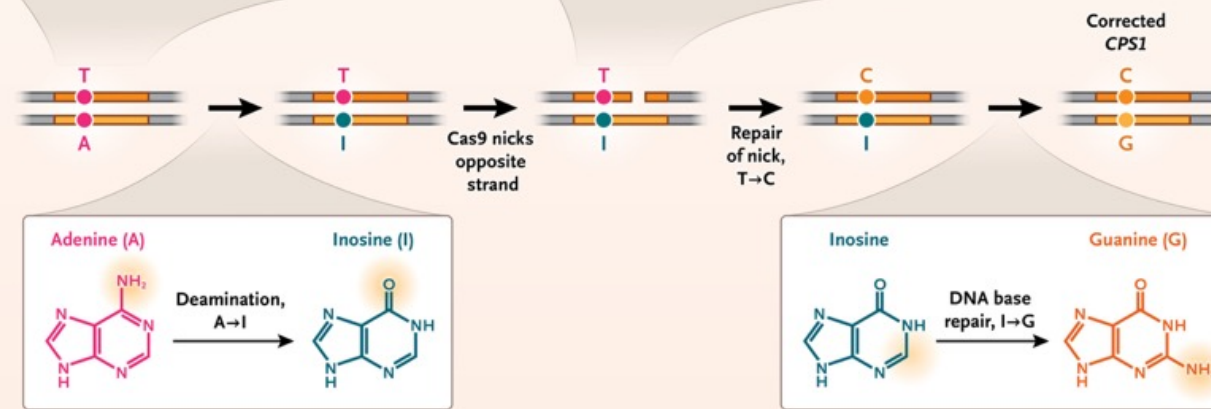
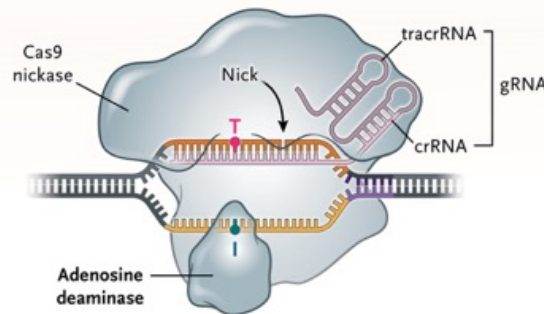


## B Adenine Base Editor–Mediated Repair of *CPS1* Variant

### *CPS1* with Pathogenic Variant



### K-abe Base Editor Bound to Target Sequence of *CPS1*



An infant described by Musunuru et al. presented with symptoms within 2 days after birth. Within 7 months, Musunuru et al. generated and carried out preclinical studies of an adenine base editor (kayjayguran abengcemeran, or k-abe) (Panel B), designed to correct one of the infant's pathogenic *CPS1* variants. The editor is made up of a modified clustered regularly interspaced short palindromic repeats–associated protein 9 (Cas9) enzyme (which does the editing) and a guide RNA (gRNA, which guides the Cas9 enzyme to the mutant *CPS1* nucleotide). In preclinical experiments, k-abe changed (or “edited”) the mutant adenine into an inosine (which resembles guanine) on the noncoding strand, which resulted in the correction of the thymine to cytosine on the coding strand and permitted synthesis of full-length *CPS1*. Reduced levels of ammonia in the infant's plasma after treatment with k-abe is consistent with correction of the pathogenic *CPS1* variant. The term crRNA denotes CRISPR (clustered regularly interspaced short palindromic repeats) RNA, PAM protospacer adjacent motif, and tracrRNA trans-activating CRISPR RNA.

## What Is Base Editing?

Base editing is a method that can be used to install single variants into the genome of live cells in a targeted, precise, and efficient manner. Thus, one can revert a pathogenic stop codon to the “original,” nonmutant sequence, allowing the synthesis of a full-length, functional protein. Musunuru et al. used an **adenine base editor (ABE)**, which comprises an enzyme (a clustered regularly interspaced short palindromic repeats–associated protein 9 [Cas9] nickase [Cas9n]–adenosine deaminase fusion) and a piece of RNA called a guide RNA (gRNA). The Cas9n enzyme is guided to a specific 20 base-pair (see Key Concepts) protospacer sequence (in this case, the region of the patient’s paternal CPS1 gene that harbors the mutation) with the gRNA. The protospacer must be next to a three-base motif, called the protospacer adjacent motif (PAM), which the Cas9n protein recognizes and binds tightly to. Once bound, the adenosine deaminase domain deaminates adenines within the protospacer, leading to the conversion of a specific A–T base pair into a G–C base pair. Base editing is therefore more precise than clustered regularly interspaced short palindromic repeats [CRISPR]–Cas9 editing, which disrupts genes by cutting the DNA rather than targeting a single base pair for mutation.

### How Can It Treat CPS1 Deficiency?

Musunuru et al. developed a base-editing strategy **to correct the CPS1 Q335X “stop” variant, a nonsense G-to-A variant** on the noncoding strand. They started out by testing several different gRNAs that target overlapping protospacers. With each gRNA, the pathogenic A variant is in a slightly different position and orientation with respect to the positioning of the adenosine deaminase domain, once the ABE has bound to the PAM and protospacer. Increasing the potential for patient-specific customization, each gRNA can be combined with an ABE variant: ABE variants differ in their preferences for specific DNA motifs. **Numerous ABE:gRNA combinations were individually generated and tested** to identify the combination with the greatest efficiency and precision. Further complicating the testing process is that it must be carried out with the use of cells that harbor the pathogenic variant and that are the same or a similar cell type to the target tissue (in the case of CPS1 deficiency, a hepatocyte) and are easy to culture and grow in the laboratory. For some rare diseases, it can take months to a year to generate such a cell line.

## How Was Gene-Editor Customization Accelerated?

To obtain a suitable cell line for testing ABE:gRNA combinations, Musunuru et al. inserted a 100 base-pair segment representing the patient's mutated *CPS1* (generated through DNA-synthesis technology) into the genome of a human hepatocyte cell line. Overall, the generation of the cell line and ABE:gRNA screening took 2 months to complete. Preclinical studies of the adenine base editor (named kayjayguran abengcemeran, or k-abe) were then conducted in two different transgenic mouse models and in nonhuman primates.

## What's Next?

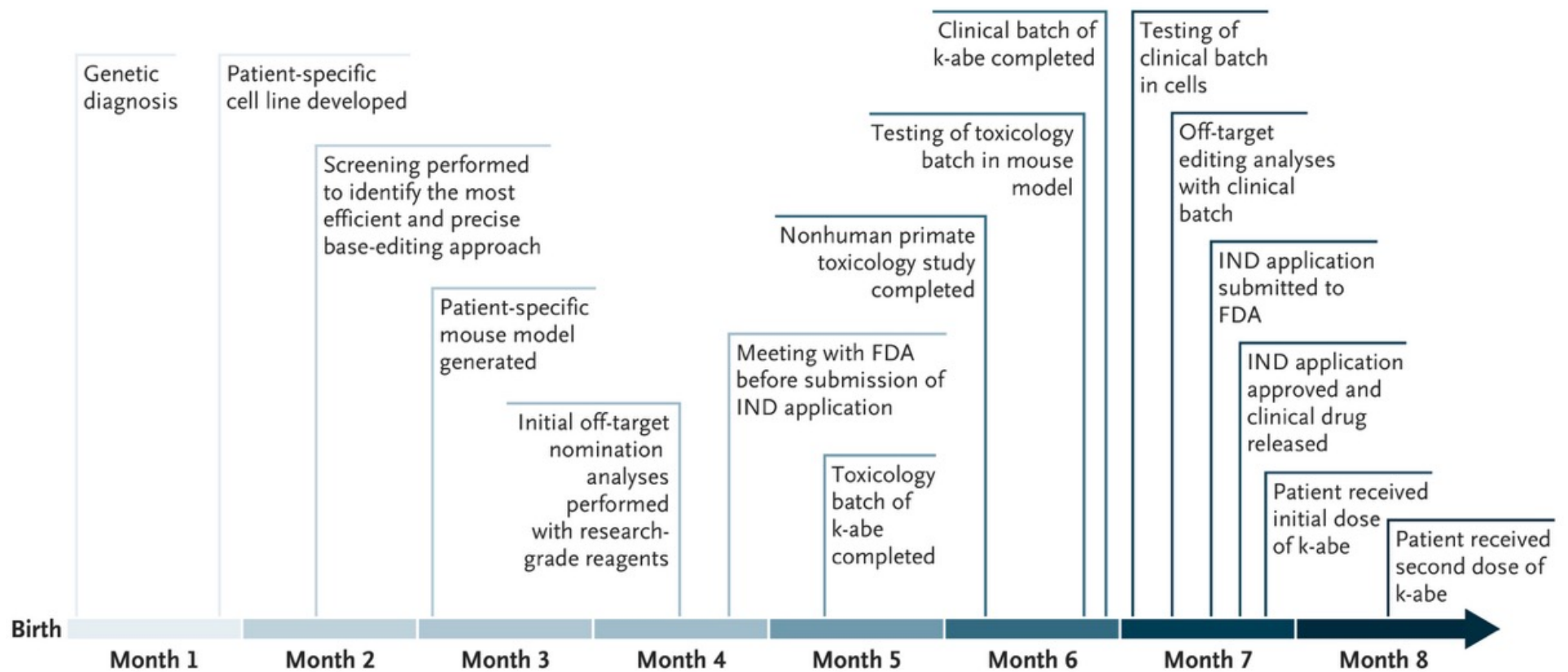
The ability to intervene at the genomic level and to directly correct the underlying genetic defect in a patient's liver shows the promise of CRISPR-based medicine. Limitations of the study include the fact that the mouse model, although carrying the patient's pathogenic *CPS1* variants, does not have a *CPS1* deficiency phenotype and so is unsuitable for testing therapeutic efficacy.

This study must be balanced against the current limitations of an N-of-1 experience in a rare or ultrarare condition. Although the authors noted clinical stabilization in the short term, the absence of direct molecular confirmation of gene editing by means of liver biopsy leaves questions unanswered, such as the durability of the therapeutic effect, the extent of mosaicism of editing, and the risks of off-target events or immune responses. Longer-term follow-up of this patient will be critical to obtaining answers.

## Patient-Specific In Vivo Gene Editing to Treat a Rare Genetic Disease

### Summary

Base editors can correct disease-causing genetic variants. After a neonate had received a diagnosis of **severe carbamoyl-phosphate synthetase 1 deficiency**, a disease with an estimated 50% mortality in early infancy, we immediately began to develop a customized lipid nanoparticle–delivered base-editing therapy. **After regulatory approval had been obtained for the therapy, the patient received two infusions at approximately 7 and 8 months of age.** In the 7 weeks after the initial infusion, the patient was able to receive an increased amount of dietary protein and a reduced dose of a nitrogen-scavenger medication to half the starting dose, without unacceptable adverse events and despite viral illnesses. No serious adverse events occurred. Longer follow-up is warranted to assess safety and efficacy. (Funded by the National Institutes of Health and others.)





## Patient-Specific Customization of Base-Editing Therapy

Reliable assessment of base editing of the *CPS1* Q335X variant would ideally use human hepatocytes with the variant; however, human hepatocytes were not available. **Therefore, we used the cultured human HuH-7 cell line as a proxy.** We synthesized a cassette harboring a 100-bp human genomic segment spanning the *CPS1* Q335X variant, as well as 100-bp segments spanning the patient's other *CPS1* variant and two reference variants in *PAH* to serve as positive controls. **We transduced HuH-7 cells with a lentiviral vector containing the cassette, thereby inserting the cassette into the genome.** This process was completed 1 month after the patient's birth.

To develop a patient-specific, bespoke gene editor, we screened **various adenine base editors** (ABEs) with guide RNAs (gRNAs) tiling the site of the Q335X variant in the lentivirus-transduced HuH-7 cells. We identified an ABE with a preference for NGC protospacer-adjacent motifs, termed NGC-ABE8e-V106W, and a gRNA with the target Q335X adenine in the eighth position of its protospacer sequence as the most efficient and precise base-editing approach; although there was bystander editing of neighboring adenines, all such edits were synonymous. This process was completed 2 months after the patient's birth. **We named the gRNA used in the lipid nanoparticle therapy "kayjayguran," the messenger RNA (mRNA) encoding the ABE "abengcemeran," and the therapy "k-abe" (for short).**

## Preclinical Studies

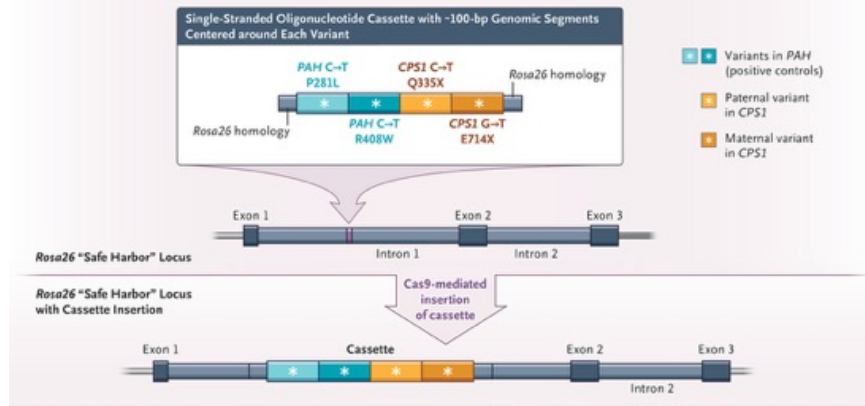
After the initial regulatory review by the FDA, we manufactured a toxicology batch of k-abe (i.e., the batch used for toxicologic testing) and undertook a limited safety study in cynomolgus monkeys to characterize single-dose toxicity of the lipid nanoparticle therapy. A total RNA dose of 1.5 mg per kilogram of body weight was administered intravenously.

On learning of the patient's genetic diagnosis, we immediately started generating mouse models to assess the *in vivo* editing efficiency of k-abe. To maximize the chance of success, we used established CRISPR reagents in mouse zygotes to insert a cassette harboring a 100-bp human genomic segment spanning the *CPS1* Q335X variant into the *Rosa26* "safe harbor" locus (the same cassette used for the lentivirus-transduced HuH-7 cells).

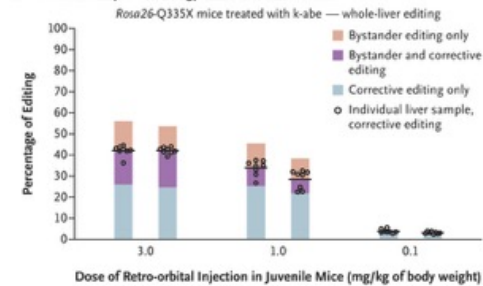
With the clinical batch of k-abe that was produced 5 months after the patient's birth, we performed a dose–response potency assessment in lentivirus-transduced HuH-7 cells.

We exposed lentivirus-transduced HuH-7 cells and primary human hepatocytes from three donors to a supersaturating dose of k-abe. Low-level synonymous bystander editing was evident at the endogenous wild-type *CPS1* genomic site in all four cell lots, a finding that is consistent with the gRNA (kayjayguran) having a 1-base mismatch to the wild-type sequence (the HuH-7 cells retained endogenous wild-type *CPS1* alleles in addition to the transduced *CPS1* Q335X variant sequence).

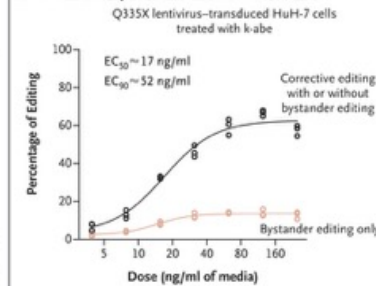
#### A Engineering a Mouse Model with Four Human Pathogenic Variant Sequences, Including Q335X Variant



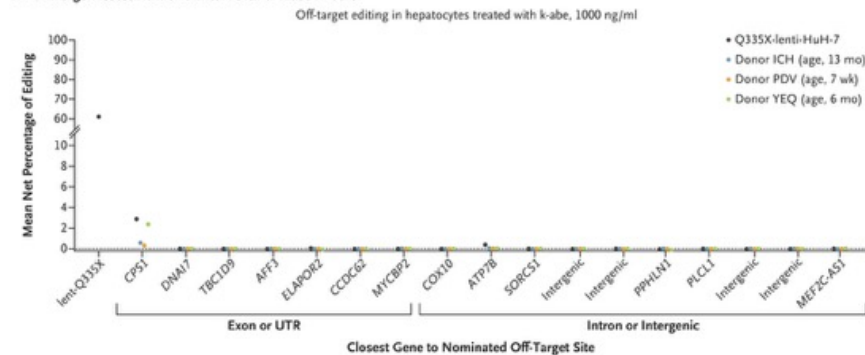
#### B In Vivo Efficacy of Toxicology Batch of K-abe in Mice



#### C In Vitro Efficacy of Clinical Batch of K-abe in Cells

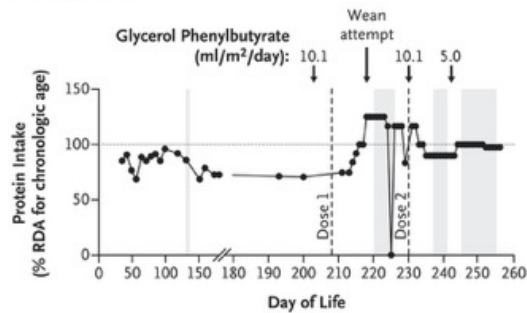
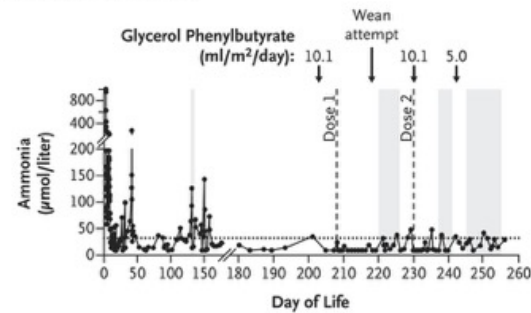
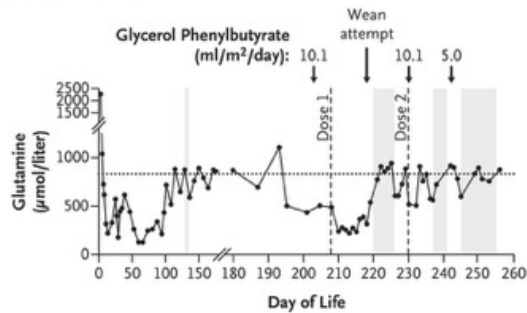
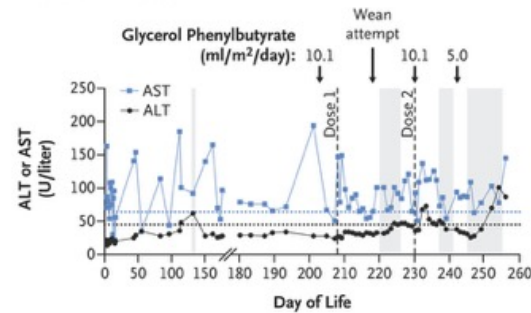
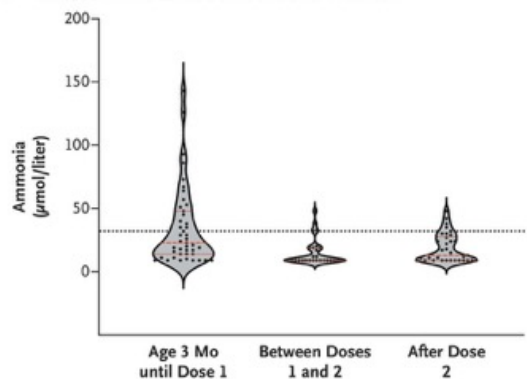
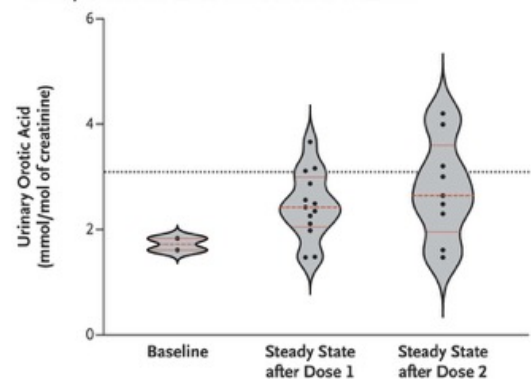


#### D Off-Target Assessment of Clinical Batch of K-abe in Cells



#### Preclinical Studies.

Panel A shows the contents of the single-stranded DNA oligonucleotide cassette inserted into the endogenous mouse *Rosa26* locus in mouse zygotes. Panel B shows the extent of whole-liver corrective adenine base editing of the *CPS1* Q335X variant in *Rosa26*-Q335X mice. Several days after administration of a single dose of k-abe from the toxicology batch, we obtained multiple samples distributed throughout the liver of each juvenile mouse on necropsy. We assessed the extent of editing in eight samples per mouse by sequencing the *Rosa26*-Q335X cassette. The two bars at each dose level (3.0, 1.0, and 0.1 mg per kilogram of body weight) represent two mice. Across the three dose groups, no more than 1% insertional or deletional mutagenesis occurred at the target site. Panel C shows corrective adenine base editing of the *CPS1* Q335X variant in lentivirus-transduced HuH-7 cells treated with k-abe. Editing was determined 3 days after treatment at the stated dose (concentration after dilution with cell medium). The best-fit agonist response curve with variable slope (four-parameter logistic regression) and 50% effective concentration (EC<sub>50</sub>) and 90% effective concentration (EC<sub>90</sub>) values were calculated with GraphPad Prism. Panel D shows the evaluation of a high-priority subset of nominated off-target sites for any adenine-to-guanine editing through individual-site targeted amplicon sequencing in the Q335X lentivirus-transduced HuH-7 cells (Q335X-lenti-HuH-7) and in primary human hepatocytes from three male donors (donor ICH [13 months of age], donor PDV [7 weeks of age], and donor YEQ [6 months of age]) after treatment with k-abe at 1000 ng per milliliter of media, as compared with untreated cells. Of 21 high-priority nominated off-target sites, 16 were successfully sequenced and shown here. Cas9 denotes clustered regularly interspaced short palindromic repeats-associated protein 9, and UTR untranslated region.

**A Protein Intake****B Plasma Ammonia Level****C Glutamine Level****D AST and ALT Levels****E Plasma Ammonia Levels before and after Treatment****F Urinary Orotic Acid Levels before and after Treatment**

### Biochemical Profile before and after Treatment with K-abe.

Shown are the timelines of protein intake (Panel A) and levels of plasma ammonia (Panel B), glutamine (Panel C), aspartate aminotransferase (AST) and alanine aminotransferase (ALT) (Panel D). The gray bars from left to right indicate periods of rotavirus-positive gastroenteritis before treatment, rhinovirus-positive upper respiratory tract infection after dose 1, and two viral illnesses after dose 2 (gastroenteritis followed by a new rhinovirus or enterovirus infection with associated viral transaminitis). In Panels B through F, the dotted horizontal lines indicate upper limits of the normal range for the laboratory value. Panels E and F show violin plots of plasma ammonia levels and urinary orotic acid levels, respectively, before and after treatment. Inside the plots, the red dashed line indicates the median, and the red dotted lines indicate the upper and lower quartiles. The clusters of dots indicate the individual data points. To convert the values for ammonia to micrograms per deciliter, divide by 0.5872. To convert the values for glutamine to micrograms per deciliter, divide by 68.42. RDA denotes recommended dietary allowance.

## Discussion

In this study, we describe a personalized base-editing therapy wholly developed in the 6-month span after a patient's birth. The patient was able to receive an increased amount of dietary protein and a reduced dose (to half the starting dose) of a nitrogen-scavenger medication, despite the “stress tests” presented by consecutive viral infections. The short follow-up is a limitation of this study; longer follow-up is needed to assess the safety and efficacy of k-abe, as well as the patient's neurologic health. Liver biopsy to assess for corrective *CPS1* editing was deferred because it posed an unacceptable risk to the infant. The potential for germline editing with k-abe could not be evaluated, although a study of a different lipid nanoparticle gene-editing drug did not detect editing in sperm samples from nonhuman primates nor germline transmission of gene edits in female mice to offspring.

We assessed k-abe for editing efficiency in mice and for safety in nonhuman primates. Such studies might not be necessary for future patient-specific treatments; perhaps cell-based studies would be sufficient. Although k-abe was developed under emergency conditions for a devastating neonatal-onset metabolic disorder, we anticipate that rapid deployment of patient-specific gene-editing therapies will become routine for many genetic diseases.



# Physical Signs of Malnutrition in Elderly



# Malnutrition in Older Adults

## KEY POINTS

### Malnutrition in Older Adults

- Malnutrition is common in older adults and has serious adverse consequences.
- The cause of malnutrition is usually multifactorial, owing to the interaction of physiological changes of aging, physical and mental impairments, diseases, medications, social settings, and dietary factors.
- The Global Leadership Initiative on Malnutrition framework is used for the syndromic diagnosis of malnutrition. Once malnutrition is confirmed, a careful search for the underlying causes is indicated.
- Effective guideline-based strategies are available to prevent and treat malnutrition in older adults.

## Possible Causes of Insufficient Food Intake and Malnutrition in Older Adults.

### Age-related physiological changes

- Loss of appetite (anorexia of aging)
- Decreased sensory perception (taste, smell, or vision)
- Incomplete compensation of weight loss

### Physical impairments

- Difficulty chewing owing to tooth loss, decayed teeth, ill-fitting dentures, inflammation, oral infections, or dry mouth
- Difficulty swallowing (dysphagia)
- Impairment in hands or arms resulting in difficulty cutting or preparing food
- Limited mobility resulting in difficulty shopping for food and cooking

### Mental impairments

- Cognitive impairment or dementia (e.g., apraxia, behavioral disorders, and apathy)
- Depression or dysthymia
- Delirium
- Altered day–night rhythm
- Psychiatric eating disorder (e.g., anorexia nervosa and delusion of slimming or poisoning)

### Health impairments

- Gastrointestinal symptoms (e.g., constipation, nausea, and vomiting)
- Gastrointestinal diseases
- Acute and chronic illness
- Acute and chronic pain
- Polypharmacy or medication side effects
- Food intolerance or allergy
- Restrictive prescription diets (e.g., low fat, low cholesterol, and low salt)

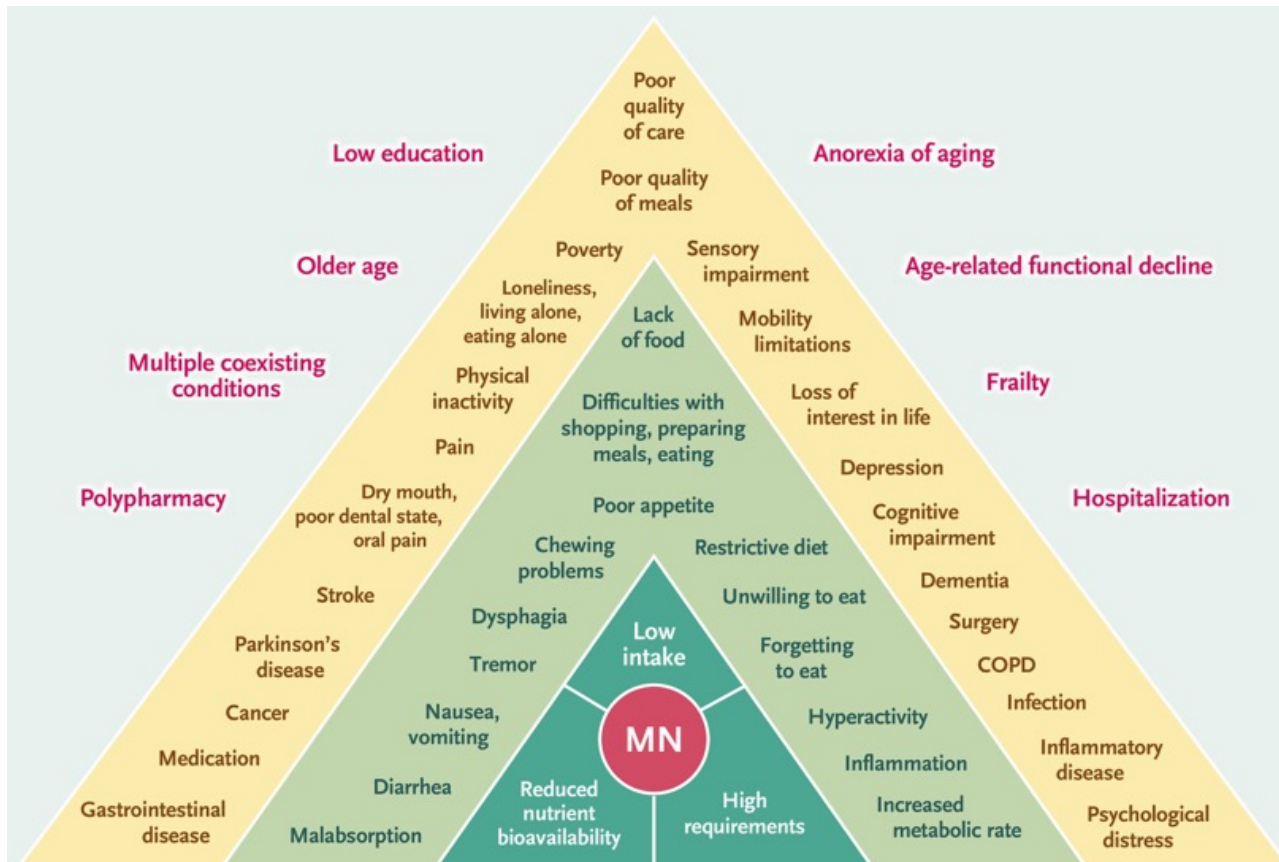
### Social and financial difficulties

- Loneliness or social isolation
- Life events (e.g., bereavement and relocation to a nursing home)
- Lack of assistance with shopping, meal preparation, and eating
- Neglect
- Unsatisfactory dining situation in an institution (e.g., environment and company)
- Low income or poverty

### Direct dietary factors and poor habits

- Restrictive diets
- Small meals or skipped meals
- Unbalanced diet or omission of valuable food groups
- Inadequate or unappealing food offered in hospitals and institutions
- High alcohol consumption or alcoholism

## Determinants of Malnutrition in Aged Persons (DoMAP) Model.



All the factors shown — regardless of their position within the DoMAP model — are considered to be potential determinants of malnutrition (MN), meaning that they may contribute to the development of malnutrition in a causative manner. The levels illustrate different modes of action: level 1 (dark green) denotes central etiologic mechanisms, level 2 (light green) denotes factors that directly lead to one of the three mechanisms in level 1 (e.g., dysphagia may directly cause low intake), and level 3 (yellow) denotes factors that indirectly lead to one or more of the three central mechanisms through one or more of the direct factors in the green triangle (e.g., stroke may cause low intake due to dysphagia or difficulties with eating). Factors shown in red text are age-related changes and general aspects that also contribute to the development of malnutrition but through means that are more indirect or subtle. The figure is adapted from the Malnutrition in the Elderly Knowledge Hub Toolbox (<https://www.healthydietforhealthylife.eu/manual-toolbox>).



## Evidence-Based Intervention Strategies and Recommendations for the Management of Malnutrition.

Strategy or Recommendation	Grade of Recommendation
Basic recommendations	
Routine screening for malnutrition with a validated tool in all older adults regardless of their nutritional status, followed by assessment, individualized intervention, and monitoring and adjustment of interventions	Good practice point
Individualized and comprehensive nutrition and hydration care	Strong evidence
Nutrition interventions as part of a multimodal and multidisciplinary team approach	Medium evidence
Nutrition education for health care professionals and informal caregivers	Medium evidence
Etiologic interventions	
Identification and management of potential causes of malnutrition and dehydration	Good practice point
Avoidance of dietary restrictions that may limit intake	Good practice point
Supportive interventions	
Mealtime assistance for persons with limited ability to feed themselves	Strong evidence in institutions, good practice point in home care

Homelike, pleasant eating environment in institutions	Strong evidence
Shared mealtimes with others	Good practice point
Energy-dense delivered meals (e.g., Meals on Wheels), with additional meals	Medium evidence
Nutrition information and education for older adults with malnutrition or at risk for malnutrition	Medium evidence
Physical activity to help maintain or improve appetite, muscle mass, and function	Good practice point
Individualized nutrition counseling for older adults and their caregivers	Medium evidence
Food modification	
Food fortification	Medium evidence
Supplementary snacks and finger foods	Good practice point
Texture-modified, fortified foods for older adults with malnutrition or at risk for malnutrition and signs of oropharyngeal dysphagia or masticatory problems	Good practice point
Oral nutritional supplements when dietary counseling and food fortification are not sufficient to meet nutritional goals	Strong evidence, good practice point (recommendations equally divided between the two grades) †
Enteral or parenteral nutrition for older adults with a reasonable prognosis (expected benefit) when oral or oral and enteral intake is expected to be impossible for more than 3 days or to be less than half the energy required for more than 1 week, despite interventions to ensure adequate oral intake	Good practice point ‡

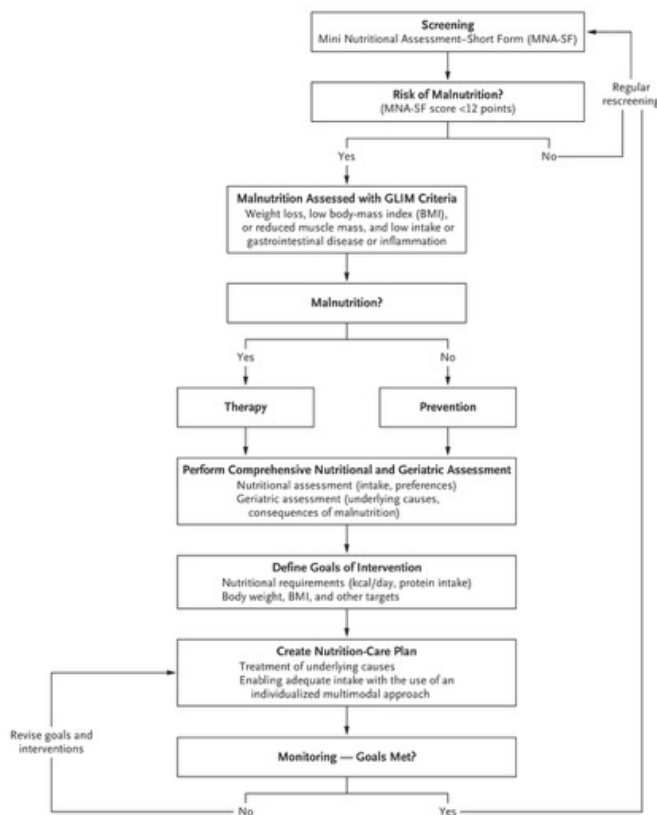


## Areas of Uncertainty

Nutrition research has been hampered by the lack of consensus on diagnostic criteria. The GLIM criteria were published in 2019, so in most of the studies on malnutrition before then, heterogeneous approaches were used to define the condition. The study populations varied in terms of nutritional status and risk factors, and this diversity partly explains the heterogeneity of results from nutrition interventions.

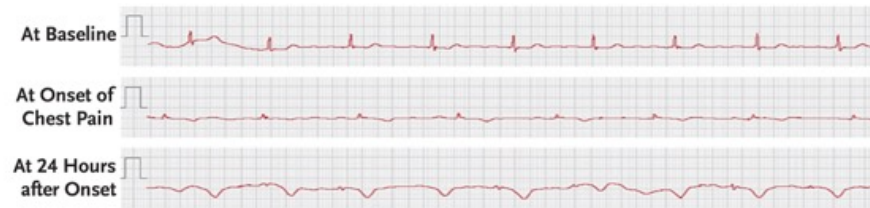
Additional challenges associated with malnutrition in older adults, as well as with younger patients, are the lack of implementation of nutritional knowledge in clinical practice, the lack of adequate funding, and the lack of dietitians in many settings. Most physicians do not receive training in nutrition in medical schools and are unaware of the relevance of incorporating nutritional intervention into the management of most common chronic diseases.

Malnutrition in older adults is underdiagnosed and undertreated. There is a need to raise awareness among health care professionals and the general public on the importance of the nutrition aspects of health and disease. Information technology may help track patient's nutritional changes over time and detect malnutrition.

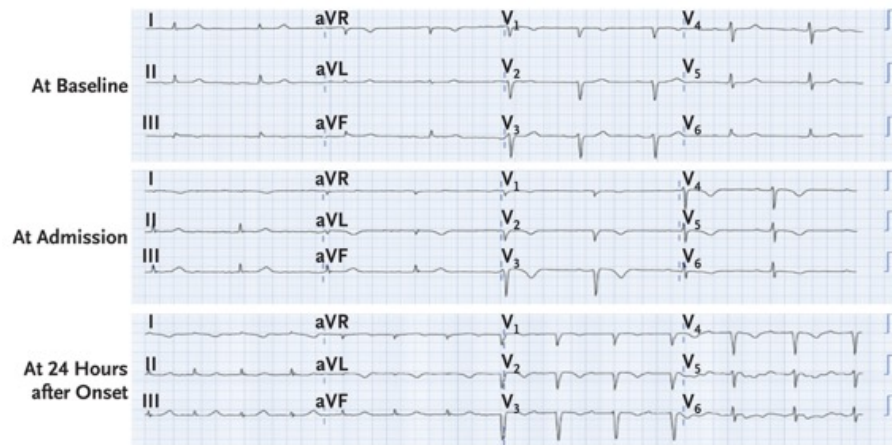


# Cardiac Injury Detected by Smartwatch

**A Smartwatch ECG** Same as Lead I (right arm -, left arm +)



**B 12-Lead ECG**



A 76-year-old retired cardiovascular nurse presented to the emergency department with a 2-hour history of chest pain that had been triggered by severe emotional distress and was associated with changes in the electrocardiogram (ECG) on her smartwatch. The physical examination was normal. The single-channel smartwatch ECG (which corresponds to lead I on a 12-lead ECG) showed new T-wave inversions and a lower QRS amplitude than had been observed at baseline (1 month before presentation). Panel A shows the findings on the smartwatch ECG over time. A 12-lead ECG showed new T-wave inversions and subtle ST-segment elevation in the V<sub>3</sub> lead as compared with baseline (2 years before presentation; Panel B). The level of high-sensitivity troponin T was 205 ng per liter (reference range, 6 to 10). A coronary angiogram showed unobstructed coronary arteries. Echocardiography revealed left ventricular apical ballooning with an ejection fraction of 35%. A diagnosis of takotsubo (stress) cardiomyopathy was made. Although this medically trained patient used her smartwatch to identify cardiac injury, smartwatch ECGs are not approved for this indication. Treatment with a beta-blocker and an angiotensin-converting-enzyme inhibitor was started. At 6 weeks of follow-up, the patient felt well, and a repeat echocardiogram was normal.

## Case 16-2025: A 34-Year-Old Man with a Nasopharyngeal Mass

A 34-year-old man was admitted to this hospital because of pain in the left ear with hearing loss, facial droop on the left side, and a nasopharyngeal mass that was identified on computed tomography (CT).

The patient had been well until approximately 8 months before the current presentation, when pain and a sensation of pressure and fullness developed in the left ear. During the subsequent 5 months, he was seen in the primary care clinic of another hospital on five occasions and received three courses of treatment with oral antibiotic agents; however, the patient's symptoms did not abate. He also received one course of prednisone treatment, which provided slight relief of symptoms.

Three months before the current presentation, treatment with neomycin ear drops was started, and the patient was referred to the otolaryngology clinic of the other hospital.

Seven weeks before the current presentation, the pain in the left ear became so severe that it awoke the patient from sleep, and he also had pain in the sinuses.

Six weeks before the current presentation, examination in the otolaryngology clinic showed that the tympanic membranes were intact and the right middle ear was well aerated, but the serous middle-ear effusion persisted in the left ear.

During the subsequent 3 days, the patient's sinus pain increased in severity and progressed from the sinuses to the top of the head and down the neck; the pain did not abate with treatment with acetaminophen and ibuprofen.

Four weeks before the current presentation, green nasal drainage and hoarseness persisted, and new swelling and clear discharge developed in the patient's left eye. He sought evaluation at the primary care clinic of the other hospital, and treatment with trimethoprim–sulfamethoxazole was started.

Three weeks before the current presentation, the patient was evaluated again in the otolaryngology clinic because of persistent pain in the left ear that radiated to the throat and ear pressure and muffled hearing that gave him the sensation of being underwater.

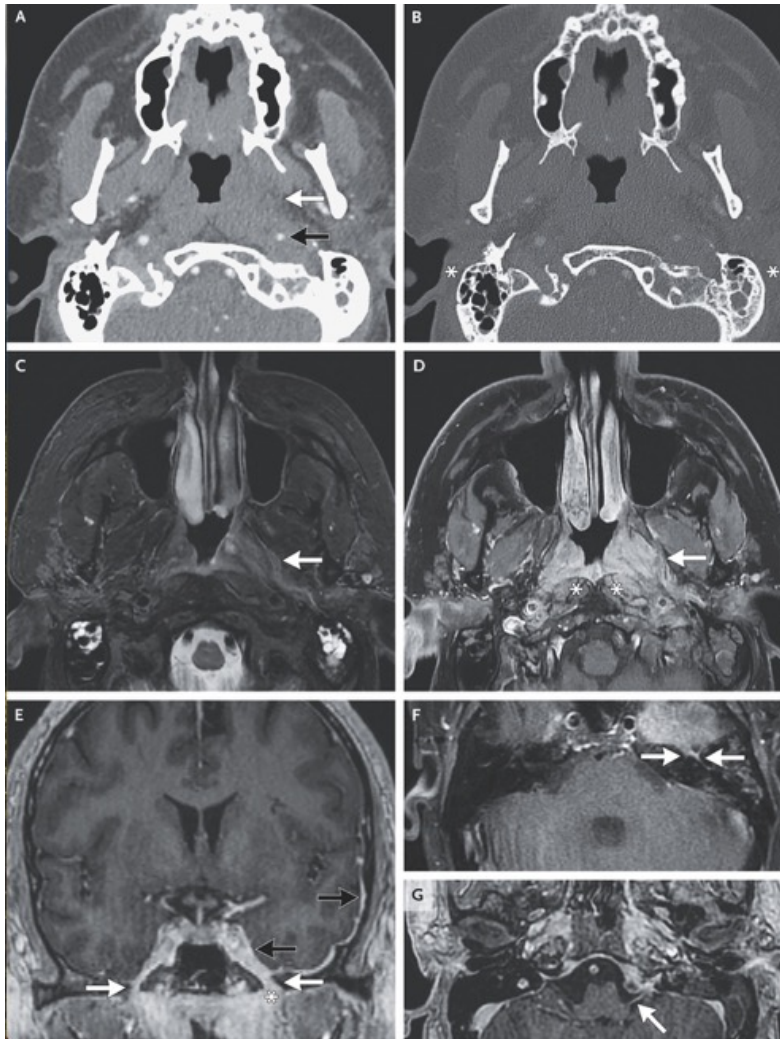
Nine days before the current presentation, an examination performed while the patient was under anesthesia revealed prominent bulges in the anterior and inferior walls of both external ear canals and intact tympanic membranes.

In the emergency department, the patient reported ongoing ear pain and hoarseness, along with new odynophagia and dysphagia. He had had an unintentional weight loss of approximately 13.6 kg in the previous month.

On physical examination, the patient appeared well. The blood pressure was 161/99 mm Hg, the heart rate 106 beats per minute, the respiratory rate 18 breaths per minute, and the oxygen saturation 97% while the patient was breathing ambient air. The external ears and ear canals were normal. The tympanic membranes had tympanostomy tubes in place, but the lumens were not visible. The pupils were equal, round, and reactive to light. The extraocular muscles and facial sensation appeared to be normal; however, the face was asymmetric, with drooping of the left cheek and flattening of the left nasolabial fold, and there was weakness on puffing the cheeks and smiling. Delayed blinking of the left eye, along with weak eye closure on the left side, was observed. On raising the eyebrows, weakness was observed in the left eyebrow. His hearing appeared to be normal, and palate elevation, shoulder shrug, tongue protrusion, and speech were also normal. Muscle tone and strength and sensation to light touch were normal in the arms and legs. The remainder of the examination was normal.

The blood level of C-reactive protein was 101.9 mg per liter (reference value, <8), and the erythrocyte sedimentation rate was 71 mm per hour (reference range, 0 to 14). The blood level of alanine aminotransferase was 137 U per liter (reference range, 10 to 55), the aspartate aminotransferase level 55 U per liter (reference range, 10 to 40), the alkaline phosphatase level 226 U per liter (reference range, 45 to 115), and the  $\gamma$ -glutamyltransferase level 300 U per liter (reference range, 8 to 61). The complete blood count with differential count was normal, as were the results of tests of renal function and coagulation. Imaging studies were obtained.





### CT and MRI Images.

An axial CT angiogram of the neck (Panel A) reveals diffuse soft-tissue prominence in the nasopharynx (white arrow) that is more pronounced on the left side than on the right side and encases the distal cervical internal carotid artery on the left side, resulting in mild asymmetric stenosis (black arrow). The posterolateral pharyngeal recesses and the eustachian tubes are effaced on both sides. A reformatted CT image to emphasize bone (Panel B) shows associated mastoid effusion (asterisks). No osseous erosion is present in the adjacent central skull base. MRI was performed. An axial T2-weighted fat-saturated image (Panel C) and an axial T1-weighted fat-saturated image, obtained after the administration of intravenous contrast material (Panel D), show an intermediate T2-hyperintense, enhancing mass in the posterior nasopharynx that is more pronounced on the left side than on the right side (arrows) and that extends into the left poststyloid parapharyngeal space. There is diffuse enhancement in the adjacent prevertebral longus colli muscles (Panel D, asterisks). No bone marrow signal abnormality is present in the base of the skull. A coronal volumetric T1-weighted image, obtained after the administration of intravenous contrast material (Panel E), shows enhancement of the V3 segments of both trigeminal nerves (white arrows), asymmetric thickening of the V3 segment of the left trigeminal nerve (asterisk), and pachymeningeal thickening and enhancement along the left middle cranial fossa, left cavernous sinus (black arrows), and left tentorial leaflet (not shown). Axial T1-weighted images (Panels F and G), performed with the administration of intravenous contrast material, show additional cranial-nerve enhancement involving the geniculate ganglion and proximal tympanic segment of the left facial nerve (Panel F, arrows) and cisternal segment of the left hypoglossal nerve (Panel G, arrow).

## Differential Diagnosis

This 34-year-old man presented with 8 months of symptoms consistent with eustachian tube dysfunction, including ear fullness, ear pain, hearing loss, middle-ear effusions, and recurrent otitis media despite treatment with multiple courses of antibiotics. Symptoms did not abate with treatment for conditions known to commonly cause eustachian tube dysfunction, such as allergic rhinitis or chronic rhinosinusitis, and progressed despite myringotomy and placement of middle-ear ventilation tubes.

Seven weeks before the current presentation, sinus pain and headache developed. Facial droop consistent with cranial neuropathy subsequently developed, and the patient was found to have elevated levels of inflammatory markers and a nasopharyngeal mass with intracranial extension on imaging studies. In constructing a differential diagnosis, I will consider cancer, infection, and autoimmune disease that could explain months of progressive eustachian tube dysfunction and the imaging findings found on presentation to this hospital.

## Nasopharyngeal Cancer

Although serous otitis media with effusion is most often caused by eustachian tube dysfunction, it is important to rule out cancer. In one systematic review of data from patients with isolated serous otitis media of unknown cause, 5.5% of the patients ultimately received a diagnosis of nasopharyngeal cancer. Nasopharyngeal carcinoma is often associated with Epstein–Barr virus (EBV) infection, with a higher prevalence among persons from Southeast Asia and northern Africa.

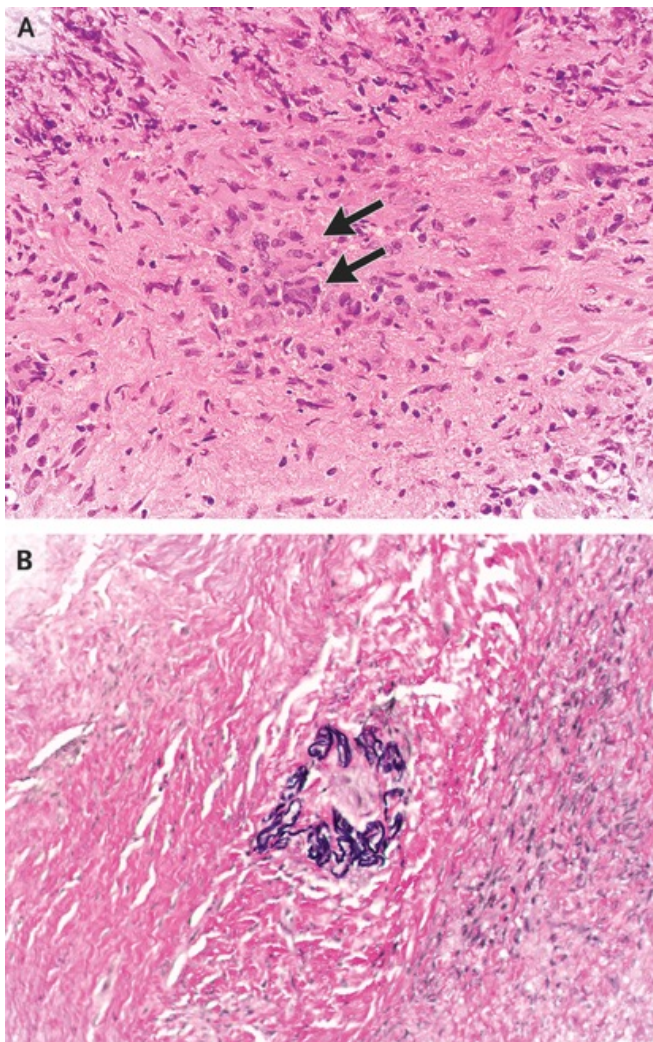
## Infection

Sinusitis can be complicated by the spread of infection into surrounding structures, such as the skull base, intracranial space, or orbits. Infections at the base of the skull usually occur in persons with clinically significant immunocompromise, such as that associated with poorly controlled diabetes, hematologic cancer, or the use of immunosuppressive medications (e.g., drugs administered for the treatment of autoimmune diseases or after organ transplantation).

## Autoimmune Disease

**Granulomatosis with polyangiitis (GPA) may lead to or manifest as sinonasal inflammatory changes.** GPA involving the head and neck can be challenging to diagnose, since biopsies of abnormal sinonasal tissue are usually nondiagnostic, without clear evidence of vasculitis. Testing for antineutrophil cytoplasmic antibodies (ANCA) can help make the diagnosis but may be negative in patients with GPA, especially in patients with disease isolated to the head and neck. Intranasal cocaine use can cause an ANCA-associated vasculitis that mimics GPA, and treatment may not be effective without cessation of the drug. Eosinophilic GPA is another vasculitis that may lead to or manifest as sinus disease.

**When determining treatment for patients with ANCA-associated vasculitis, it is essential to evaluate the extent of the disease with the Birmingham Vasculitis Activity Score (BVAS),** which helps to determine whether the condition is organ-threatening or life-threatening. **This patient's BVAS was 19** (scores range from 0 to 63, with higher scores reflecting more severe disease). He had organ-threatening disease with cranial-nerve involvement and narrowing of the internal carotid artery due to severe nasopharyngeal disease. Therefore, an immediate and aggressive treatment was required.



No evidence of a lymphoproliferative disorder was present on histopathological analysis with the use of ancillary immunohistochemical staining, or on a separately performed flow cytometric evaluation of biopsy specimens. Chromogenic in situ hybridization for EBV-encoded RNA, which was performed to rule out EBV-associated sinonasal neoplasms such as nasopharyngeal carcinoma and extranodal natural killer T-cell lymphoma, was negative. No fungal forms were identified on Grocott's methenamine silver staining, a finding that helps to rule out a destructive fungal process.

Positive indirect immunofluorescence staining revealed ANCA with a cytoplasmic pattern. An enzyme-linked immunosorbent assay (ELISA) confirmed the presence of **anti-proteinase 3 antibodies (PR3-ANCA), with antibody activity measured at 77 units (reference value, <20).**

An ELISA for antibodies to myeloperoxidase was negative.

The findings of the biopsy performed on hospital day 6, interpreted in the context of the clinical presentation of this patient and the positive test for PR3-ANCA, were diagnostic of GPA.

#### **Pathological Diagnosis**

**Granulomatosis with polyangiitis.**



Two weeks after the patient started immunosuppressive therapy, his facial numbness resolved and facial nerve paresis abated; repeat transnasal nasopharyngoscopy showed a decrease in the inflammation of the nasopharynx on the left side. After 1 month of treatment, he had an increase in headache and fatigue that corresponded to tapering of the dose of prednisone, and the prednisone taper was extended from 3 months to 5 months. After 2 months of treatment, headache and fatigue had completely resolved and repeat laboratory testing showed normal blood levels of aspartate aminotransferase, alanine aminotransferase, and alkaline phosphatase. The patient had residual autophony of breath and voice, a symptom suggestive of patulous eustachian tube dysfunction in the left ear. A hearing test revealed moderately severe, symmetric sensorineural hearing loss. Three months after receiving a diagnosis of GPA, the patient was evaluated by the facial plastic surgery consultant because of residual subtle depression of the left eyebrow and left oral commissure; no intervention was planned. Five months after initiation of immunosuppressive therapy, the ANCA level was less than 20 units. Fifteen months after the initial diagnosis, the patient continues to receive rituximab infusions every 4 months.



Der **Birmingham Vasculitis Activity Score, kurz BVAS**, ist ein validiertes Instrument zur quantitativen Dokumentation der Krankheitsaktivität bei Patienten mit systemischen Vaskulitiden. Er dient der Einschätzung der Krankheitsschwere, der Überwachung von Veränderungen im Krankheitsverlauf sowie der Unterstützung von Behandlungsentscheidungen und der objektiven Bewertung des Therapieansprechens.

Der BVAS umfasst neun **Organsysteme**, in denen typische Manifestationen der Vaskulitis dokumentiert werden:

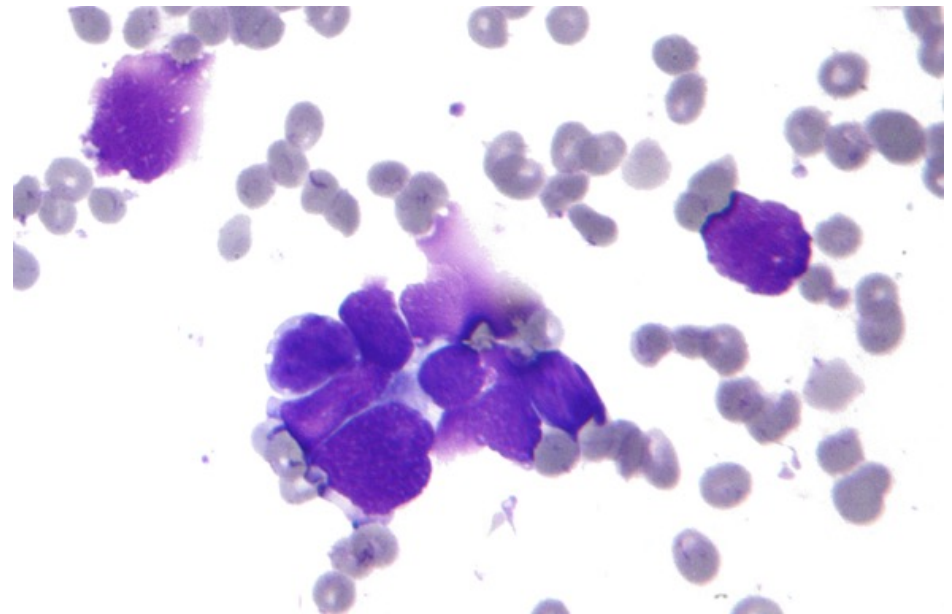
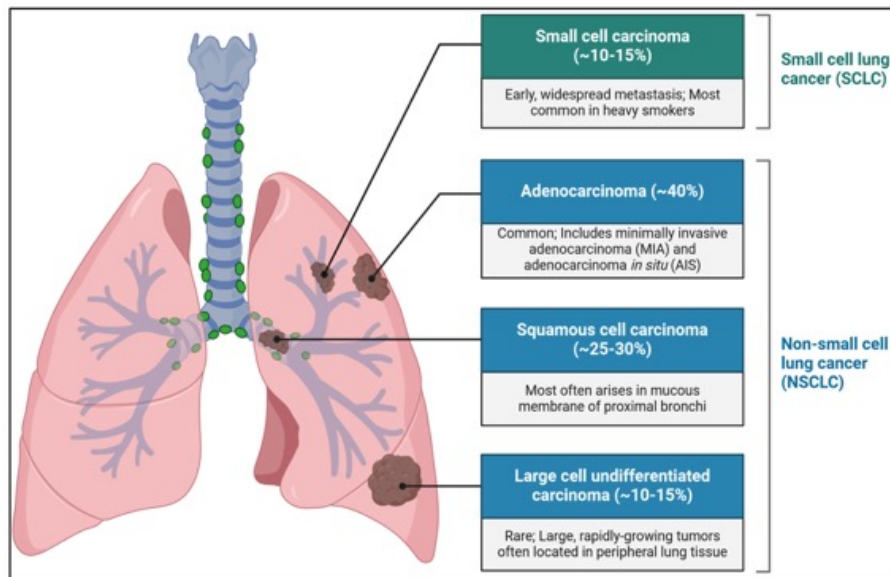
- **Allgemeinsymptome** (z.B. Fieber, Gewichtsverlust)
- **Haut**
- **Schleimhäute/Augen**
- **Hals-Nasen-Ohren-Bereich (HNO)**
- **Brustkorb** (z.B. **pulmonale Infiltrate**)
- **Herz**
- **Gastrointestinaltrakt**
- **Nieren**
- **Nervensystem**

#### **Interpretation**

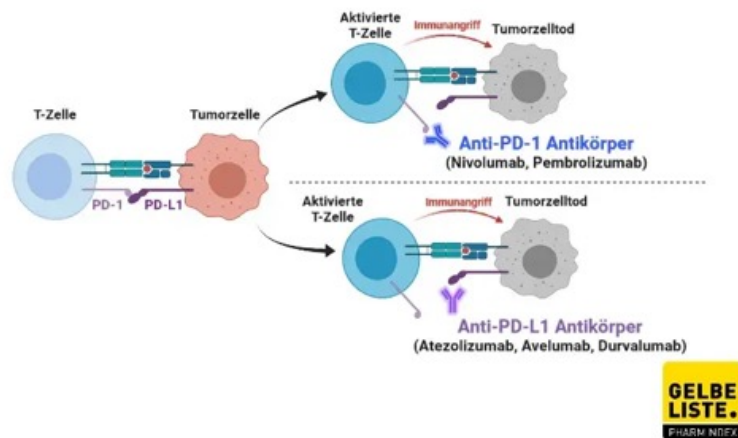
- 0 Punkte: Keine aktive Vaskulitis
- 1 bis 10 Punkte: Geringe bis moderate Krankheitsaktivität
- > 10 Punkte: Hohe Aktivität, oft mit Organbeteiligung

Jedes Symptom wird mit einer vordefinierten Punktzahl bewertet, wobei nur neue oder sich verschlechternde Symptome berücksichtigt werden, die innerhalb eines festgelegten Zeitraums (meist 4 Wochen) auftreten. Die Summe der Punkte ergibt den Gesamtscore.

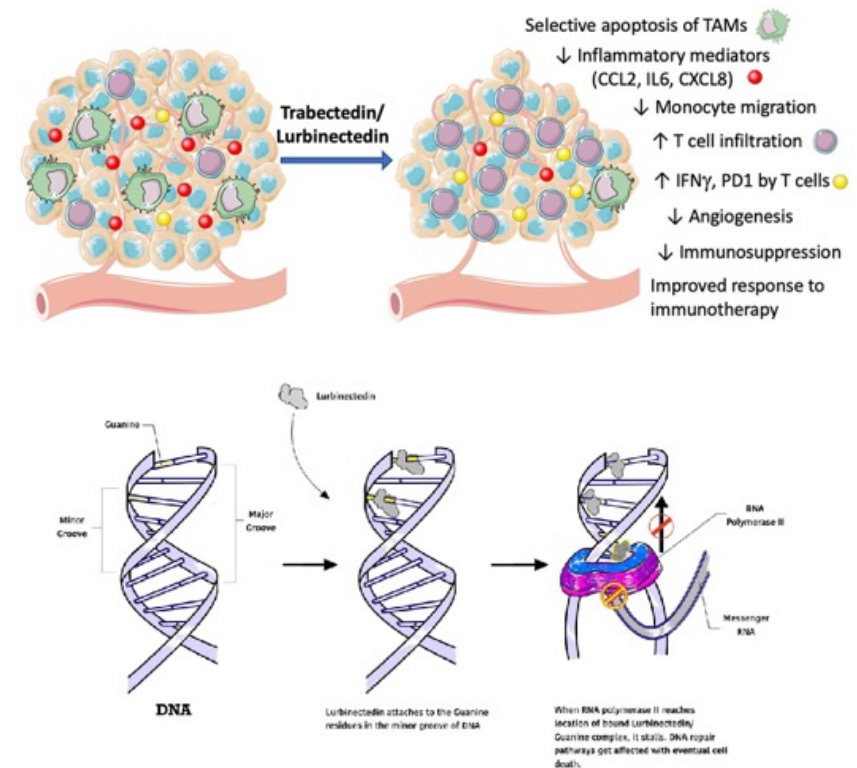
Small cell lung cancer (SCLC), also known as oat cell carcinoma, is a fast-growing and aggressive type of lung cancer that typically starts in the bronchi (airways) of the lungs. It's considered the most aggressive form of lung cancer, often spreading quickly to other parts of the body.



Atezolizumab ist ein monoklonaler Antikörper, der zur Behandlung verschiedener Krebsarten eingesetzt wird, insbesondere von nicht-kleinzelligem Lungenkrebs (NSCLC) und Urothelkarzinom. Er gehört zur Gruppe der PD-L1-Inhibitoren, die die Interaktion zwischen dem PD-L1-Protein auf Tumorzellen und dem PD-1-Rezeptor auf Immunzellen blockieren, was die Aktivität des Immunsystems gegen den Tumor verstärken kann.



Lurbinectedin ist ein Medikament, das bei Erwachsenen mit kleinzelligem Lungenkrebs (SCLC) eingesetzt wird, insbesondere wenn die Krankheit fortgeschritten ist oder bei der platinbasierten Chemotherapie nicht mehr wirksam ist. Es handelt sich um einen Zellgift eine Alkylanz, die sich an die DNA bindet und dadurch bestimmte Zellprozesse stört.



## Efficacy and safety of first-line maintenance therapy with lurbinectedin plus atezolizumab in extensive-stage small-cell lung cancer (IMforte): a randomised, multicentre, open-label, phase 3 trial

### Summary

**Background** Despite improved efficacy with first-line immune checkpoint inhibitors plus platinum-based chemotherapy for extensive-stage small-cell lung cancer (ES-SCLC), survival remains poor. In this study, we aimed to compare lurbinectedin plus atezolizumab and atezolizumab alone as maintenance therapies in patients with ES-SCLC without progression after induction therapy with atezolizumab, carboplatin, and etoposide.

**Methods** IMforte was a randomised, open-label, phase 3 trial done at 96 hospitals and medical centres in 13 countries (Belgium, Germany, Greece, Hungary, Italy, Mexico, Poland, South Korea, Spain, Taiwan, Türkiye, the UK, and the USA). Eligible patients were aged 18 years or older with treatment-naïve ES-SCLC. Patients received four 21-day cycles of induction treatment (atezolizumab, carboplatin, and etoposide). After completing induction treatment, eligible patients without disease progression were randomly assigned (1:1) using permuted blocks (Interactive Voice/Web Response System) to receive maintenance treatment intravenously every 3 weeks with lurbinectedin ( $3 \cdot 2 \text{ mg/m}^2$ ; with granulocyte colony-stimulating factor prophylaxis) plus atezolizumab (1200 mg) or atezolizumab (1200 mg). The two primary endpoints were independent review facility-assessed (IRF) progression-free survival and overall survival, measured from randomisation into the maintenance phase. Efficacy endpoints were assessed in the full analysis set, which included all patients who were randomly assigned to maintenance phase treatment, regardless of whether they received their assigned study treatment. Safety was assessed in all patients who received at least one dose of lurbinectedin or atezolizumab, and was analysed according to the treatment received. This study is registered with ClinicalTrials.gov, NCT05091567, and is closed for recruitment.

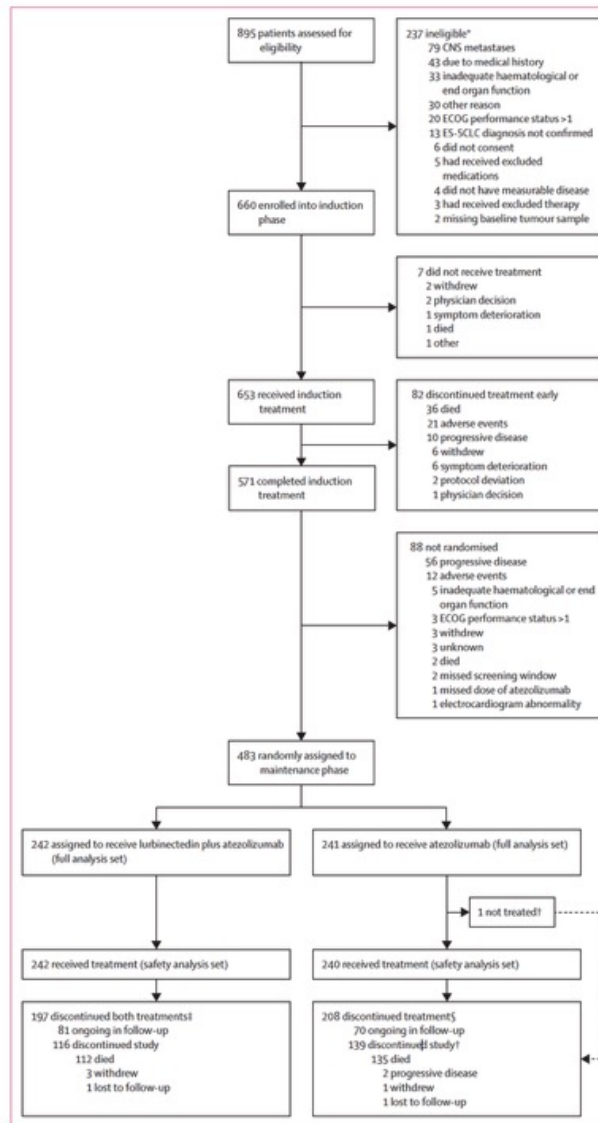
**Findings** Between Nov 17, 2021, and Jan 11, 2024, 895 patients were screened for enrolment, of whom 660 (74%) were enrolled into the induction phase. Between May 24, 2022, and April 30, 2024, 483 (73%) of 660 patients entered the maintenance phase and were randomly assigned to lurbinectedin plus atezolizumab (n=242) or atezolizumab (n=241). At the data cutoff (July 29, 2024), IRF progression-free survival was longer in the lurbinectedin plus atezolizumab group than the atezolizumab group (stratified hazard ratio [HR] 0·54 [95% CI 0·43–0·67];  $p < 0·0001$ ), as was overall survival (stratified HR 0·73 [0·57–0·95];  $p = 0·017$ ). 92 (38%) of 242 patients in the lurbinectedin plus atezolizumab group and 53 (22%) of 240 patients in the atezolizumab group had grade 3–4 adverse events. The most common grade 3–4 events in the lurbinectedin plus atezolizumab group were anaemia (20 [8%] of 242 patients), decreased neutrophil count (18 [7%] patients), and decreased platelet count (18 [7%] patients) and the most common events in the atezolizumab group were hyponatremia (five [2%] of 240 patients), dyspnoea (four [2%] patients), and pneumonia (four [2%] patients). Grade 5 adverse events occurred in 12 (5%) of 242 patients in the lurbinectedin plus atezolizumab group and six (3%) of 240 patients in the atezolizumab group. The incidence of myelosuppressive toxicities (eg, neutropenia and leukopenia) was higher in the lurbinectedin plus atezolizumab group than the atezolizumab group.

**Interpretation** IRF progression-free survival and overall survival were longer in the lurbinectedin plus atezolizumab group than the atezolizumab group for patients with ES-SCLC, albeit with a higher incidence of adverse events. Lurbinectedin plus atezolizumab represents a novel therapeutic option for first-line maintenance treatment in this setting.



**Figure 1: Trial profile**

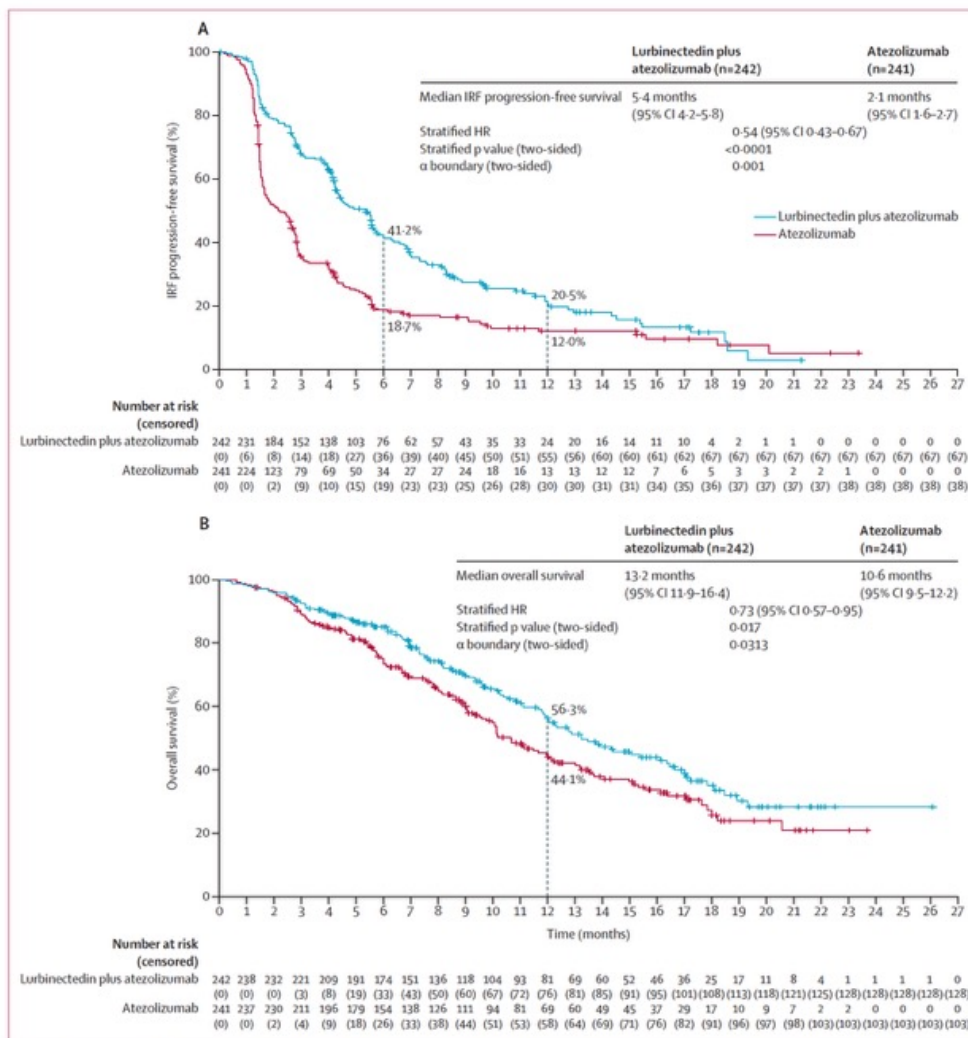
ECOG=Eastern Cooperative Oncology Group. ES-SCLC=extensive-stage small-cell lung cancer. \*Two patients were enrolled after their second screening and were therefore counted as ineligible at screening and as enrolled. Additionally, one patient was deemed ineligible at screening twice. †One patient was not treated and had discontinued the study. ‡198 patients in the lurbinectedin plus atezolizumab group discontinued lurbinectedin and 197 patients in the lurbinectedin plus atezolizumab group discontinued atezolizumab. Reasons for discontinuation of lurbinectedin were progressive disease (n=155), death (n=16), adverse events (n=13), withdrawal (n=8), deterioration of symptoms (n=5), and physician's decision (n=1). Reasons for discontinuation of atezolizumab were progressive disease (n=160), death (n=16), adverse events (n=6), withdrawal (n=9), deterioration of symptoms (n=5), and physician's decision (n=1). §208 patients in the atezolizumab group discontinued treatment. Reasons for discontinuation of atezolizumab were progressive disease (n=185), death (n=6), adverse events (n=9), deterioration of symptoms (n=5), withdrawal (n=2), and physician's decision (n=1).



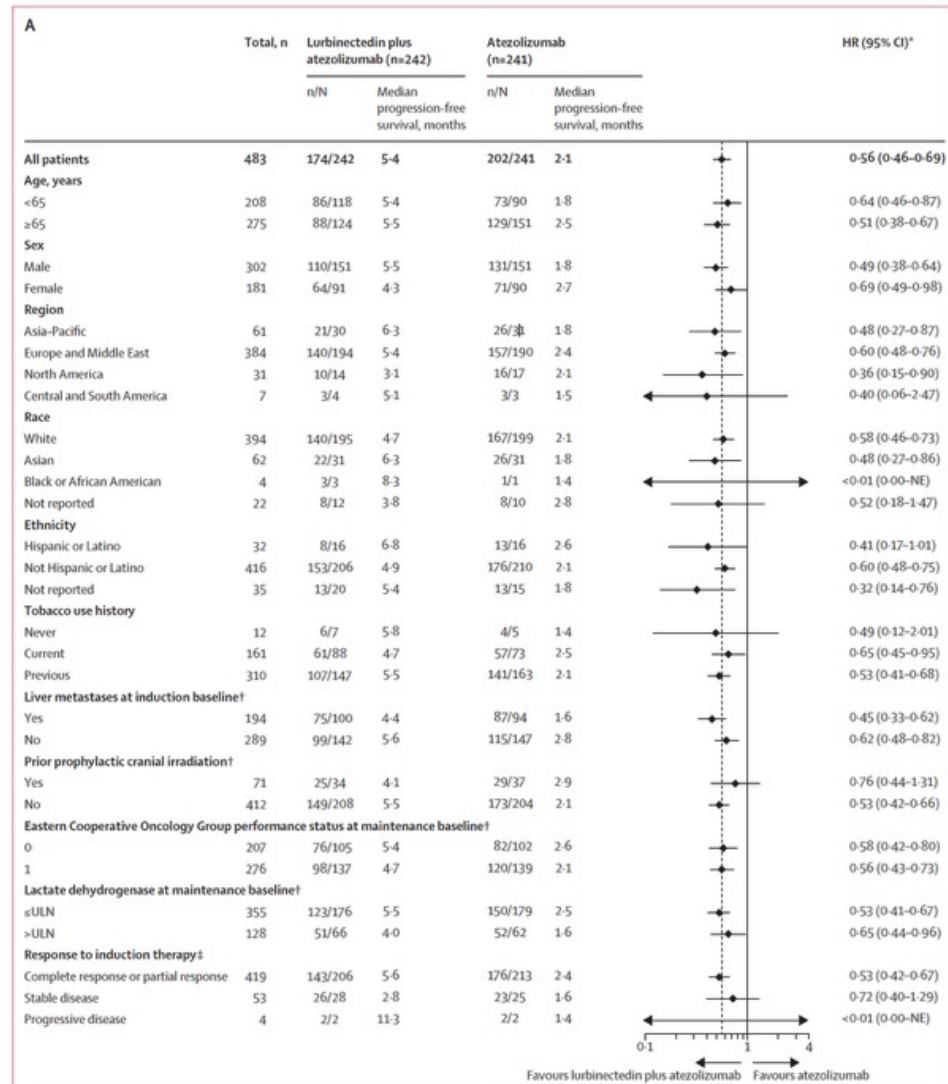
	Lurbinectedin plus atezolizumab (n=242)	Atezolizumab (n=241)
Age, years	65.0 (60.0-71.0)	67.0 (61.0-72.0)
<65 years	118 (49%)	90 (37%)
≥65 years	124 (51%)	151 (63%)
Sex		
Male	151 (62%)	151 (63%)
Female	91 (38%)	90 (37%)
Region		
Asia-Pacific	30 (12%)	31 (13%)
Europe and Middle East	194 (80%)	190 (79%)
North America	14 (6%)	17 (7%)
Central and South America	4 (2%)	3 (1%)
Race		
White	195 (81%)	199 (83%)
Asian	31 (13%)	31 (13%)
Black or African American	3 (1%)	1 (<1%)
American Indian or Alaska Native	1 (<1%)	0
Not reported	12 (5%)	10 (4%)
Ethnicity		
Hispanic or Latino	16 (7%)	16 (7%)
Not Hispanic or Latino	206 (85%)	210 (87%)
Not reported	20 (8%)	15 (6%)
Tobacco use history		
Never	7 (3%)	5 (2%)
Current	88 (36%)	73 (30%)
Previous	147 (61%)	163 (68%)
Liver metastases at induction baseline*		
Yes	100 (41%)	94 (39%)
No	142 (59%)	147 (61%)
Previous prophylactic cranial irradiation*		
Yes	34 (14%)	37 (15%)
No	208 (86%)	204 (85%)
Eastern Cooperative Oncology Group performance status at maintenance baseline*		
0	105 (43%)	102 (42%)
1	137 (57%)	139 (58%)
Lactate dehydrogenase at maintenance baseline*		
≤ULN	176 (73%)	179 (74%)
>ULN	66 (27%)	62 (26%)
Time from day 1 of induction cycle 1 to randomisation, months	3.2 (2.9-3.5)	3.2 (3.0-3.5)
Response to induction therapy†		
Complete response or partial response	206/236 (87%)	213/240 (89%)
Stable disease	28/236 (12%)	25/240 (10%)
Progressive disease	2/236 (1%)	2/240 (1%)

Data are median (IQR), n (%), or n/N (%). ULN=upper limit of normal. \*Data were obtained from electronic case-report forms. †Seven randomly assigned patients did not have a maintenance screening tumour assessment.

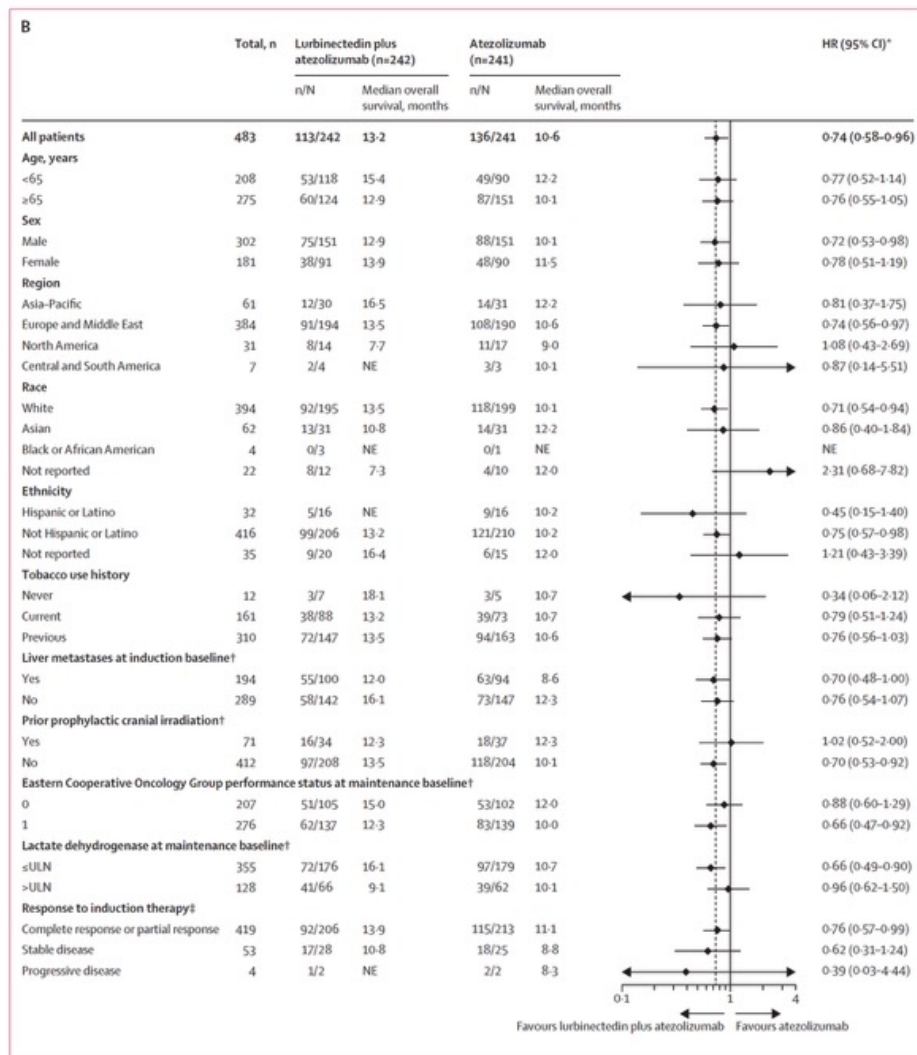
**Table 1: Baseline characteristics in the full analysis set (n=483)**



**Figure 2:** IRF progression-free survival and overall survival from randomisation into the maintenance phase in the full analysis set  
Kaplan-Meier estimates of IRF progression-free survival (A) and overall survival (B) in the full analysis set. Stratification factors included in the stratified p value and Cox model are the same stratification factors used for randomisation. Censored events are indicated with a + symbol. HR=hazard ratio. IRF=independent review facility-assessed.



(Figure 3 continues on next page)



**Figure 3:** Subgroup analysis of IRF progression-free survival (A) and overall survival (B)

IRF=independent review facility-assessed. n=events. N=number of patients. HR=hazard ratio. NE=not estimable. ULN=upper limit of normal. \*HRs are unstratified.

†Data were determined from electronic case report forms. ‡Seven randomised patients did not have a maintenance screening tumour assessment.

	Lurbinectedin plus atezolizumab (n=242)	Atezolizumab (n=240)
Patients with ≥1 adverse event	235 (97%)	194 (81%)
Treatment-related adverse events	202 (83%)	96 (40%)
Grade 3-4 adverse events	92 (38%)	53 (22%)
Treatment-related grade 3-4 adverse events	62 (26%)	14 (6%)
Grade 5 adverse events	12 (5%)	6 (3%)
Treatment-related grade 5 adverse events	2 (1%)	1 (<1%)
Serious adverse events	75 (31%)	41 (17%)
Treatment-related serious adverse events	28 (12%)	9 (4%)
Adverse events leading to treatment discontinuation of any study drug	15 (6%)	8 (3%)
Adverse events leading to dose interruption/modification of any study drug	92 (38%)	33 (14%)
Adverse events of special interest for lurbinectedin	93 (38%)	62 (26%)
Grade 3-4	18 (7%)	12 (5%)
Grade 5	7 (3%)	4 (2%)
Serious	28 (12%)	16 (7%)
Adverse events of special interest for atezolizumab	76 (31%)	54 (23%)
Grade 3-4	15 (6%)	8 (3%)
Grade 5	0	0
Serious	10 (4%)	5 (2%)
Requiring corticosteroids	40 (17%)	18 (8%)

Data are n (%).

**Table 2:** Adverse events during the maintenance phase (safety analysis set; n=482)

	Lurbinectedin plus atezolizumab (n=242)	Atezolizumab (n=240)
Anaemia	20 (8%)	2 (1%)
Decreased neutrophil count	18 (7%)	0
Decreased platelet count	17 (7%)	0
Neutropenia	11 (5%)	1 (<1%)
Thrombocytopenia	11 (5%)	1 (<1%)
Fatigue	8 (3%)	3 (1%)
Nausea	6 (2%)	2 (1%)
Increased alanine transaminase	6 (2%)	1 (<1%)
Dyspnoea	5 (2%)	4 (2%)
Pneumonia	5 (2%)	4 (2%)
Hypokalaemia	5 (2%)	3 (1%)
Decreased white blood cell count	5 (2%)	0
Hyponatremia	3 (1%)	5 (2%)

Data are n (%). All events that occurred in at least 2% of patients in either group are shown.

**Table 3:** Grade 3-4 adverse events

## Research in context

### Evidence before this study

Extensive-stage small-cell lung cancer (ES-SCLC), which accounts for approximately 15% of lung cancers, is an aggressive and highly lethal disease. The current standard of care is induction therapy with a combination of etoposide, platinum chemotherapy, and immunotherapy, followed by maintenance therapy with the same immunotherapy agent, based on the findings from the IMpower133 and CASPIAN trials, which showed significant improvements in overall survival and progression-free survival with atezolizumab or durvalumab, respectively, compared with chemotherapy alone. IMforte was designed to improve patient outcomes using a novel treatment approach in the first-line maintenance therapy setting. We searched PubMed on Feb 28, 2025, for publications describing phase 3 studies of first-line maintenance therapy in ES-SCLC published in English between Jan 1, 2011, and Dec 31, 2021, using the combined search terms “extensive-stage small-cell lung cancer”, “extensive-disease small-cell lung cancer”, “maintenance”, “first-line”, “phase 3”, and “phase III”. Our search identified two phase 3 trials of maintenance therapy: CheckMate 451, involving maintenance therapy with nivolumab or nivolumab plus ipilimumab, and MERU, involving maintenance therapy with rovalpituzumab tesirine, an antibody-drug conjugate targeting delta-like ligand 3. Although progression-free survival was favourable compared with placebo in both studies, formal statistical testing was not done, and neither study was able to demonstrate significant improvement in overall survival with experimental treatment. MERU met futility for overall survival and was discontinued early.

### Added value of this study

To our knowledge, IMforte is the first phase 3 trial to meet the primary endpoints of progression-free survival and overall survival in the first-line maintenance setting in ES-SCLC. In IMforte, compared with patients in the atezolizumab group, patients in the lurbinectedin plus atezolizumab group had statistically significant and clinically meaningful improvement in both independently-assessed progression-

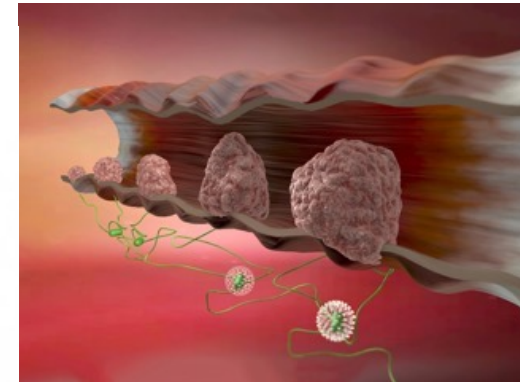
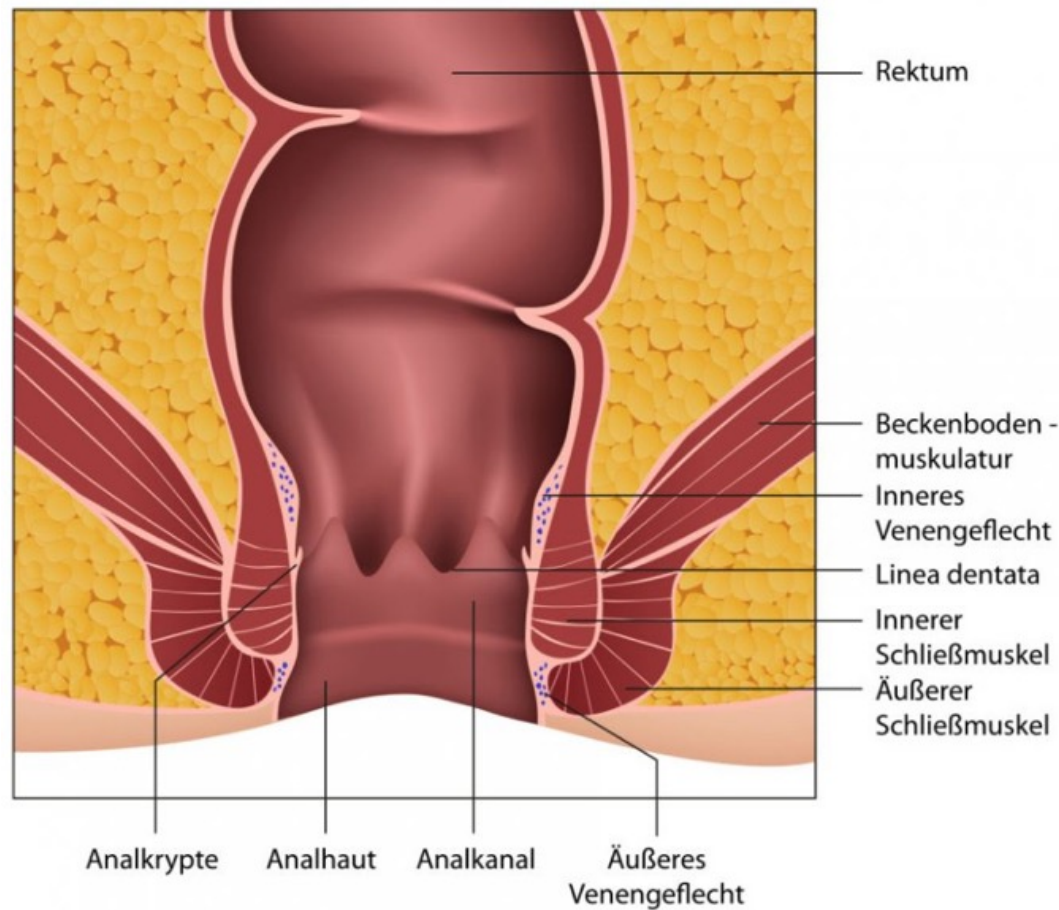
free survival and overall survival, with a 46% reduction in the risk of disease progression or death and a 27% reduction in the risk of death versus atezolizumab alone as the active comparator in first-line maintenance treatment. Although the incidence of adverse events was higher in the lurbinectedin plus atezolizumab group than the atezolizumab group, the safety profile of the combination was considered manageable and consistent with the known safety profiles of each agent, with no new safety signals identified. These findings build on the regimen of atezolizumab combined with platinum-based chemotherapy followed by atezolizumab maintenance therapy that was first established as a standard of care based on the results of IMpower133 in 2019.

### Implications of all the available evidence

Due to the high attrition rate in ES-SCLC, effective first-line treatment strategies are crucial to improve the prognosis of this aggressive disease. Patients whose disease did not progress on induction therapy with atezolizumab, etoposide, and carboplatin and who were administered lurbinectedin plus atezolizumab in the maintenance phase had significantly longer independent review facility-assessed progression-free survival and overall survival compared with those given maintenance atezolizumab alone. When putting IMforte into context with previous trials that have shown significant improvement in study outcomes with experimental treatment in the first-line setting of ES-SCLC (eg, IMpower133 and CASPIAN) it is important to note that in IMforte, progression-free survival and overall survival were measured from randomisation into the maintenance phase rather than from the start of the induction phase, and patients randomly assigned to maintenance treatment had favourable outcomes from induction therapy (ie, without early disease progression and without significant toxicity from induction therapy). The clinical benefits observed in IMforte highlight the potential of lurbinectedin plus atezolizumab as a new first-line maintenance treatment for patients with ES-SCLC, a population for whom improved treatment outcomes are urgently needed.



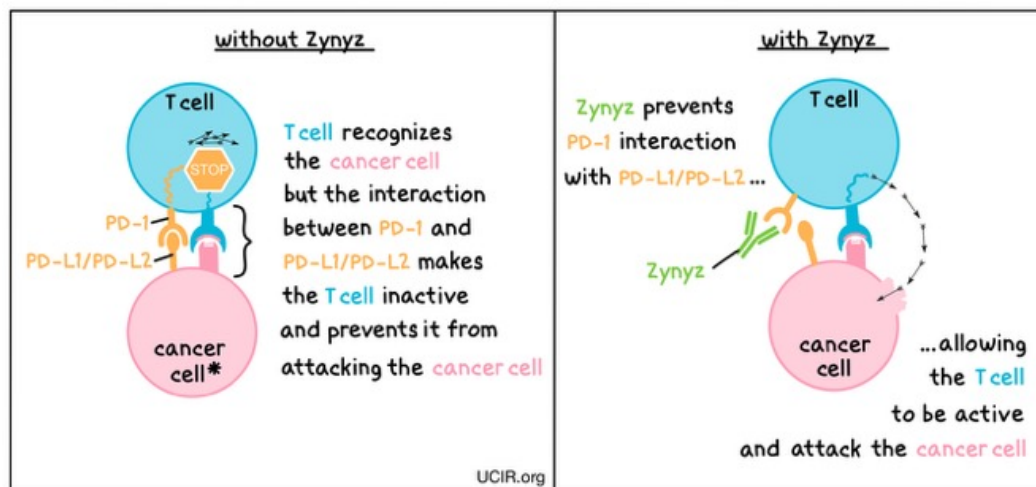
Ein Analkanalkarzinom ist eine bösartige Neubildung im Analkanal, dem Teil des Darms, der den Enddarm mit dem Anus verbindet. Es ist eine relativ seltene Krebsart, aber es gibt eine Reihe von Faktoren, die das Risiko erhöhen, darunter **Infektionen mit humanen Papillomviren (HPV)**.



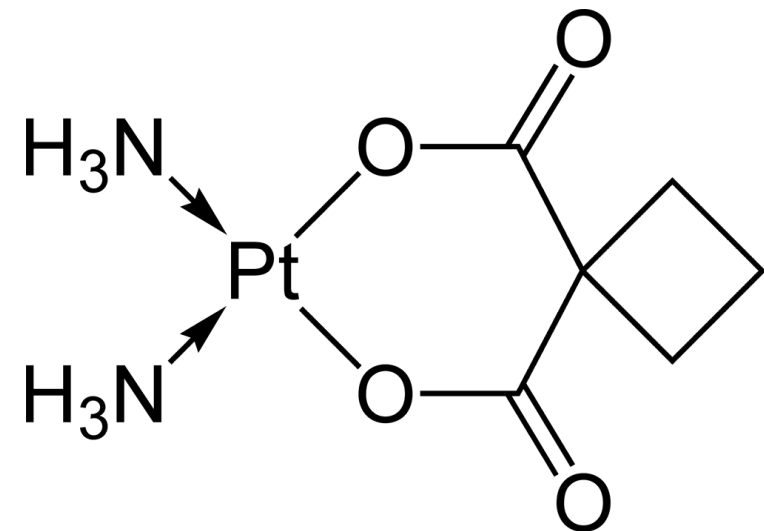


Retifanlimab ist ein Antikörper, der bei der Behandlung von Merkelzellkarzinom (MCC) eingesetzt wird. Er ist ein monoklonaler Antikörper, der den programmierten Zelltod-Rezeptor 1 (PD-1) blockiert, was die Immunantwort des Körpers gegen Krebszellen verstärkt.

Carboplatin ist ein sehr verbreitetes Zytostatikum (Mittel zur Bekämpfung von Krebserkrankungen). Die chemische Struktur enthält ein komplex gebundenes Platinatom, es handelt sich um einen Cisplatin-Abkömmling. Die Wirkung gegen Krebszellen beruht auf einer Vernetzung der DNA-Moleküle (Erbsubstanz), die dadurch funktionsunfähig werden.



\*other cells within the tumor mass or elsewhere can also display PD-L1/PD-L2 on their surface and make T cells inactive



# Retifanlimab with carboplatin and paclitaxel for locally recurrent or metastatic squamous cell carcinoma of the anal canal (POD1UM-303/InterAACT-2): a global, phase 3 randomised controlled trial

## Summary

**Background** Retifanlimab has activity in programmed death ligand 1-positive advanced squamous cell anal carcinoma (SCAC) that has progressed on platinum chemotherapy. We aimed to prospectively assess the benefit of adding retifanlimab to initial carboplatin–paclitaxel for this disease.

**Methods** This global, multicentre, double-blind, randomised, controlled, phase 3 trial was done at 70 centres in 12 countries across the EU, Australia, Japan, the UK, and the USA. Patients aged  $\geq 18$  years with inoperable locally recurrent or metastatic SCAC, an Eastern Cooperative Oncology Group performance status of 0 or 1, no previous systemic therapy, and well controlled HIV (ie, CD4+ count  $>200/\mu\text{L}$  and undetectable viral load) were eligible. Patients were randomly assigned (1:1) to retifanlimab (500 mg intravenous) or placebo every 4 weeks with standard carboplatin–paclitaxel for up to 1 year. Patients in the placebo group could cross over to retifanlimab monotherapy on confirmed disease progression. The primary endpoint was independently assessed progression-free survival (ie, time from date of randomisation to date of first documented progressive disease or death due to any cause) per Response Evaluation Criteria in Solid Tumours version 1.1. Efficacy was assessed by intention to treat. This trial is registered with ClinicalTrials.gov (NCT04472429) and EUDRA-CT (2020–000826–24) and is active but closed to enrolment.

**Findings** Between Nov 12, 2020, and July 3, 2023, 376 patients were assessed for eligibility and 308 were randomly assigned to retifanlimab plus carboplatin–paclitaxel (n=154) or placebo plus carboplatin–paclitaxel (n=154). 222 (72%) of 308 patients were female and 86 (28%) were male. Median progression-free survival was 9·3 months (95% CI 7·5–11·3) in the retifanlimab group and 7·4 months (7·1–7·7) in the placebo group (hazard ratio 0·63 [95% CI 0·47–0·84]; one-sided p=0·0006). Serious and grade 3 or worse adverse events were more frequent in the retifanlimab plus carboplatin–paclitaxel group compared with the placebo plus carboplatin–paclitaxel group (47·4% vs 38·8% and 83·1% vs 75·0%, respectively). The most common grade  $\geq 3$  adverse events were neutropenia (35·1% for retifanlimab plus carboplatin–paclitaxel vs 29·6% for placebo plus carboplatin–paclitaxel) and anaemia (19·5% vs 20·4%). Four fatal adverse events occurred in the retifanlimab plus carboplatin–paclitaxel group, only one (pancytopenia) of which was treatment related. One fatal adverse event occurred in the placebo plus carboplatin–paclitaxel group and was not treatment related.

**Interpretation** Retifanlimab provides clinical benefit, with a manageable safety profile, when added to first-line chemotherapy in advanced squamous cell carcinoma of the anal canal. These results suggest retifanlimab with carboplatin plus paclitaxel should be considered as the new standard of care for patients with advanced squamous cell anal carcinoma.

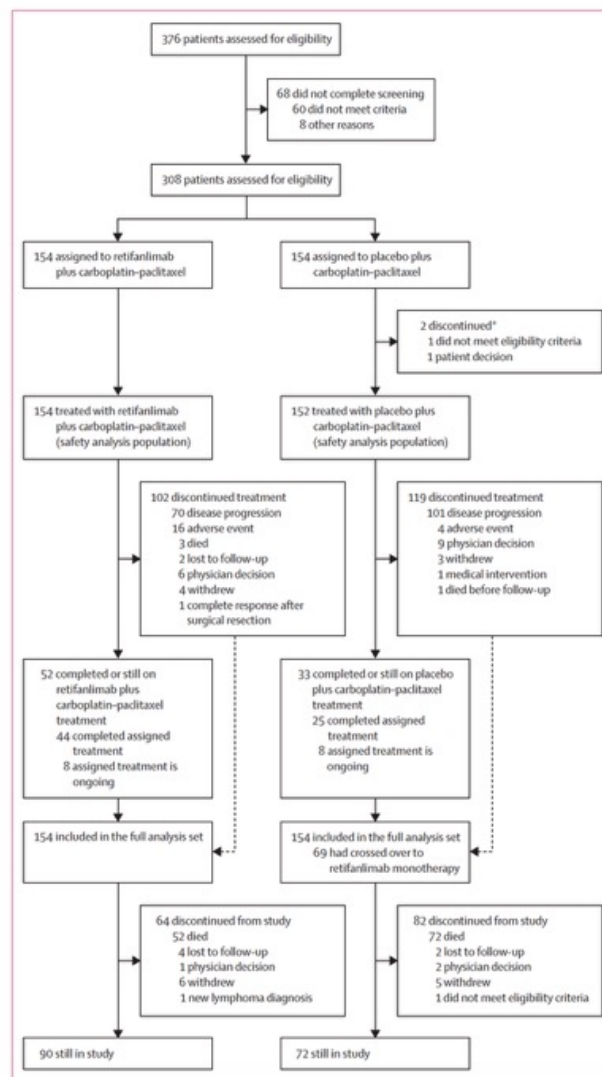


Figure 1: Trial profile

\*Two patients included in full analysis set for overall survival.

	Retifanlimab plus carboplatin-paclitaxel (n=154)	Placebo plus carboplatin-paclitaxel (n=154)
Age, years	62 (29–86)	61 (35–84)
Sex		
Female	104 (68%)	118 (77%)
Male	50 (32%)	36 (23%)
Race		
White	132 (86%)	137 (89%)
Black or African American	3 (2%)	2 (1%)
Asian	10 (6%)	8 (5%)
Other	3 (2%)	2 (1%)
Geographical location		
Australia, the EU, North America, or the UK	146 (95%)	146 (95%)
Rest of the world	8 (5%)	8 (5%)
Previous radiotherapy	104 (68%)	113 (73%)
Locally recurrent disease	28 (18%)	27 (18%)
Metastatic disease*	126 (82%)	127 (82%)
Liver	55 (36%)	56 (36%)
ECOG PS 0	82 (53%)	86 (56%)
HIV positive	6 (4%)	5 (3%)
HPV status†		
Positive	29 (19%)	28 (18%)
Negative	3 (2%)	4 (3%)
Unknown or missing	122 (79%)	122 (79%)
P16 status‡		
Positive	76 (49%)	74 (48%)
Negative	16 (10%)	15 (10%)
Indeterminate or missing	62 (40%)	65 (42%)
PD-L1 expression status ≥1*§	139 (91%)	140 (91%)

Data are median (range) or n (%). ECOG PS=Eastern Cooperative Oncology Group performance status. HPV=human papillomavirus. PD-L1=programmed cell death ligand 1. \*Stratification factor. †Samples available from local testing. ‡Samples available from central testing. §PD-L1 expression <1 also includes patients with non-evaluable tumour tissue; PD-L1 expression data were unavailable for three patients in the retifanlimab plus carboplatin-paclitaxel group and seven in the placebo plus carboplatin-paclitaxel group.

Table 1: Baseline demographics and disease characteristics

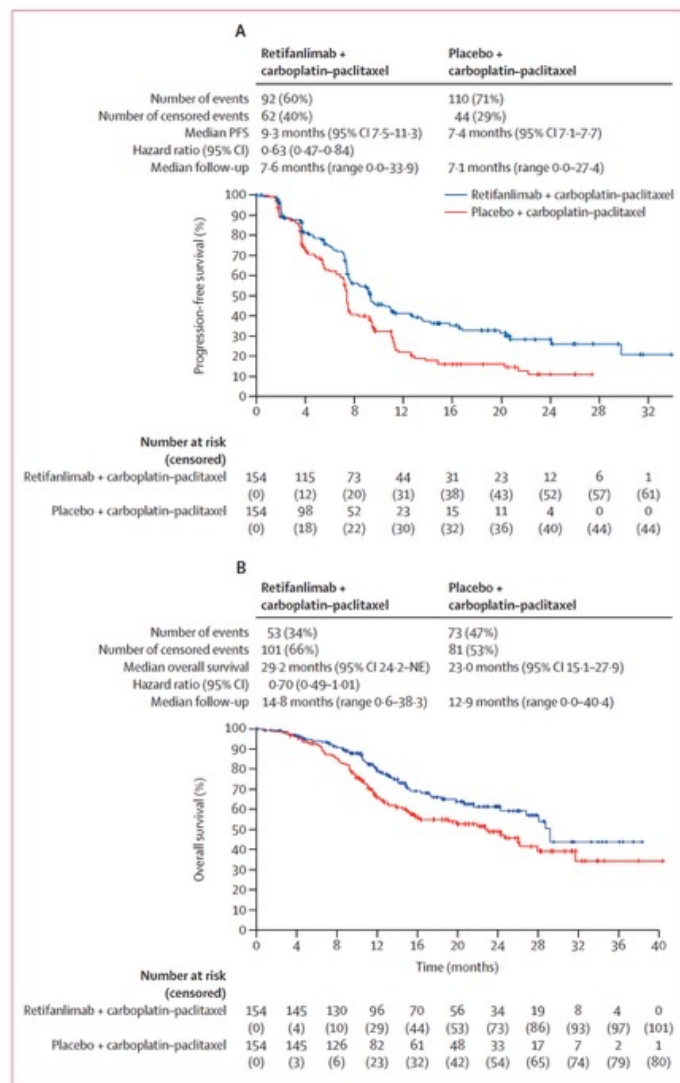


Figure 2: Kaplan-Meier analysis of progression-free survival (A) and overall survival (B) in the full analysis set  
NE=not evaluable, PFS=progression-free survival

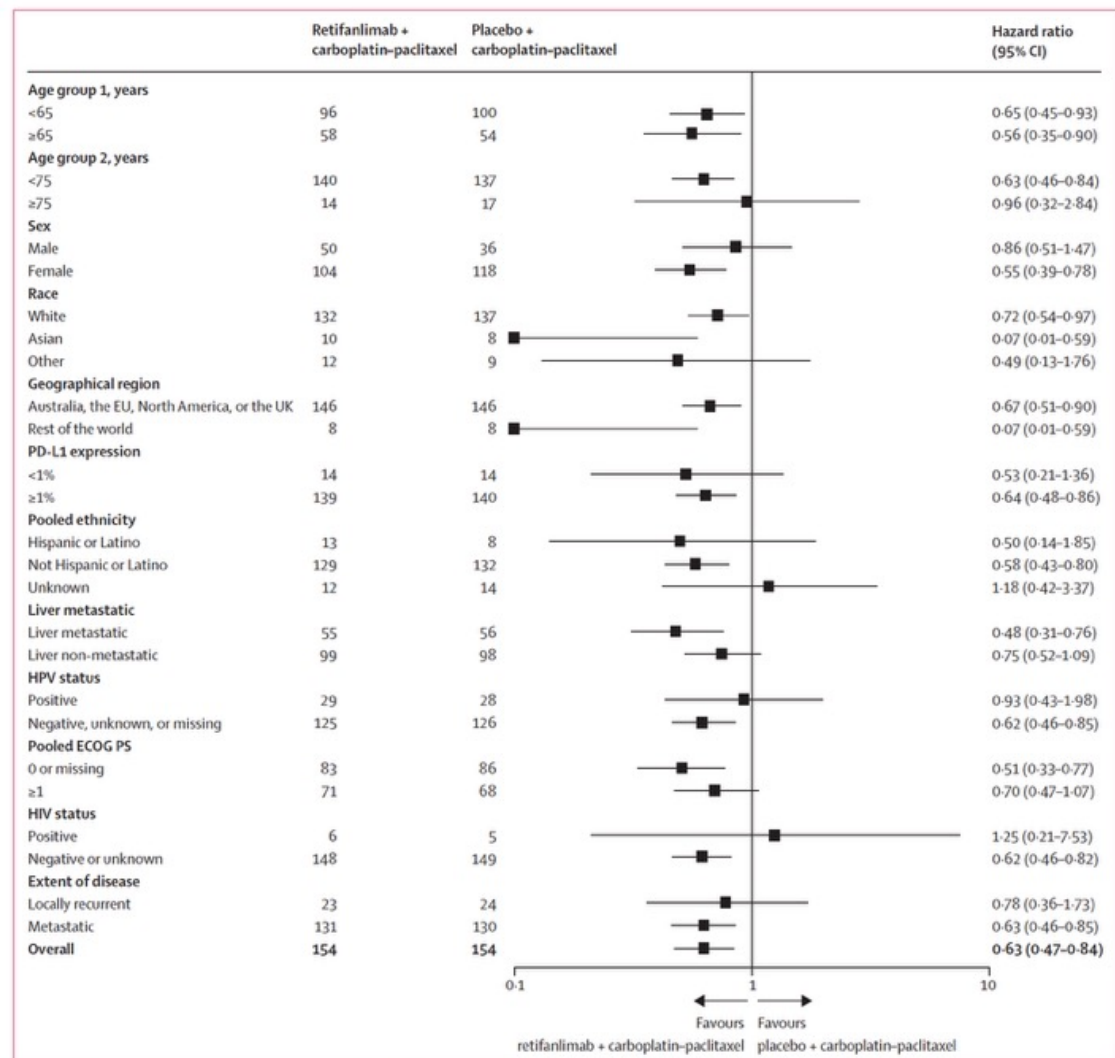


Figure 3: Forest plot of progression-free survival by masked independent central review in the full analysis set  
ECOG PS=Eastern Cooperative Oncology Group performance status. HPV=human papillomavirus. PD-L1=programmed death ligand 1.



	Retifanlimab plus carboplatin- paclitaxel (n=154)	Placebo plus carboplatin- paclitaxel (n=152)	Total (n=306)
Treatment duration, months	7.4 (0.03–14.6)	6.8 (0.03–14.6)	7.2 (0.03–14.6)
Patients with any adverse events	154 (100%)	152 (100%)	306 (100%)
Patients with grade $\geq 3$ adverse events	128 (83%)	114 (75%)	242 (79%)
Deaths	4 (3%)*	1 (1%)†	5 (2%)
Patients with serious adverse events	73 (47%)	59 (39%)	132 (43%)
Treatment-related serious adverse events	25 (16%)	10 (7%)	35 (11%)
Immune-related adverse events	75 (49%)	40 (26%)	115 (38%)
Adverse events leading to discontinuation of retifanlimab or placebo	17 (11%)	4 (3%)	21 (7%)

Data are median (range) or n (%). \*Events were metastases to peritoneum (n=1), pancytopenia (n=1), pneumonia (n=1), and sepsis (n=1). †Fatal pneumonia.

**Table 2: Summary of safety**

## Research in context

### Evidence before this study

We searched ClinicalTrials.gov from database inception to Nov 12, 2024, for phase 3 clinical trials of systemic therapies for the treatment of advanced squamous cell carcinoma of the anal canal (SCAC) using the keywords “squamous cell carcinoma of the anal canal” or “anal cancer, squamous cell carcinoma” (Condition/disease) and “systemic therapy” (Other terms), and filtered by phase 3 studies. To our knowledge, there are no US Food and Drug Administration-approved therapies, and treatment options for patients with advanced SCAC have remained largely unchanged over several decades due to few studies being done in this patient population. Carboplatin with weekly paclitaxel is the current recommended regimen based on the phase 2 InterAACT trial results and European Society for Medical Oncology and National Comprehensive Cancer Network guidelines. However, the progression-free survival and overall survival with this regimen are short (8.1 months and 20.0 months, respectively). Retifanlimab is an anti-programmed cell death-1 (PD-1) humanised monoclonal antibody that is approved in the USA and Europe for advanced Merkel cell carcinoma. Retifanlimab showed improved clinical responses and a favourable safety profile compared with previous salvage chemotherapy in a phase 2 study of patients with platinum-refractory advanced SCAC. The aforementioned studies have led to the phase 3 study of retifanlimab in combination with standard-of-care chemotherapy in patients with advanced SCAC reported here.

### Added value of this study

The phase 3 POD1UM-303/InterAACT-2 study evaluated the ability of retifanlimab to provide additive benefit to standard-of-care chemotherapy in patients with locally advanced or

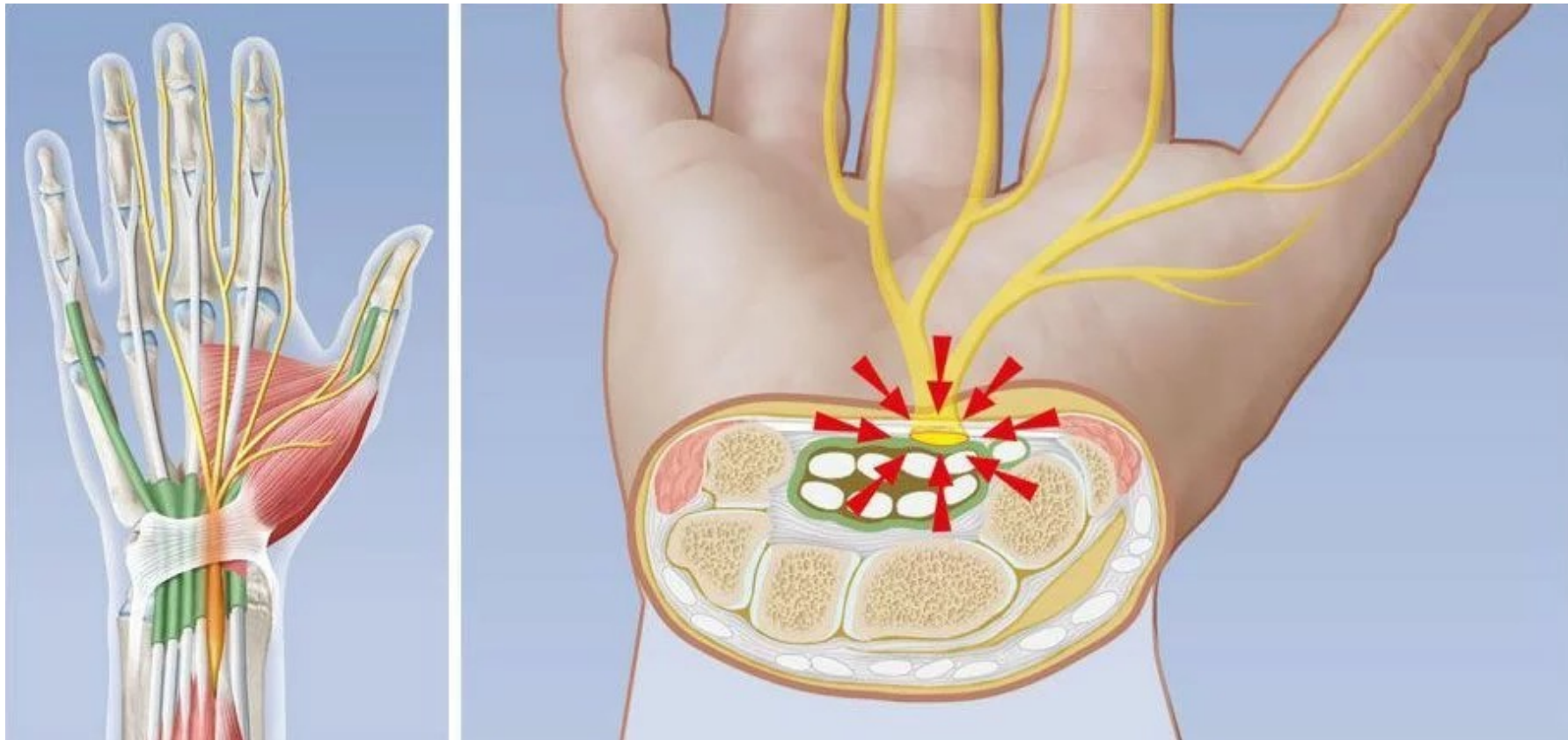
metastatic SCAC not previously treated with systemic therapy. Although the current standard-of-care platinum-based chemotherapy provides high initial response rates, patients commonly experience disease progression and have short median survival times, highlighting an unmet medical need. To our knowledge, this is the first and largest well controlled trial in recurrent or metastatic SCAC, a rare disease.

The addition of retifanlimab to carboplatin–paclitaxel led to significantly longer median progression-free survival than placebo plus carboplatin–paclitaxel, with a consistent benefit in favour of retifanlimab plus chemotherapy observed for all subgroup comparisons. At the interim analysis, despite the immature data, results suggested a possible improvement of overall survival. Similar rates of carboplatin–paclitaxel dose interruption were observed in both groups, with higher rates of serious and grade  $\geq 3$  adverse events observed with retifanlimab that could be managed with standard measures and did not compromise administration of carboplatin–paclitaxel.

### Implications of all the available evidence

Data from our study demonstrate clinically meaningful improvements in survival and tumour control with retifanlimab plus carboplatin–paclitaxel compared with the current preferred carboplatin plus paclitaxel regimen in patients with previously untreated advanced SCAC. Retifanlimab with carboplatin plus paclitaxel should be considered as the new standard of care for this difficult-to-treat disease. Future studies could investigate the combination of retifanlimab with novel targeted agents added to standard-of-care chemotherapy for the treatment of patients with advanced SCAC including those with HIV who are most at risk for SCAC.

Durch den Karpaltunnel am Handgelenk verlaufen Sehnen und der Mittelnerv. Bei einem Karpaltunnelsyndrom schwillt das Gewebe im Karpaltunnel an. Drückt es auf den Mittelnerv, können Empfindungsstörungen und Schmerzen auftreten. Über- und Fehlbelastungen der Hand erhöhen das Risiko für ein Karpaltunnelsyndrom.



# Surgery versus corticosteroid injection for carpal tunnel syndrome (DISTRICTS): an open-label, multicentre, randomised controlled trial

## Summary

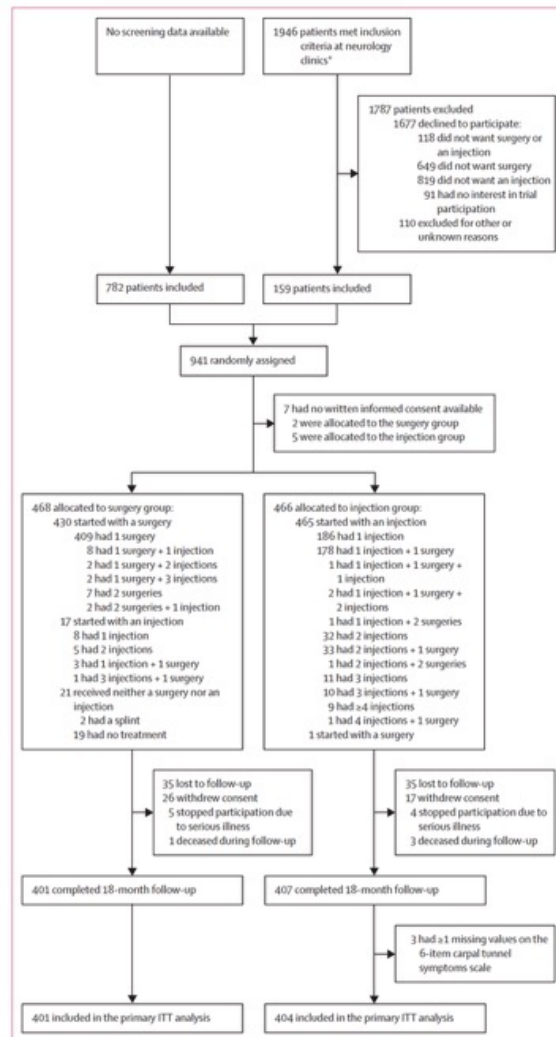
**Background** Surgery and corticosteroid injections are established treatments for carpal tunnel syndrome, but the optimal treatment strategy remains unclear. This study aimed to compare starting treatment with surgery versus starting with a corticosteroid injection.

**Methods** We conducted an open-label, randomised controlled trial across 31 hospitals in the Netherlands. Eligible patients, diagnosed with carpal tunnel syndrome for at least 6 weeks and confirmed by electrophysiological or sonographic testing, were randomly assigned (1:1) to start treatment with either surgery or an injection via a web-based system. Randomisation was stratified by unilateral or bilateral symptoms, carpal tunnel syndrome with or without concomitant disease as risk factor, and previous ipsilateral injections. If needed, additional treatments were allowed, such as additional injections or surgery. The primary outcome, assessed in the intention-to-treat population, was the proportion of patients who were recovered (defined as a score of less than eight points on the six-item carpal tunnel syndrome scale) at 18 months. The trial was preregistered with the ISRCTN Registry (ISRCTN13164336) and is now completed.

**Findings** From Nov 7, 2017, to Nov 4, 2021, 934 participants (545 female and 389 male participants) were included. 468 were randomised to the surgery group and 466 to the injection group. At 18 months, 805 (86%) of 934 participants had primary outcome data. In the surgery group, 243 (61%) of 401 participants had recovered, significantly higher than the 180 (45%) of 404 participants recovered in the injection group (relative risk 1.36; 95% CI 1.19–1.56;  $p < 0.0001$ ). One or more adverse event occurred in 376 (86%) of 436 participants in the surgery group and in 384 (85%) of 453 participants in the injection group. One participant in the surgery group was hospitalised due to complications. No treatment-related deaths were reported.

**Interpretation** In patients with carpal tunnel syndrome, initiating treatment with surgery offers a higher chance of recovery after 18 months compared with starting with a corticosteroid injection, even with the possibility of additional interventions.





**Figure 1: Trial profile**  
ITT=intention-to-treat. \*Due to logistical complexity, screening data were not completely registered. Eight recruiting hospitals registered patients with carpal tunnel syndrome that visited centralised outpatient clinics, a streamlined care process designed to deliver efficient and standardised diagnosis and treatment for patients, during their inclusion time period.

	Surgery group, n=468	Injection group, n=466
Sex		
Female	269 (57%)	276 (59%)
Male	199 (43%)	190 (41%)
Age, years*	59.0 (51.0–69.0)	58.0 (48.3–71.0)
BMI, kg/m <sup>2</sup> *	27.5 (24.9–31.6)	27.7 (25.2–31.3)
Unilateral or bilateral CTS		
Unilateral	175 (37%)	178 (38%)
Bilateral	293 (63%)	288 (62%)
Dominant side more severely affected*		
Yes	290 (62%)	286 (61%)
No	173 (37%)	176 (38%)
Duration of CTS symptoms, months*	8.0 (4.0–24.0)	9.0 (5.0–23.3)
CTS symptoms, in terms of a sensation of pins and needles (with or without pain) and numbness in median nerve innervated area of the hand		
Yes	467 (100%)	466 (100%)
No	1 (<1%)	0 (0%)
CTS symptoms at night, which wake the patient		
Yes	416 (89%)	416 (89%)
No	52 (11%)	50 (11%)
Worsening of CTS symptoms during specific hand or wrist movements*		
Yes	411 (88%)	414 (89%)
No	56 (12%)	52 (11%)
Neurological examination*		
Sensory disturbances	236 (50%)	244 (52%)
Paresis	87 (19%)	90 (19%)
Atrophy	80 (17%)	87 (19%)
Concomitant disease as risk factor for CTS		
Diabetes	48 (10%)	44 (9%)
Rheumatoid arthritis	17 (4%)	16 (3%)
Thyroid disease	30 (6%)	26 (6%)
Renal failure requiring dialysis	2 (<1%)	1 (<1%)
Anatomical abnormality at the carpal tunnel†	3 (1%)	2 (<1%)
Ipsilateral CTS injections >1 year ago	18 (4%)	19 (4%)
CTS symptom severity (CTS-6 sum score)*‡	19.0 (16.0–22.0)	18.0 (15.0–21.0)
Upper limb functioning (QuickDASH)*§	43.2 (27.3–56.8)	40.9 (27.3–56.8)

Data are n (%) or median (IQR). CTS=carpal tunnel syndrome. \*Data not available for all randomised participants (between two and eight participants missing per group). †Abnormality that could have induced changes in structures at the level of the carpal tunnel (eg. space-occupying lesion or status after trauma or surgery). ‡The CTS-6 score is a disease-specific six-item scale that measures symptoms for a typical 24-h period during the past 2 weeks; the sum score ranges from six (best) to 30 (worst). §The QuickDASH is an 11-item measure of upper limb functioning. The score ranges from 0 (no disability) to 100 (most severe disability).

**Table 1: Demographical and baseline clinical characteristics**



	Surgery group	Injection group	Mean difference (95% CI)	p value
<b>Primary outcome after 18 months</b>				
Recovered	243/401 (61%)	180/404 (45%)	1.36 (1.19 to 1.56)*	<0.0001
<b>Secondary outcomes after 18 months</b>				
QuickDASH score	12.45 (10.78 to 14.11)	19.80 (17.76 to 21.84)	-7.35 (-9.99 to -4.72)	-
Participants' global perception of recovery†	6.21 (6.08 to 6.34)	5.43 (5.25 to 5.60)	0.78 (0.57 to 1.00)	-
Participants' satisfaction†	5.94 (5.80 to 6.11)	5.33 (5.16 to 5.51)	0.61 (0.37 to 0.84)	-
<b>Interventions‡</b>				
Surgeries	443	230	-	-
Injections	44	617	-	-

Data are n, n/N (%) or mean (95% CI), unless otherwise specified. p values are from  $\chi^2$  tests. \*Data are relative risk (95% CI). †Participants' global perception of recovery and participants' satisfaction were measured with seven-point Likert-type items of 1 (much worse), 2 (worse), 3 (a little worse), 4 (similar), 5 (a little improved), 6 (improved), or 7 (vastly improved) and 1 (very dissatisfied), 2 (dissatisfied), 3 (a little dissatisfied), 4 (similar), 5 (a little satisfied), 6 (satisfied), and 7 (very satisfied). ‡Some participants had more than one of each intervention (figure 1).

Table 2: Outcomes

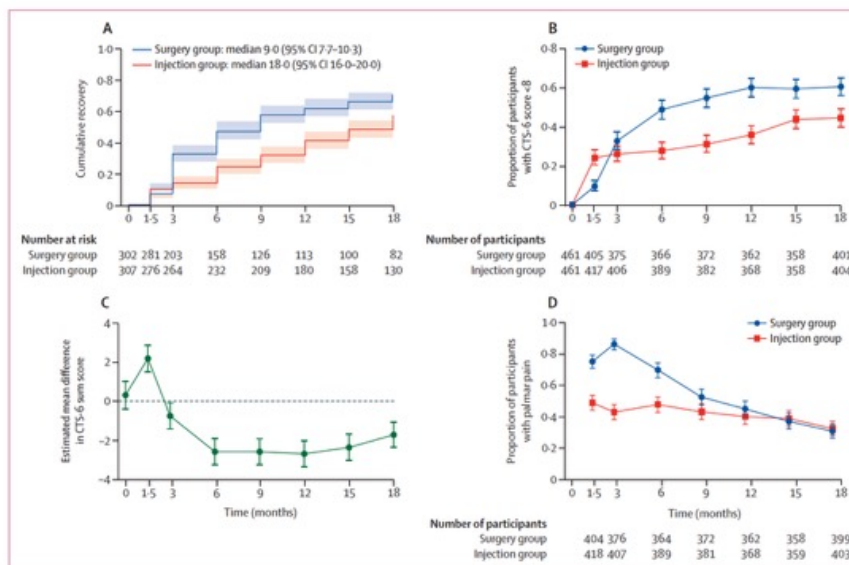


Figure 2: Graphs of four of the secondary outcomes

(A) Inverse Kaplan-Meier curves estimating the cumulative time to recovery during 18 months of follow-up. The median time to recovery was 9.0 months (95% CI 7.7-10.3) in the surgery group and 18.0 months (16.0-20.0) in the injection group. Time to recovery was defined as the first timepoint after the last self-reported carpal tunnel syndrome intervention (eg, additional injection, surgery, or splint) with a CTS-6 sum score of less than eight if this timepoint was followed by a CTS-6 sum score of less than eight at the next available timepoint or if this was the last available timepoint. (B) The proportion (with 95% CIs) of participants with a CTS-6 sum score of less than eight per timepoint in the surgery group and in the injection group. (C) The estimated mean difference of the CTS-6 sum score, generated with a linear mixed model, for the two trial groups. (D) The proportion (with 95% CIs) of participants with scar or proximal palm pain (or both) in the surgery group and in the injection group during 18 months of follow-up.

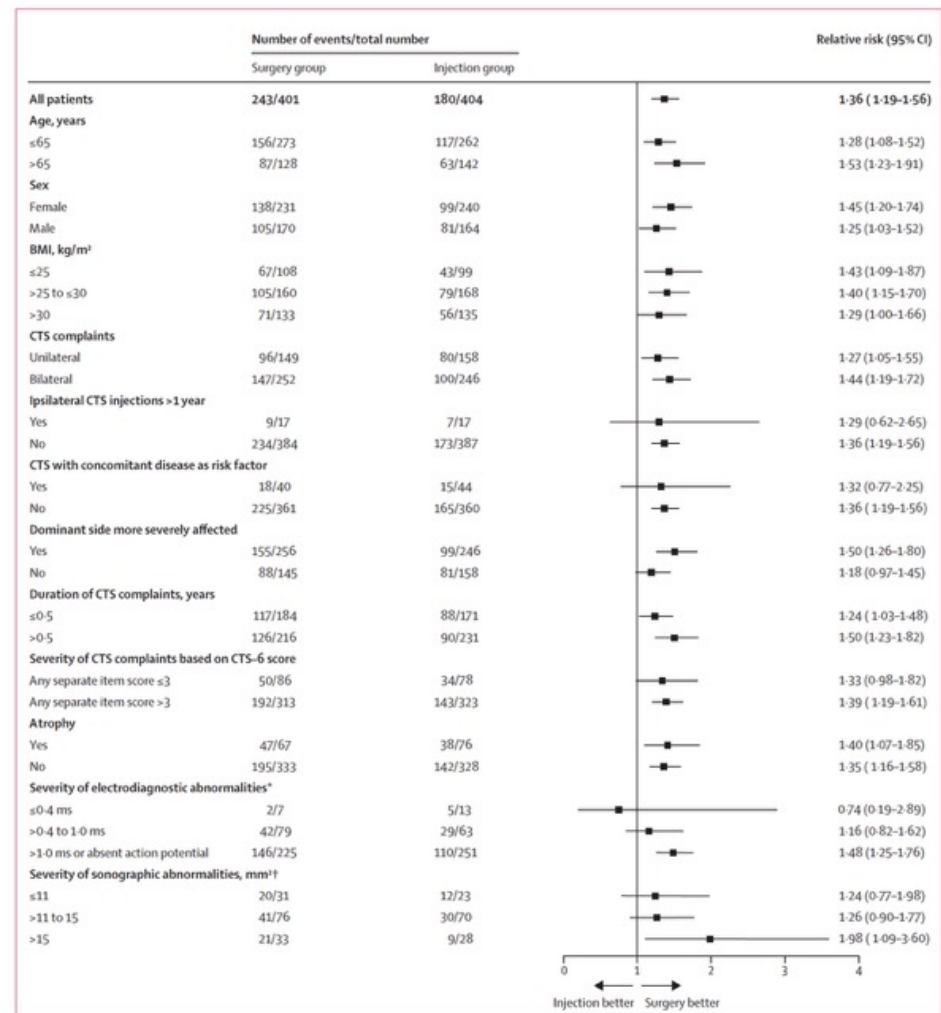


Figure 3: Rate of recovery in subgroups as part of the prespecified subgroup analysis

Relative risks and 95% CIs show the effect within each subgroup. CTS=carpal tunnel syndrome. CTS-6=six-item carpal tunnel symptoms scale. \*The distal sensory latency difference of the 4th finger between the median and the ulnar nerve in milliseconds was recorded, with a greater difference or absence of a median sensory nerve action potential indicating more severe electrodiagnostic abnormalities. †The median nerve cross-sectional area in mm² was recorded, with a higher cross-sectional area indicating more severe sonographic abnormalities.

	Surgery group	Injection group	Risk difference (95% CI)	p value*
<b>Adverse events during surgery†</b>				
Nerve injury	0/441	1/226 (<1%)	0.00 (−0.01 to 0.01)	0.56
Tendon injury	0/441	0/226	0.00 (0.00 to 0.00)	1.00
Haematoma	0/441	2/226 (<1%)	−0.01 (−0.02 to 0.00)	0.12
Pain	1/441 (<1%)	2/226 (<1%)	−0.01 (−0.02 to 0.01)	0.27
<b>Adverse events during injection‡</b>				
Nerve injury	NA	0/465	..	..
Tendon injury	NA	0/465	..	..
Haematoma	NA	1/465 (<1%)	..	..
Pain	NA	2/465 (<1%)	..	..
<b>Adverse events during follow-up</b>				
Wound or skin problem requiring treatment§	60/435 (14%)	30/453 (7%)	0.07 (0.03 to 0.11)	0.0004
Pain in the hand, wrist, or scar¶	273/435 (63%)	291/453 (64%)	−0.01 (−0.08 to 0.05)	0.65
Changed sensation in the hand	287/435 (66%)	326/453 (72%)	−0.06 (−0.12 to 0.00)	0.05
Diminished strength of the hand	287/435 (66%)	289/453 (64%)	0.02 (−0.04 to 0.08)	0.50
Decreased dexterity of the hand	264/435 (61%)	259/453 (57%)	0.04 (−0.03 to 0.10)	0.29
Allergic reaction	1/436 (<1%)	0/453	0.00 (−0.00 to 0.01)	0.49
Sleep and mood complaints	1/436 (<1%)	2/453 (<1%)	−0.00 (−0.01 to 0.01)	0.51
Increased complaints or treatment at contralateral side	18/436 (4%)	11/453 (2%)	0.02 (−0.01 to 0.04)	0.15
Admitted to hospital for other reasons	46/436 (11%)	45/453 (10%)	−0.05 (−0.10 to 0.01)	0.14
Other adverse events (not related)	153/436 (35%)	159/453 (35%)	−0.00 (−0.06 to 0.06)	1.00
Data are n/N, unless otherwise indicated. NA=not available. *p values are from $\chi^2$ tests and, for cases with fewer than five observations, Fisher's exact test. †The number of surgeries includes 11 revision surgeries; nine for the surgery group and two for the injection group. For two participants in the surgery group and for four participants in the injection group, adverse events during surgery were not reported because no surgery report was available. ‡Only available for injection group for the initial injection. §One participant in the surgery group was hospitalised due to a serious wound infection. ¶Reported separately from the palmar pain scale.				
<b>Table 3: Physician-reported adverse events during surgery or injection and participant-reported adverse events during follow-up</b>				

## Research in context

### Evidence before this study

Surgical release of the transverse carpal ligament and an injection of corticosteroids near the median nerve in the wrist are both effective treatments for carpal tunnel syndrome. Often, the treatment starts with a steroid injection because it is considered less invasive and easy to do. However, there is also a substantial group of clinicians who refer patients directly for surgery, believing that injections offer only temporary relief and thus delay more effective surgical treatment. To determine which treatment is more effective in adults with carpal tunnel syndrome, we searched databases for randomised controlled trials from database inception to Feb 3, 2015, with search terms covering carpal tunnel and corticosteroid injections and surgery (for the full search strategy and terms see the appendix p 43). Three randomised controlled trials were identified that compared surgical treatment directly to one or two steroid injections for carpal tunnel syndrome. The quality of these single-centre studies was moderate and sample sizes were small. The two trials with a follow-up shorter than 6 months indicated that surgery might be more beneficial. The only trial with a follow-up of more than 6 months indicated that injection was initially more beneficial but this was not found at the 2-year follow-up, with participants who had additional surgery in the injection group excluded from analysis. Informal updates of the search aligned with a recently published Cochrane review (which covered literature up to November, 2022), showing insufficient evidence on the most effective treatment strategy with long-term follow-up for carpal tunnel syndrome to end the unwanted treatment variation in medical practice.

### Added value of this study

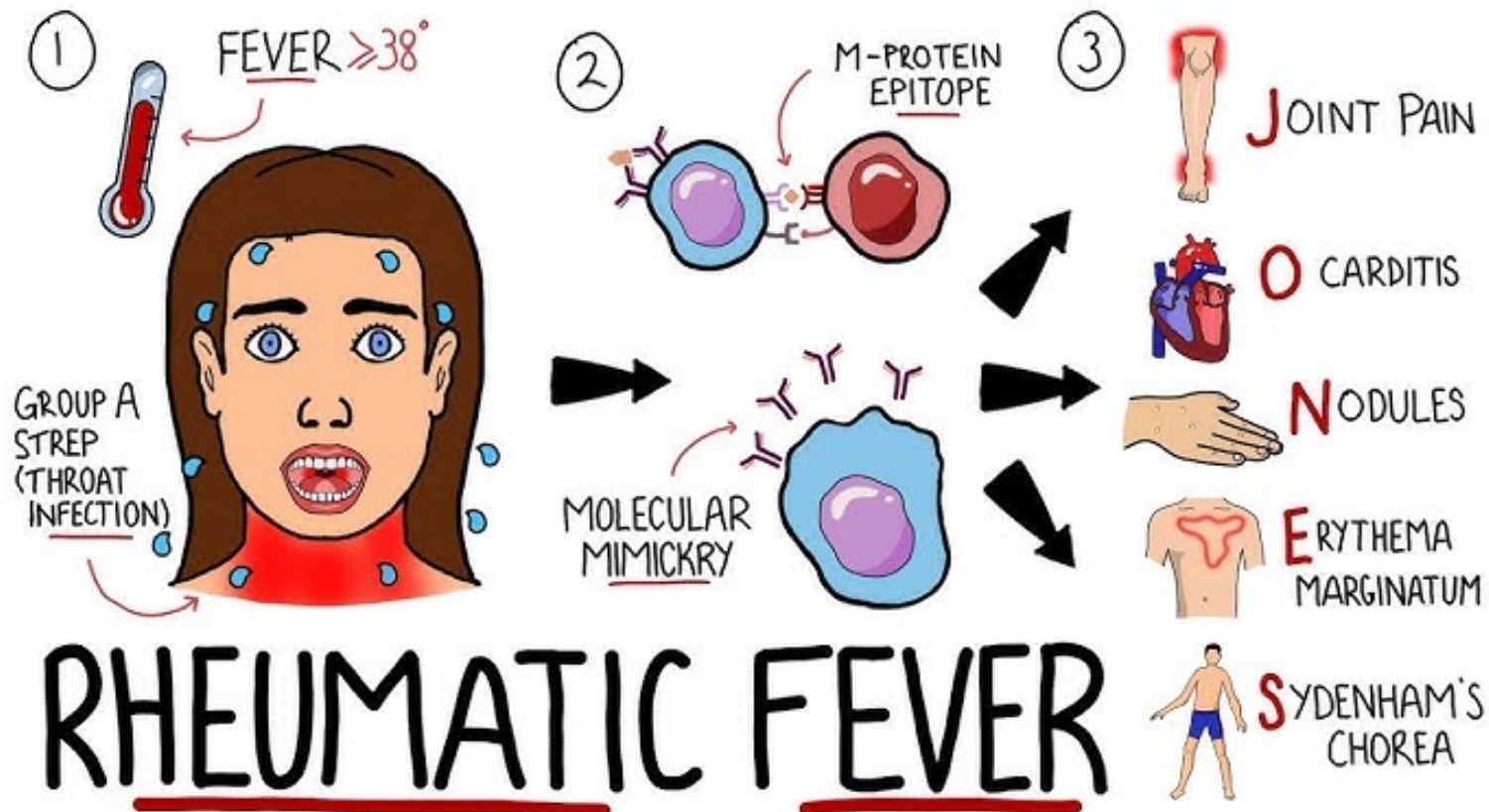
This study is the first adequately powered randomised controlled trial comparing the effectiveness of starting with

surgery versus starting with injections for carpal tunnel syndrome with a long-term follow-up of 18 months. We found that starting treatment for carpal tunnel syndrome with surgery had a greater chance of recovery at 18 months than starting with injections, even with the option of additional treatments. Furthermore, the survival analysis showed that the median time to recovery in the surgery group was around half that in the injection group. We also found better outcomes in the surgery group than in the injection group regarding upper-limb functioning, the participant's global perception of recovery, and the participant's satisfaction with the results of treatment. From 6 weeks to 9 months, more participants in the surgery group had palmar pain than in the injection group; thereafter, the proportion of participants with palmar pain were similar in both groups. The results for the proportion of participants with limitations due to palmar pain showed the same pattern. Physician-reported adverse events were scarce. Participant-reported adverse events were similar between both treatment strategies, except for more wound or skin problems requiring treatment in the surgery group and more often reported changed sensation in the hand in the injection group.

### Implications of all the available evidence

This is the first study that shows that initial surgery is more effective than initial corticosteroid injection, with a higher and earlier chance for long-term recovery and relatively few adverse events. In clinical practice, patients can be advised convincingly that early surgery is more beneficial in the long term.

Molekulare Mimikry (im Deutschen auch Antigen-Mimikry genannt) bezeichnet die Ähnlichkeit von Molekülen auf der Oberfläche von Krankheitserregern (z.B. Bakterien, Viren) mit körpereigenen Strukturen. Diese Ähnlichkeit kann dazu führen, dass das Immunsystem den Erreger als "Fremd" nicht richtig erkennt und sich infolgedessen auch gegen körpereigenes Gewebe richtet, was zu Autoimmunerkrankungen führen kann.







## Acute rheumatic fever

Acute rheumatic fever (ARF) is an autoimmune disorder resulting from Group A Streptococcus (GAS) pharyngitis or impetigo in children and adolescents, which may evolve to rheumatic heart disease (RHD) with persistent cardiac valve damage. RHD causes substantial mortality and morbidity globally, predominantly among socioeconomically disadvantaged populations, with an interplay of social determinants of health and genetic factors determining overall risk. ARF diagnosis is based on a constellation of clinical and laboratory features as defined by the 2015 Jones Criteria, although advances in molecular point-of-care testing and the ongoing search for ARF biomarkers offer the potential to revolutionise diagnostics. There are persistent gaps in ARF pathophysiology with little progress in therapeutics over the last several years. The greater focus towards primordial, primary, and secondary prevention such as advances in GAS vaccine development, innovations in digital health technology, improved antibiotic formulations for secondary prevention, and decentralised programmatic implementation to improve health-care delivery offer feasible solutions towards reducing future ARF burden globally.

	Age-standardised incidence rate (95% UI)	Age-standardised prevalence rate (95% UI)	Age-standardised death rate (95% UI)	Disability-adjusted life years (95% UI)
Global	50.7 (40.1–63.1)	684.2 (540.4–848.9)	4.5 (3.9–5.3)	162.1 (139.1–190.5)
African region	93.7 (72.9–118.0)	1336.7 (1021.2–1691.8)	2.7 (2.4–3.2)	139.1 (110.2–178.9)
Region of the Americas	42.9 (34.8–52.8)	641.2 (521.2–783.5)	0.9 (0.8–1.0)	55.0 (43.4–71.2)
South-East Asia region	44.2 (34.8–55.6)	628.9 (429.1–787.5)	11.2 (9.3–15.1)	346.3 (292.1–439.8)
Eastern Mediterranean region	53.4 (42.1–66.5)	758.7 (601.0–933.1)	6.5 (5.2–8.6)	240.3 (197.1–305.7)
Western Pacific region	35.6 (28.3–44.2)	542.2 (431.3–666.3)	3.3 (2.7–4.1)	97.9 (81.7–117.4)
European region	12.8 (11.0–14.9)	167.6 (145.6–194.7)	1.6 (1.4–1.7)	42.6 (38.9–47.5)

95% UI=95% uncertainty interval. Disability-adjusted life-years are age-standardised. All measures are reported per 100 000 of the population.

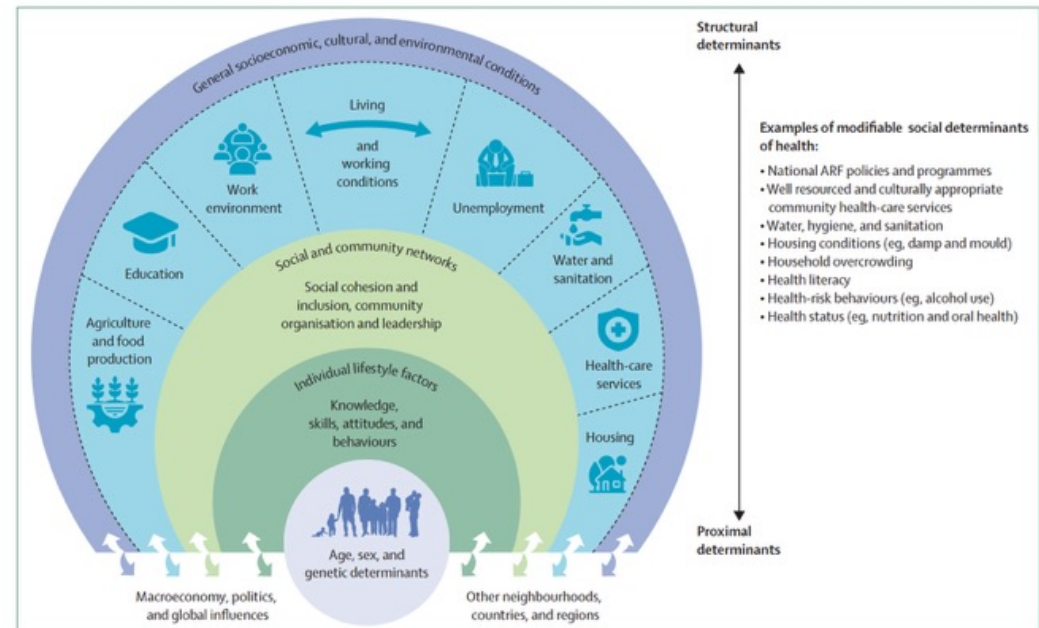
*Table: 2021 Global Burden of Disease estimates for rheumatic heart disease globally and across WHO regions<sup>a</sup>*



**Panel 1: Key genome-wide association studies supporting genetic susceptibility to rheumatic heart disease**

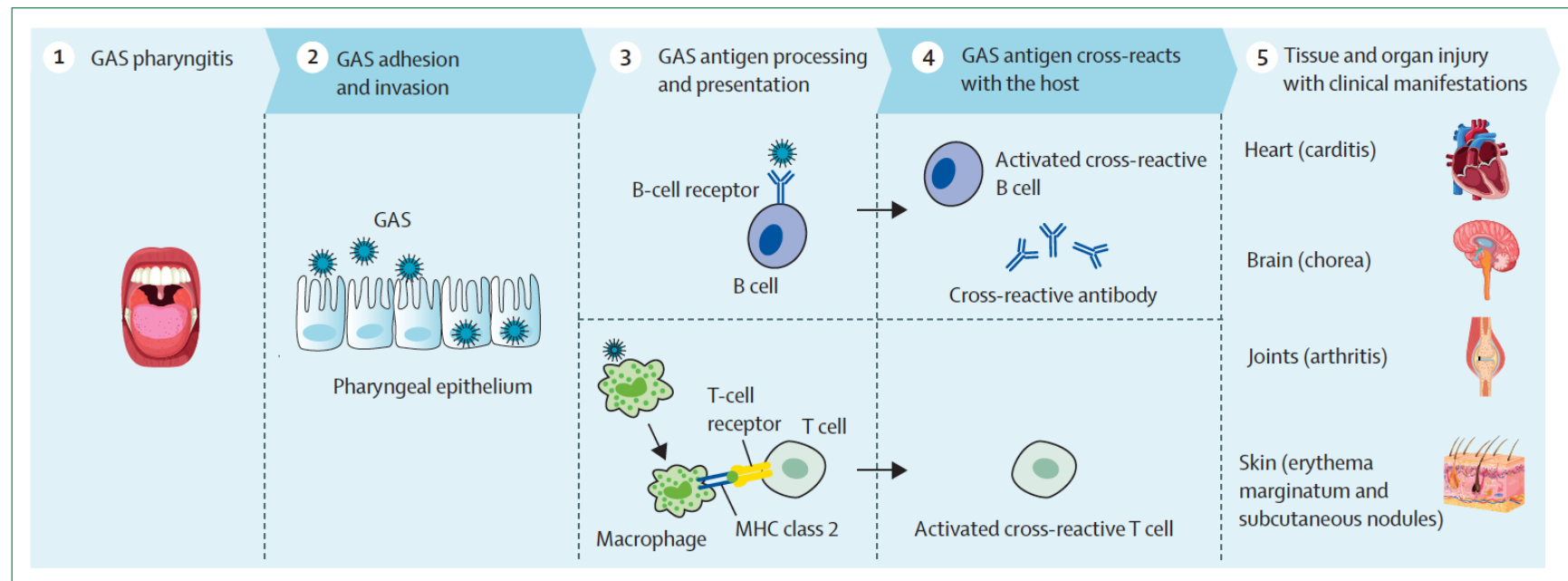
- *IGHV4-61\*02*: a susceptibility signal in the immunoglobulin heavy chain locus corresponding to the *IGHV4-61\*02* allele has been associated with a 1.4-fold increased risk of rheumatic heart disease among 1016 Indigenous peoples of the South Pacific (399 cases; 617 controls).<sup>29</sup>
- *HLA-DQA1\_DQB1*: specific risk (*HLA-DQA1\*0101\_DQB1\*0503*; *HLA-DQA1\*0103\_DQB1\*0601*) and protective (*HLA-DQA1\*0301\_DQB1\*0402*) haplotypes for rheumatic heart disease have been identified with variations in *HLA-DQA1\_DQB1* among 1263 Aboriginal Australians (398 RHD cases; 865 controls).<sup>30</sup>
- Class 3 region of the HLA complex: a rheumatic heart disease susceptibility signal in this region has been identified among 1163 South Asians (672 cases; 491 controls) in India and Fiji, and subsequently confirmed with a European Biobank dataset (150 cases; 1309 controls).<sup>31</sup>
- 11q24.1: the genetics of RHD (RHDGen) study, a multi-centred genome-wide association study comprising 4809 participants (2548 rheumatic heart disease cases and 2261 controls) from eight African nations, identified a single rheumatic heart disease susceptibility locus (11q24.1) among Black African individuals.<sup>32</sup>

HLA=human leukocyte antigen. RHD=rheumatic heart disease.



**Figure 1: Social determinants of health**

The Dahlgren and Whitehead model<sup>12-19</sup> depicts social determinants of health that influence the risk of Group A streptococcus infection, acute rheumatic fever, and progression to rheumatic heart disease in a population. Social determinants of health include structural (eg, economic and political systems) and proximal determinants, consisting of components of daily life (eg, family environment, housing, traditional practices), the socioeconomic environment (including macroeconomic measures such as wealth), demography, lifestyle, and behaviour. ARF=acute rheumatic fever.



**Figure 2: The process of molecular mimicry in the pathophysiology of acute rheumatic fever**

Following GAS pharyngitis (1), there is adhesion and invasion of the pharyngeal epithelium (2). Presentation of GAS antigens results in activation of B cells and T cells (3). Activated T cells and antibodies produced by activated B cells cross-react with antigenic epitopes (4) in the heart, brain, joints, and skin and subcutaneous tissues resulting in clinical manifestations of acute rheumatic fever (5). Cross-reactive antibodies bind to Group A carbohydrates, triggering increased expression of vascular cell adhesion molecule 1 in the cardiac valve endothelium, causing T-cell infiltration and cytokine-mediated immune damage. Cross-reactive antibodies binding to dopamine receptors and lysogangliosides result in Sydenham's chorea. A delayed hypersensitivity reaction causes the skin and subcutaneous tissue manifestations while immune-complex deposition in the joints results in arthritis. GAS=group A *Streptococcus*. MHC=major histocompatibility complex.

### Panel 2: Common clinical features of acute rheumatic fever

#### Joint manifestations

Joint manifestations occur in approximately 60–80% of ARF cases, commonly presenting as a nonsuppurative, asymmetric, migratory polyarthritis predominantly affecting the large joints (eg, wrist, elbow, ankle, knee).<sup>39</sup> Monoarthritis and polyarthralgia are seen in high-incidence areas. Symptoms are managed with non-steroidal anti-inflammatory drugs and largely resolve spontaneously within 4 weeks. Rarely, Jaccoud arthropathy, a non-erosive arthropathy classically resulting in ulnar deviation of metacarpophalangeal joints, can occur.<sup>40</sup>

#### Carditis

Endocarditis (valvulitis) involving regurgitation of the mitral valve followed by the aortic valve is the hallmark of rheumatic carditis. Pericarditis can occur and usually resolves without long-term sequelae. Systolic dysfunction from primary myocarditis is uncommon, however can occur in cases of recurrent acute rheumatic fever.<sup>41</sup>

Mitral regurgitation classically presents with a high-pitched, apical, holosystolic murmur radiating to the axilla or a low-pitched mid-diastolic Carey Coombs murmur. A pericardial rub can be heard in the presence of pericarditis. Approximately 12–21% of cases are, however, subclinical.<sup>39</sup> Cardiac rhythm disturbances are often self-limiting and can occur in the absence of valvulitis with approximately half of patients showing prolonged PR intervals. Rarer rhythm disturbances include accelerated junctional tachycardia, premature contractions, and second-degree heart block. QTc prolongation in the early phase of acute rheumatic fever is likely benign, but QT prolonging medications should be used with caution.<sup>42</sup>

Severe cardiac complications such as complete heart block, cardiomegaly, and congestive cardiac failure are relatively uncommon.

#### Sydenham's chorea

Chorea is a cardinal feature of acute rheumatic fever, occurring in 10–30% of cases with a female predominance and peak incidence in pre-pubertal children.<sup>39</sup> Sydenham's chorea commonly presents with carditis, but can occur in isolation with a latent period of 1–6 months and the absence of serological evidence of Group A streptococcus infection. The typical presentation is purposeless, involuntary movements of the extremities and trunk, which disappear during sleep.<sup>43</sup> Other presenting features include neuropsychiatric disturbance, dysarthria, dysgraphia, and hypotonia.<sup>44,45</sup> Symptoms commonly remit within 6 months, however can persist for up to 2 years, and relapses can occur.

#### Skin and subcutaneous manifestations

Skin and subcutaneous manifestations are rare (<10%) and consist of erythema marginatum and subcutaneous nodules.<sup>41</sup> Erythema marginatum is a non-pruritic, evanescent, maculopapular, blanching rash with a serpiginous border.<sup>46</sup> The rash manifests on the trunk and limbs, sparing the face, palms, and soles, and might not be evident on dark skin tones. Subcutaneous nodules are small, firm, mobile, and painless nodules occurring over extensor joint surfaces (eg, elbows, knees, and ankles), the occiput, and vertebrae, and are usually associated with carditis.

### Panel 3: 2015 Jones Criteria for diagnosis of ARF<sup>39</sup>

#### For all patient populations with evidence of preceding Group A Streptococcus infection

- Diagnosis of initial ARF: two major manifestations or one major plus two minor manifestations
- Diagnosis of recurrent ARF: two major criteria or one major and two minor criteria or three minor criteria

#### Major criteria

##### Low-risk populations\*

- Carditis (clinical or subclinical)†
- Arthritis (polyarthritis only)
- Chorea
- Erythema marginatum
- Subcutaneous nodule

##### Moderate-risk to high-risk populations

- Carditis (clinical or subclinical)
- Arthritis (monoarthritis or polyarthritis); polyarthralgia‡
- Chorea
- Erythema marginatum
- Subcutaneous nodule

#### Minor criteria

##### Low-risk populations\*

- Polyarthralgia
- Fever (>38.5°C)
- ESR greater than 60 mm/h, CRP greater than 3 mg/dL (>30 mg/L), or both§
- Prolonged PR interval, after accounting for age variability (unless carditis is a major criterion)

##### Moderate-risk to high-risk populations

- Monoarthralgia
- Fever (>38°C)
- ESR greater than 30 mm/h, CRP greater than 3 mg/dL (>30 mg/L), or both§
- Prolonged PR interval, after accounting for age variability (unless carditis is a major criterion)

ARF=acute rheumatic fever. CRP=C-reactive protein. ESR=erythrocyte sedimentation rate. \*ARF incidence is less than 2 per 100 000 school-aged children per year or all-age rheumatic heart disease prevalence of less than or equal to 1 per 1000 population per year. †Subclinical carditis indicates echocardiographic valvulitis. ‡Polyarthralgia should only be considered as a major manifestation in moderate-risk to high-risk populations after exclusion of other causes. Joint manifestations can only be considered in either the major or minor categories, but not as both in the same patient. §The CRP value must be greater than the upper limit of normal for the laboratory. Also, because ESR might evolve during ARF, peak ESR values should be used.



#### **Panel 4: Confirmatory criteria for pathological valve dysfunction (2023 World Heart Federation guidelines)<sup>64</sup>**

##### **Pathological mitral regurgitation (at least mild; all criteria must be met)**

- Observed in at least two views
- Observed in at least one view, mitral regurgitation jet length measures equal to or greater than 1.5 cm (in individuals weighing equal to or less than 30 kg) or equal to or greater than 2.0 cm (in individuals weighing equal to or greater than 30 kg)
- Velocity equal to or greater than 3.0 m/s for one complete envelope
- Pansystolic jet in at least one envelope

##### **Pathological aortic regurgitation (at least mild; all criteria must be met)**

- Observed in at least two views
- Observed in at least one view, aortic regurgitation jet length equal to or greater than 1.0 cm
- Velocity equal to or greater than 3.0 m/s in early diastole
- Pandiastolic jet in at least one envelope

#### **Panel 5: Symptomatic and supportive therapy of acute rheumatic fever**

##### **Arthritis**

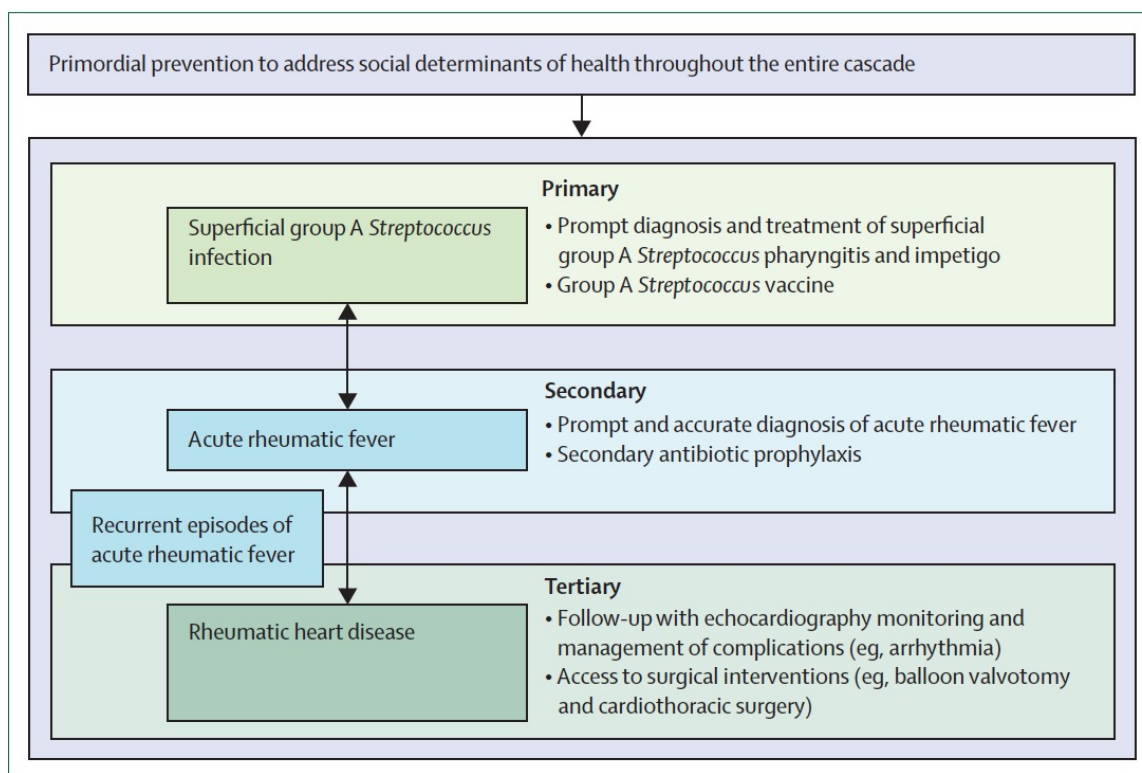
Non-steroidal anti-inflammatory drugs are recommended for management of arthritis and arthralgia, with naproxen and ibuprofen replacing aspirin as first-line therapy due to a more favourable safety profile.<sup>69,70</sup> Rapid symptomatic improvement is generally achieved with high-dose therapy which is weaned after 1–2 weeks based on clinical response and decline in inflammatory markers.<sup>71</sup> Resolution occurs in 90% of cases within 12 weeks, although rebound symptoms can occur on withdrawal of therapy warranting medication reintroduction.<sup>72</sup> Alternative diagnoses should be sought in individuals who are not responsive to non-steroidal anti-inflammatory drugs.

##### **Carditis**

Almost half of latent rheumatic heart diseases cases resolve within 5 years.<sup>73</sup> Mild to moderate rheumatic carditis is managed conservatively, with pharmacological therapy targeting management of complications such as heart failure (eg, angiotensin-converting enzyme inhibitors, diuretics, and nitrates). Emergency valve replacement surgery is sometimes warranted for chordae tendineae rupture. Although older studies did not suggest the benefit of corticosteroids and intravenous immunoglobulin in preventing subsequent rheumatic heart disease, subsequent smaller studies have shown improvements in laboratory and radiological parameters with the use of corticosteroids in severe carditis.<sup>71,74–76</sup> Screening and treatment of latent infections (eg, strongyloides, tuberculosis) should be performed before commencing immunosuppressive treatment. Hydroxychloroquine has shown the ability to control inflammation and pericarditis in a case series of two patients with protracted rheumatic carditis, with ongoing studies offering potential to provide further insight on its use.<sup>77,78</sup>

##### **Chorea**

The management of Sydenham's chorea is geared towards improving daily function and consists of symptomatic and immunomodulatory therapy, although the evidence base is scarce. Dopamine antagonists might provide symptomatic benefit, but their use is limited by extra-pyramidal side-effects. Anti-epileptic agents such as carbamazepine and sodium valproate are used most. Immunomodulatory therapies including corticosteroids, intravenous immunoglobulin, and plasmapheresis are reserved for severe and refractory cases. Recent retrospective studies suggest corticosteroid therapy might provide quicker resolution of chorea and are associated with a lower risk of relapse.<sup>44,79</sup> Randomised controlled trials aim to provide further evidence (eg, NCT06259006).



**Figure 3: Opportunities for prevention and treatment of group A *Streptococcus* infection, acute rheumatic fever, and rheumatic heart disease**

#### Panel 6: GAS vaccine pipeline

##### M protein vaccine candidates

The M protein is encoded by the *emm* gene and consists of a coiled-coil structure with a hypervariable N-terminal, central domain, and conserved C-terminal region. There are currently four M protein-based candidate GAS vaccines on a product development track.<sup>114-116</sup> The most advanced is StreptNova, a 30-valent vaccine comprised of four recombinant proteins containing N-terminal peptides.<sup>117</sup> The vaccine has reported to be well tolerated, immunogenic, and safe, with no evidence of cross-reactivity or clinical autoimmunity among 23 healthy adult volunteers in a phase 1a trial completed in 2020.<sup>117</sup> The J8/S2 combivax and P\*17/S2 combivax incorporate peptides from the conserved C-terminal region and also include non-M peptides into their formulation.<sup>118</sup> Animal studies have shown immunogenicity with no clinical toxicity and the candidates have progressed to clinical trials in 2022. StreptInCor, which consists of a 55-amino acid peptide from the derived from C-terminal region, has shown safety and efficacy in animal studies and is due to progress to clinical trial.<sup>119,120</sup>

##### Non-M protein vaccine candidates

Non-M protein-based vaccines target highly conserved factors across GAS isolates (eg, *Streptococcus pyogenes* adhesion and division protein [SpyAD], streptolysin O, C5a peptidase) and have shown promising results in preclinical trials.<sup>114-116</sup> These consist of subsets of protein antigens such as the Combo5 and Teevax vaccines. Some candidates also feature GAC, which is a surface polysaccharide present across all GAS isolates (eg, Combo4 and VAX-A1).<sup>121</sup> Experimental evidence has, however, shown autoantibodies to GlcNAc, an immunodominant side chain in GAC, which can cross-react with cardiac and brain tissue raising theoretical safety concerns. VAX-A1 consists of a modified version of GAC in which the GlcNAc side chains are removed and conjugated to SpyAD. Animal studies have shown VAX-A1 to be immunogenic with no evidence of cross-reactivity to cardiac or brain tissue.<sup>122</sup> There is ongoing research to explore novel technologies that feature modified GAC subunits with the goal for a universal GAS vaccine.<sup>123</sup>

GAC=Group A carbohydrate. GAS=Group A streptococcus. GlcNAc=N-acetylglucosamine.



## Conclusion

There have been considerable advances in ARF in the last several years, with major progress in the search for GAS point-of-care testing, ARF biomarkers, GAS vaccine development, SAP, innovations in AI, and development of decentralised health-care services to better serve affected populations. Further research to better understand the pathophysiology and global distribution of ARF and GAS is required to move these initiatives forward. The huge disparity in funding as compared to the global scale of disease burden remains problematic, but increasing global advocacy with ongoing efforts to strengthen international collaborations and streamline national efforts has potential in pushing primordial, primary, and secondary prevention strategies to reduce the morbidity and mortality resulting from GAS infections, ARF, and RHD.

## Jones Criteria for Rheumatic Fever

Mnemonic



Learn  
Medicine  
Atop

JONES (Major Criteria)	PEACE (Minor Criteria)
J - Joints Involvement (Migratory polyarthritis)	P - Previous Rheumatic Fever or Preceding Streptococcal Infection
C - Carditis	E - Electrocardiogram (ECG) with PR prolongation
N - Nodules (Subcutaneous Nodules)	A - Arthralgia
E - Erythema Marginatum	C - CRP and ESR Increased
S - Sydenham's Chorea (St. Vitus' dance)	E - Elevated Temperature (Fever)

✓ Two major criteria

or

✓ One major and two minor criteria





## Rethinking jaundice

Figueiredo *et al.* report a genetic trait that may provide protection from the disease—the decreased expression of a bilirubin conjugation enzyme. As a result, unconjugated bilirubin concentrations increase, which has antimalarial effects.

Natural lines of defense against malaria have evolved in malaria-endemic regions over millions of years. These include genetic traits that confer partial resistance or protect from severe malaria. For example, mutations in the gene encoding glucose-6-phosphate dehydrogenase results in an enzyme deficiency that increases oxidative stress in red blood cells. This has a negative effect on the parasite (the *Plasmodium* life cycle includes an asexual phase in host red blood cells). A decrease in hemoglobin production by red blood cells caused by mutations in genes encoding the globin subunits of hemoglobin (a condition known as thalassemia) makes these cells less hospitable to *Plasmodium* and increases their clearance from the host. Mutations in the gene that encodes glycophorin cause Dantu, a condition characterized by high surface tension in red blood cells that makes it difficult for malaria parasites to invade and multiply. And red blood cells that lack Duffy antigens, the receptors for one species of *Plasmodium*, hinder the parasite's ability to invade these cells. These genetic traits are often associated with substantial host trade-offs, such as the development of sickle cell disease or an increased risk of anemia, and are therefore not predominant in the global population. However, the protective effect against malaria has made these traits prevalent in malaria-endemic regions, where coevolution of the parasite and its host has shaped their genomes.

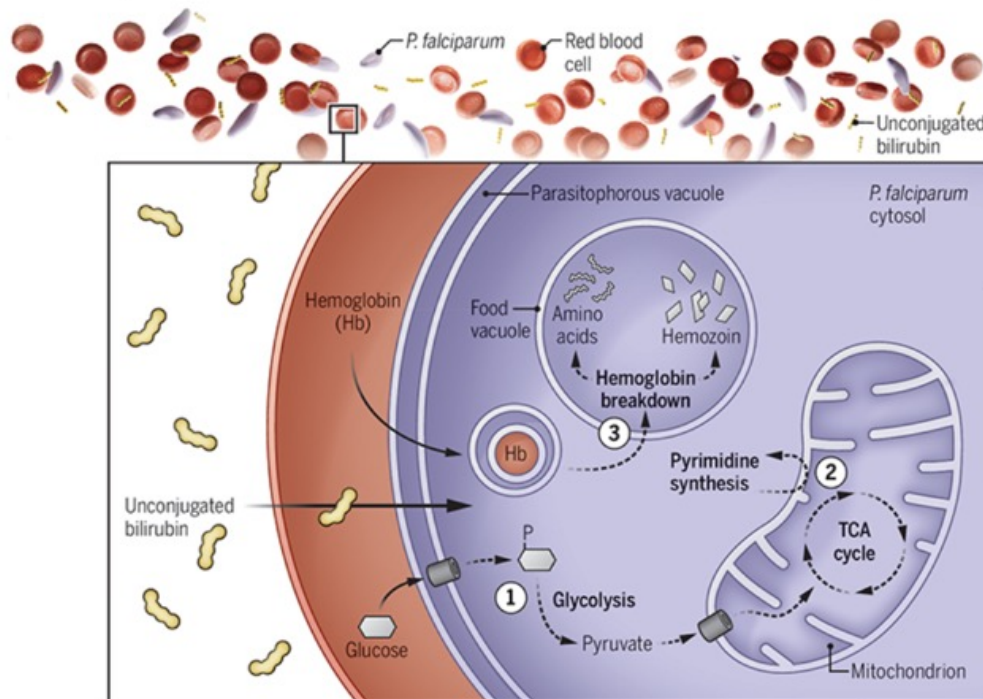
Increased amounts of unconjugated bilirubin are a characteristic of Gilbert's syndrome, a benign liver condition caused by a polymorphism in the promoter region of the gene encoding the enzyme UDP glucuronosyltransferase family 1 member A1 (UGT1A1), resulting in its reduced transcription. UGT1A1 catalyzes the addition of glucuronic acid to bilirubin, a yellowish pigment that is a by-product of red blood cell breakdown. This modification occurs in hepatocytes and transforms insoluble unconjugated bilirubin into a water-soluble conjugated form that is excreted through bile and urine. Hence, repressing UGT1A1 causes unconjugated bilirubin to accumulate, which manifests as mild jaundice. Jaundice, the yellowing of the skin and eyes, is a common feature in malaria and has been associated with hemolysis or liver dysfunction and considered a marker of disease severity. However, Figueiredo *et al.* suggest, through experiments in cultured infected red blood cells and rodent models and by examining human data, that unconjugated bilirubin serves a host-beneficial function during *Plasmodium* infection. Increasing unconjugated bilirubin amounts, through direct administration to infected red blood cells, impaired parasite development and halted disease progression. Conversely, mice genetically engineered to lack bilirubin production were hypersensitive to *Plasmodium* infection, a vulnerability that was reversed by administration of unconjugated bilirubin. Additionally, asymptomatic humans with *Plasmodium falciparum* parasitemia had increased amounts of unconjugated bilirubin relative to parasite burden compared with symptomatic infected individuals. Consistent with a protective effect of unconjugated bilirubin, the UGT1A1-repressing polymorphism is overrepresented in populations of African origin, where malaria is endemic.

Increased unconjugated bilirubin has been frequently observed in people suffering from malaria. However, Figueiredo *et al.* present a paradigm-shifting view of bilirubin-associated jaundice in the context of *Plasmodium* infection, challenging the conventional notion that the accumulation of unconjugated bilirubin in plasma is solely a consequence of liver dysfunction. Instead, the authors propose that this metabolic alteration constitutes a protective, adaptive host response that limits malaria severity.

### The antimalarial effects of unconjugated bilirubin

In one phase of its infectious life cycle, the malaria parasite *Plasmodium falciparum* resides in its parasitophorous vacuole within a red blood cell.

Unconjugated bilirubin in the host plasma disrupts several metabolic processes in the parasite, including (1) glucose catabolism in the cytosol and (2) the tricarboxylic acid (TCA) cycle and pyrimidine synthesis in the mitochondrion. Furthermore, (3) hemoglobin in the pathogen's food vacuole is also affected, including its breakdown to obtain amino acids and detoxification into hemozoin.



The findings of Figueiredo *et al.* suggest a multifactorial antimalarial mode of action for unconjugated bilirubin. The authors show that unconjugated bilirubin impairs the parasite's energy metabolism, pyrimidine biosynthesis, and hemozoin crystallization (which converts toxic heme to harmless hemozoin) and also reduces mitochondrial membrane potential and volume (see the figure). However, it is unclear whether these processes are targeted directly by unconjugated bilirubin or are downstream effects of the actual target (or targets), which has yet to be identified. Also, it is unclear whether the antimalarial properties of unconjugated bilirubin are limited to direct effects on the parasite or have broader effects, including immune modulatory functions. That unconjugated bilirubin is not just a by-product of *Plasmodium*-induced hemolysis but acts as a host-derived antimalarial agent reshapes the notion of jaundice in individuals with malaria. The study of Figueiredo *et al.* paves the way for new views on disease resistance, therapeutic development, and evolutionary biology.



## A metabolite-based resistance mechanism against malaria

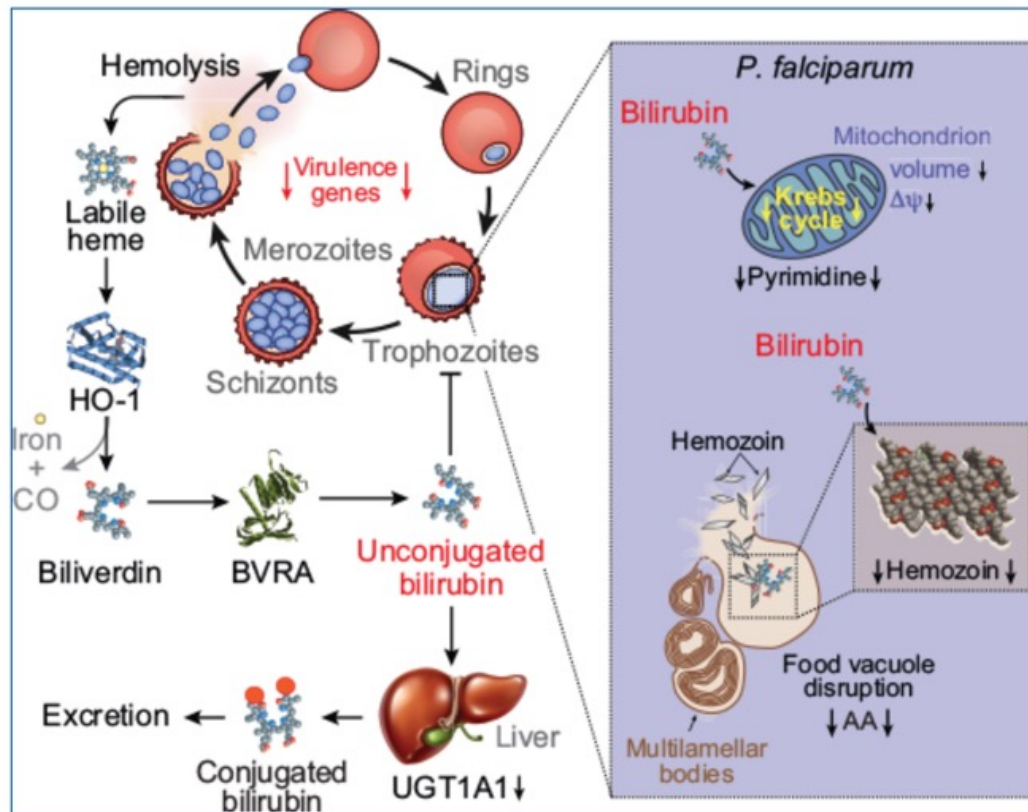
**INTRODUCTION:** Jaundice arises when bilirubin, a yellow pigment, accumulates in plasma and gives a yellowish color to the skin and the sclera (the white portion of the eyeball). Bilirubin has long been considered as a “waste product” of heme catabolism. Because of its lipophilic nature, bilirubin excretion requires conjugation to glucuronic acid through a reaction catalyzed in hepatocytes by UDP glucuronosyltransferase family 1 member A1 (UGT1A1). The less toxic water-soluble conjugated bilirubin is then excreted via the bile into the intestinal lumen. Because bilirubin conjugation occurs in the liver, its accumulation in plasma is a reliable biomarker of liver dysfunction. Although accurate, this has led to the widespread perception of jaundice being a maladaptive and eventually pathogenic response. However, several investigators have shown that bilirubin participates in various activities, acting as a lipophilic antioxidant and presumably as a ligand of receptors involved in different metabolic functions.

**RATIONALE:** Jaundice is a common presentation of malaria, the ancestral infectious disease caused by parasites that evolved to invade and proliferate inside the red blood cells of their hosts, causing hemolysis and the accumulation of extracellular hemoglobin in plasma. When the prosthetic heme groups of hemoglobin are detached from the globin chains of hemoglobin, there is an accumulation of labile heme. Survival from experimental malaria is contingent on the capacity of the infected host to catabolize heme into biliverdin, the substrate used by biliverdin reductase to produce bilirubin. This raised the hypothesis that bilirubin production by biliverdin reductase participates in a metabolism-based defense strategy against malaria.



**RESULTS:** Using a highly specific approach to measure bilirubin in plasma, we found a correlation between the levels of circulating unconjugated bilirubin and the onset of symptomatic *P. falciparum* malaria in humans. We established that bilirubin is protective against malaria in an experimental model of malaria in mice, where repressing bilirubin production through genetic loss of function of biliverdin reductase precipitated malaria mortality. This lethal phenotype could be reversed by the administration of bilirubin, verifying that unconjugated bilirubin can be protective against experimental malaria. Repression of bilirubin conjugation by hepatic UGT1A1 was also protective against experimental malaria in mice, further supporting the protective effect of unconjugated bilirubin against malaria. Using several orthogonal approaches in vivo and in vitro, we found that unconjugated bilirubin targets *Plasmodium* inside the red blood cell to repress its proliferation and virulence. Bilirubin targets the parasite's mitochondrion and simultaneously interferes with heme detoxification, disrupting the parasite food vacuole and therefore inhibiting the acquisition of essential amino acids from hemoglobin.

**CONCLUSION:** The induction of bilirubin production and inhibition of its conjugation in response to *Plasmodium* spp. infection is an evolutionarily conserved resistance mechanism against malaria. Presumably, this metabolism-based defense strategy has a major evolutionary trade-off, namely, the insidious incidence of neonatal jaundice, which can potentially damage neurons in the brain. To what extent this defense strategy can be targeted therapeutically to overcome the enormous burden imposed by malaria on human populations remains to be established.



**Antimalarial effect of bilirubin.** Malaria is associated with hemolysis and labile heme accumulation, which is catabolized into biliverdin by heme oxygenase-1 (HO-1) and converted into bilirubin by biliverdin reductase A (BVRA). Repression of bilirubin conjugation by UGT1A1 increases unconjugated bilirubin to target the *Plasmodium* mitochondrion and inhibit hemozoin crystallization, compromising the parasite's food vacuole and amino acid (AA) acquisition.  $\Delta\psi$ , mitochondrial membrane potential.

## How many years do I have left? An app gave me some helpful insights.



When a friend mentioned that he'd used a new artificial-intelligence-powered smartphone app called Death Clock AI to learn when his ticker would give out, I wanted to know my end date as well. I had used a rudimentary web-based calculator nearly a decade ago, which said my time would be up in 2031 — now just six years away! I was hoping an app combining AI and statistical modeling to predict my personal life expectancy would buy me more time.

It did! I am pleased to report that I won't die until 2042, at age 84. Those early death clocks — or longevity calculators — used only basic information to estimate how much time you had left. (The web-based tool I used previously asked four questions — about birth date, body mass index, smoking and mental health status.) There are, of course, other life expectancy calculators — the Social Security Administration provides one, as do such insurance companies as John Hancock and Northwest Mutual. But Death Clock AI is a giant step ahead with its reliance on artificial intelligence, which is fed by user data and trained on more than 1,200 life expectancy studies, allowing for a more personalized prediction of a death date.

# DEATH CLOCK: AI'S TAKE ON LIFE, LONGEVITY, AND BEYOND



## What Is the Death Clock?

The Death Clock is more than a curiosity — it's a tool combining AI and statistical modeling to predict individual life expectancy. Developed by Brent Franson, it leverages data from over 1,200 life expectancy studies and 53 million participants to create personalized predictions.

## How It Works

1. **Data Input:** Users provide information on their lifestyle, including dietary habits, sleep quality, and physical activity.
2. **AI Analysis:** Using machine learning algorithms, the app compares user data against its extensive database of longevity studies.
3. **Personalized Predictions:** The app generates a “death day” card, providing an estimated date of death.

Test taken: Friday, 13th June 2025.

**At time of testing you are 83 years, 3 months and 9 days old.**

Current age in: Days: (30,417), Weeks: (4,345), Months: (1,014)

Based on our calculations you will die on: **Sunday, 25th September 2044**

[f Share on facebook](#)

[X Post](#)

**You will live to be 102 years, 6 months and 21 days old!**

That's **7044 Days, 03 Hours, 25 Minutes, 43 Seconds** remaining...

Or approx: **19 years**